

Decay of dyonic black holes

Rahul Nigam

Department of Theoretical Physics
Tata Institute of Fundamental Research
Mumbai, India.

A thesis submitted for the degree of

Doctor of Philosophy

November, 2008

Declaration

I state that the work, embodied in this thesis, forms my own contribution to the research work carried out under the guidance of Professor Sunil Mukhi. I also collaborated with Anindya Mukherjee while he was a student at TIFR. This work has not been submitted for any other degree to this or any other University or body. Whenever references have been made to previous works of others, it has been clearly indicated.

(Rahul Nigam)

In my capacity as the supervisor of the candidate's thesis, I certify that the above statements are true to the best of my knowledge.

(Sunil Mukhi)

Acknowledgements

Firstly, I would like to thank my advisor, Sunil Mukhi for all his help during my research span in TIFR. He always supported and guided me patiently while I was struggling with the new ideas. Discussions with him were always fun and revealing at the same time. Most importantly while working with him I learnt that there is always a solution to every problem, its just one has to look for it at right place and not to give up before finding it.

I would also like to thank Atish Dabholkar, Avinash Dhar, Gautam Mandal, Shiraz Minwalla, Sandip Trivedi and Spenta Wadia for all the help I received from them during my stay in TIFR. They were always very approachable . Other members of the theory group have also been very helpful. In particular I would like to thank Deepak Dhar, Mustansir Barma and Sridhar K. for their help and support. My collaborator and a good friend Anindya Mukherji has helped me with stimulating discussions when we were finding it difficult to solve a problem. I want to thank Debashis Ghoshal, Rajesh Gopakumar and Ashoke Sen for their help whenever I visited HRI.

I had the good fortune to befriend a lot of students and postdocs in TIFR. Presence of Costis, Kevin, Lars, Rakesh, Rudra, Sashideep, Suresh and Suvrat made it a very joyable journey with all the serious discussions on random topics. I am thankful to Basu, Shamik and Tridib to patiently answer all my computer related queries. My special thanks to my friends Anil and Anuradha for their emotional support and for keeping me updated with the world outside institute.

My thanks are due to the DTP office staff, Raju Bathija, Girish Ogale, Rajan Pawar and Mohan Shinde who have helped me with any official matters. They have always been very friendly. I wish to specially thank Ajay Salve, our system administrator for his friendship and prompt help whenever things went wrong with the student room computers.

Finally I thank my parents and brother for all their love and support.

I dedicate this thesis to my loving parents and brother. I further dedicate it to all the researchers in India for their sustained contribution to the field of fundamental sciences.

Contents

1	Introduction	1
2	Decay of Dyonic black holes	7
2.1	Introduction	7
2.2	The system	10
2.3	Decays into a pair of dyons	12
2.4	Analysis of the marginal stability curves: $\frac{1}{2}$ -BPS decay products .	17
2.4.1	Equations of the curves	17
2.4.2	Farey fractions and Ford circles	20
2.4.3	Analysis of the decays: Sen circles and Ford circles	21
2.4.4	Analysis of the decays: higher torsion case	23
2.5	Analysis of the marginal stability curves: $\frac{1}{4}$ -BPS decay products .	26
2.5.1	Decays into a $\frac{1}{2}$ -BPS and a $\frac{1}{4}$ -BPS dyon	26
2.5.2	Decays into two $\frac{1}{4}$ -BPS dyons	27
2.6	Discussion	31
3	Constraints on “rare” dyon decays	32
3.1	Introduction	32
3.2	Marginal stability for $\mathcal{N} = 4$ dyons	34
3.3	Rare dyon decays	37
3.3.1	Analysis and implicit solution	37
3.3.2	Explicit solution: special cases	38
3.3.3	General charges, “triangular” moduli	45

3.3.4	Explicit solution: the general case	48
3.4	Multi-particle decays	50
3.5	Multi-centred black holes	51
3.6	Discussion	58
4	String Networks	59
4.1	String Networks	59
4.2	Classification of periodic string networks	64
4.2.1	Some general properties	64
4.2.2	Dual grid diagrams	66
4.2.3	Periodic identifications	73
4.3	Discussion	76
5	Kinematical Analogy for Marginal Dyon Decay	77
5.1	Introduction and review	77
5.1.1	Kinematic Analogy	78
5.1.2	Momentum ellipsoid	82
5.1.3	Multiparticle decays and the issue of codimension	84
5.1.4	Decay widths on marginal stability curves	85
6	Conclusions	86
	References	91

Chapter 1

Introduction

Black holes in String theory

String theory is a prominent candidate for being the quantum theory of gravity. The physical idea of this theory is that instead of elementary point like particles, the most basic building blocks of the nature are string like objects. The different vibrational modes of these strings give rise to different particles. Extended objects called “D-Branes” also contribute to the spectrum of the particles in string theory. Physical consistency requires that a supersymmetric string theory has a 10-dimensional space-time background¹. This superstring theory can still describe a 4 dimensional real world spacetime if we assume that the 6 extra dimensions are compact, and too small to be detected by present experiments. Hence a 10-dimensional critical string theory is a quantum theory of supergravity coupled to supersymmetric matter.

String theory has become a very powerful tool in understanding the very interesting objects known as black holes. Classical black holes are solutions to Einstein’s equation with very unique properties. Its a region of space in which the gravitational field is so powerful that nothing, not even electromagnetic radiation, can escape its pull after having fallen past its event horizon. The term “black hole” derives from the fact that the absorption of visible light renders the hole’s interior invisible, and indistinguishable from the black space around

¹Theories in less than 10d are subcritical and more than 10d are referred to as supercritical.

it. While general relativity describes a black hole as a region of empty space with a point-like singularity at the center and an event horizon at the outer edge, the description changes when the effects of quantum mechanics are taken into account. It's been shown that rather than holding captured matter forever, black holes may slowly leak a form of thermal black body energy called Hawking radiation and may well have a finite life.

This leads to a striking correspondence between the laws of thermodynamics and the laws of black hole mechanics. The first law of thermodynamics states that the variation of the total energy is equal to the temperature times the variation of the entropy plus the work. The corresponding formula for black holes states that the variation of the black hole mass is related to the variation of the horizon area plus the work term proportional to the variation of all the charges.

$$\delta M = \frac{\kappa_s}{2\pi} \frac{\delta A}{4} + \mu \delta Q + \Omega \delta J \quad (1.1)$$

Consequently, it was shown that the temperature of the black hole is given as $T = \kappa_s/2\pi$, κ_s being the surface gravity. This leads to the identification of the black hole entropy in terms of the event horizon area,

$$S_{macro} = \frac{A_{hor}}{4G_N \hbar} \quad (1.2)$$

It was shown that the total area of the event horizons of any collection of classical black holes can never decrease, even if they collide and merge. This is remarkably similar to the second Law of Thermodynamics, with area playing the role of entropy.

Although general relativity can be used to perform a semi-classical calculation of black hole entropy, this situation is theoretically unsatisfying. In statistical mechanics, entropy is understood as counting the number of microscopic configurations of a system which have the same macroscopic qualities (such as mass, charge, etc.). But without a satisfactory theory of quantum gravity, one cannot perform such a computation for black holes. However, it has been one of the successes of string theory that it provides such a microscopic quantum description for black hole entropy. Black holes are identified with certain states in the spectrum of string theory and the logarithm of the degeneracy of these states is identified with the black hole entropy.

In string theory, black holes are viewed as a bound state of strings and Dbranes wrapped around non-contractible cycles of a compact manifold. If g_s is the string coupling constant and N is the order of the number of strings/branes then the effective perturbation coupling constant is $g_s N$. For N large so that $g_s N \gg 1$, this bound state can gravitate and form a black hole which can be analyzed as solutions of the low energy effective action. The black hole entropy then can be computed for this using the Bekenstein-Hawking formula. Now, in the regime where $g_s N \ll 1$ and $N \gg 1$, the field theory associated with the strings/branes bound state becomes weakly coupled and amenable to perturbation. Hence the degeneracies of various states in the Hilbert space of this theory can be computed in the weak coupling limit. Now to compare the entropy in two limits we need to vary $g_s N$ gradually from small to large values. However we have no control over the system for intermediate values of $g_s N$ and hence it is not possible to compare the two limits. This problem can be avoided in a supersymmetric string theory if we study a certain class of black holes known as BPS black holes. Supersymmetry provides a lower bound called the Bogomol'nyi-Prasad-Sommerfield bound on the mass of a state in the theory. For any state, the mass is always greater than or equal to the central charge in the supersymmetry algebra. The states which saturate this bound are referred to as BPS states. These states are annihilated by some subset¹ of the total of 16 supercharges and therefore many of their properties, like mass and degeneracy, are protected under the flow of coupling constant. In 1996 in a 5-dimensional supersymmetric example, Strominger and Vafa[2] calculated the leading order degeneracy of the microscopic BPS states and showed that it was equal to the Bekenstein-Hawking entropy. Subsequent works in 4-dimensions were performed in this direction and this relation was established there also.

Black holes which have both electrical and magnetic charges are called dyons. Extremal dyonic black holes are those that carry minimum mass for a given set of charges. So, regarding them as states in superstring theory its easy to see that they saturate the BPS bound, and hence a BPS state which can be counted at weakly coupling and reliably extrapolated to strong coupling. Therefore counting

¹A $\frac{1}{2}$ -BPS state is annihilated by half of these supercharges while a $\frac{1}{4}$ -BPS is annihilated by one-fourth of them.

the degeneracy of this class of black hole is an important problem which can give insight into the non-perturbative aspect of the theory. A degeneracy counting formula for such an extremal dyonic black hole in four dimensional $\mathcal{N} = 4$ string theory was proposed by [16]. In this formula, degeneracy is generated by the inverse of a Siegel modular form of $Sp(2, Z)$. This modular form has well defined modular transformation properties under the group $Sp(2, Z)$ and is invariant under the subgroup of $Sp(2, Z)$, which is isomorphic to $SL(2, Z)$. The degeneracy is extracted from this inverse modular form by taking its Fourier transform. The leading order degeneracy, in the large charge expansion, must be equal to the Bekenstein-Hawking entropy. The question arises as to what structures in gravity correspond to these subleading terms. This problem is intimately connected with the idea of curve of marginal stability, as we explain now. The zeroes of the modular form are poles of the integrand and the residues of these poles cause discrete jumps in the degeneracy formula [10, 11, 14] as we vary the parameters of the theory. It was argued that this change in degeneracy corresponds to appearance and disappearance of a two-centered $\frac{1}{2}$ -BPS black hole along with the original single-centered solution. [10, 13, 14, 15] The single-centered solutions exist everywhere in the moduli space while the two-centered ones can decay on “curves of marginal stability”. Hence information about curve of marginal stability can potentially throw light on the various states in string theory that contribute to the counting formula and their supergravity realization.

A black hole in 4-dimensions is uniquely characterized by its angular momentum, mass and electric and magnetic charges. However we will see that instead of each charge component, the properties of a black hole depend on certain parameters which can be constructed out of these charges. These parameters are invariant under the dualities of the theory and hence play an important role in defining the entropy. For given electric and magnetic charge vectors q_e and q_m , one can combine them as

$$q = \begin{pmatrix} q_e \\ q_m \end{pmatrix} \quad (1.3)$$

Both q_e and q_m are Lorentzian vectors which lie in $\Gamma^{22,6}$ Narain lattice. There are three quadratic combinations $q_e^2, q_m^2, q_e \cdot q_m$ which are invariant under $O(22, 6; Z)$

transformations. It was shown that the partition function that counts the degeneracies of dyonic black holes is given in terms of the Igusa cusp form which is a modular form of weight ten of the group $Sp(2, Z)$. It depends on three complex variables with a Fourier expansion given by :

$$\frac{1}{\Phi_{10}(p, q, l)} = \sum c(m, n, l) p^m q^n y^l \quad (1.4)$$

Where sum is over $m, n \geq -1$ and $l \in Z$. Then the degeneracies is given in terms of the Fourier coefficients:

$$d(\Gamma) = c(q_e^2/2, q_m^2/2, q_e \cdot q_m) \quad (1.5)$$

This calculation requires an integration over a three real dimensional subspace of the Seigel upper half plane where the integrand involves the inverse of the above mentioned modular form. However as this integrand develops poles at different points in the parameter space and whenever these poles are crossed, the degeneracy picks up an extra contribution. The degeneracy of these black holes depends on the charges and the moduli fields at infinity. This jump in the entropy indicated the presence of curves of marginal stability in the moduli space at which the black holes become marginally stable. These marginal curves were studied in detail for the case where product black holes were both $\frac{1}{2}$ BPS[13]. The curve of marginal stability for this case are of codimension 1.

We studied this phenomenon of marginal dyon decay for the cases where either one or both of the products were $\frac{1}{4}$ BPS. This led to the generalization of the equation of marginal curve. Since the products have less supersymmetry in this case, extra constraints have to be imposed on the moduli fields. Because of the extra constraints the codimension of the curve in this case is two or more and hence can be avoided in the moduli space. Therefore these decay modes are called "rare decays" and they do not lead to any discrete jumps in the entropy of the system. We did an intensive study of these rare decay modes and derived the formula for the marginal curve. We also extended this work to the case where the original dyon decays into an N-centered dyon. These are also rare decays and do not change the entropy. We found the maximum codimension of the curve for any given decay process and our investigation completes the study of a $\frac{1}{4}$ -BPS dyon

decay. We also discovered a kinematic analogy for the dyon decay phenomenon and using this analogy we derived the curve of marginal stability in a somewhat different way.

There is an alternate string network representation to study the dynamics of a $\frac{1}{4}$ BPS dyonic state. It was shown that supersymmetric string theories have a stable configuration in which three strings of different type meet in a plane. If the three strings are of type (p_i, q_i) , $(1 \leq i \leq 3)$, where p and q are the magnetic and electric charges respectively, then the charge conservation requires:

$$\sum_i^3 p_i = \sum_i^3 q_i = 0 \quad (1.6)$$

The angles between different strings are adjusted such that the net force on the vertex due to the tensions between different strings cancel. It $T_{p,q}$ denotes the tension of the (p, q) string and n_i denotes the direction of the i_{th} string meeting at the vertex, then we must have

$$\sum_i^3 T_{p,q} n_i = 0 \quad (1.7)$$

It was proved that such a configuration satisfies BPS condition. Now given such a configuration, a string network is constructed by joining many of these vertices together with above equations satisfied at each vertex. We did a thorough study of these string networks of arbitrary torsion. The mass of a general dyonic state can be looked at as a product of the string tension and the length of string network. We elaborated this geometric way of deriving the mass formula for a $\frac{1}{4}$ BPS dyonic state. The marginal decay of a dyon occurs when one of the intermediate strings in the network vanishes. The lengths of different strings can be written as a function of the torus modular parameter. As this length shrinks to zero, the string network breaks into two disjoint networks. This is exactly the same process of a $\frac{1}{4}$ BPS dyon marginally decaying into two different dyons. Therefore the constraint which makes the length vanish is same as the constraint of marginal equation. We further provided a complete classification procedure for periodic string networks, in the process re-deriving and extending some of the considerations in Ref.[11].

Chapter 2

Decay of Dyonic black holes

In this chapter we study general two-body decays of arbitrary torsion $\frac{1}{4}$ -BPS dyons in four-dimensional type IIB string compactifications. We find a “master equation” for marginal stability that generalizes the curve found by Sen for $\frac{1}{2}$ -BPS decay, and analyze this equation in a variety of cases including decays to $\frac{1}{4}$ -BPS products. For $\frac{1}{2}$ -BPS decays, an interesting and useful relation is exhibited between walls of marginal stability and the mathematics of Farey sequences and Ford circles. We exhibit an example in which two curves of marginal stability intersect in the interior of moduli space.

2.1 Introduction

In the last couple of years there has been renewed interest in the properties of dyonic black holes in four dimensions, particularly those associated to $\mathcal{N} = 4$ compactifications (type II strings on $K3 \times T^2$ or heterotic/type I strings on T^6 , as well as supersymmetry-preserving orbifolds of these systems) [1, 3, 4, 5, 6, 7, 8, 9, 10, 11, 12, 13, 14, 15]. A key advance has been a better understanding of a classic degeneracy formula due to Dijkgraaf, Verlinde and Verlinde[16]¹. This DVV counting formula was a conjecture based on some essential requirements that the answer was required to satisfy, including reduction to the correct formula for purely electric states, duality invariance and a suitable asymptotic growth. In

¹This formula really computes a supersymmetric index, and in what follows when we say “degeneracy” we will always be referring to this index

more recent times this result has been put on a firmer footing by using dualities involving M-theory, namely the 4d-5d connection[1] and the duality between M-theory on $K3$ and the heterotic string[3]. Among other things, the generalization of this formula to CHL orbifolds and the origin of a genus-2 modular form have been illuminated in many of these works.

However this formula has been considerably refined from its original form. To start with any such formula must satisfy the symmetries of the theory. The symmetry group of the theory under consideration is a 4 dimensional U-duality group. This can be expressed as the product of a T-duality and a S-duality group. The T-duality group keeps the norms of the electric charges and magnetic charges as well as their inner product fixed. While the S-duality group keeps only one quartic combination of the T-duality invariants fixed. The degeneracy formula is expressed in terms of the T-duality invariants. S-duality of course changes the argument of the degeneracy formula but also changes the moduli and the contour of integration which depends upon the moduli and the T-duality invariants. On deforming the new contour to the old one a residue corresponding to poles that the partition function might have, are picked up. Hence degeneracy specification includes specifying the integration contour in the degeneracy formula and noting that different contours can lead to different answers for the degeneracy [10, 11]. The effect of varying the integration contours is in the form of discontinuous jumps in the degeneracy whenever the contour crosses a pole in the integration variable and picks up the corresponding residue. This has been interpreted as due to the decay of some $\frac{1}{4}$ -BPS dyons into a pair of $\frac{1}{2}$ -BPS dyons at curves of marginal stability, which are computed using the BPS mass formula.

Because for large charges the decaying states are black holes, a mechanism is needed to explain exactly how these decay on curves of marginal stability. The answer turns out to be [13, 14] that $\frac{1}{4}$ -BPS black holes (for a given set of charges) exist both in single-centre and multi-centre varieties. For the latter, the separations of the centres are determined by the moduli [25]. If we specialize to two-centred dyons with both centres being $\frac{1}{2}$ -BPS, then it was shown in Ref.[13] that as we approach a curve of marginal stability the two centres fly apart to infinity. On the other side of the curve the constraint equation has no solutions. This explains (in principle, though no method is known to explicitly count states

of a two-centred black hole) the phenomenon of marginal stability and jumping in the counting formula, in terms of the disintegration of two-centred black holes. It should be noted that the degeneracy of single-centred black holes with the same charges does not vary across moduli space, therefore they exist either everywhere or nowhere.

In these developments, the only type of marginal decay that plays a role is into two $\frac{1}{2}$ -BPS final states. Also, the only multi-centred black holes needed to complete the explanation are those with a pair of $\frac{1}{2}$ -BPS centres. Though the correspondence between these two situations was derived for some special cases, it is believed to hold in general, namely for any charge vectors and any point in the entire $\frac{SL(2)}{U(1)} \times \frac{SO(6,22)}{SO(6) \times SO(22)}$ moduli space of $\mathcal{N} = 4$ compactifications.

Recent work has focused on the issue of marginal stability of these dyons. Curves of marginal stability for specific decays have been obtained[10], the impact of such decays on the degeneracy formula has been studied[10, 11, 14] and the decays across such walls have been identified with the disappearance of two-centred black holes from the spectrum[13, 14], following previous ideas in the $\mathcal{N} = 2$ context[17]. A formula has been proposed in [14] to count the “immortal” dyons which exist everywhere. And very recently, Sen has considered the case of unit torsion dyons decaying into $\frac{1}{4}$ -BPS states[15] and demonstrated that this takes place only on surfaces of codimension 2 or more in moduli space.

In the present chapter we take a step towards resolving the first problem. We consider the most general decay of a $\frac{1}{4}$ -BPS dyon into two decay products, each one of which can be either $\frac{1}{2}$ - or $\frac{1}{4}$ -BPS. We find a necessary condition for marginal two-body decays and study the resulting equation in a variety of cases. It turns out that some solutions of our equation are “spurious” in the sense that they describe an inverse decay process rather than the forward decay. This puts constraints on the possible decay products which are identical to those found in [15]. We are also able to reproduce some of the results in Refs.[10] as a special case, as well as generalize them to the case of higher torsion dyons. On the way we will see that a known mathematical construction, that of Farey sequences and Ford circles, bears a remarkably close relation to the circles of marginal stability in Ref.[10] and helps us understand the properties of these circles.

2.2 The system

We consider type IIB string theory first compactified on $K3$. This is a very special background, being chiral and half-maximally supersymmetric in six dimensions. In this background there are no 1-form gauge fields, and therefore no BPS particles. However, there are 26 2-form fields in six dimensions, of which 5 are self-dual and the remaining anti-self-dual. Correspondingly there is a spectrum of charged BPS strings. These can be enumerated as follows: the NS-NS field B and the RR field $C^{(2)}$ in 10d each reduce to a 2-form in 6d that can be decomposed into its self-dual and anti-self-dual parts. The self-dual RR 4-form $C^{(4)}$ in 10d can be decomposed over each of the 22 2-cycles of $K3$. The resulting 2-forms in 6d are self-dual or anti-self-dual depending on which cycle of $K3$ they come from: as is well known, there are 3 self-dual and 19 anti-self-dual 2-cycles of $K3$. The corresponding charged objects arise as follows: two strings correspond to the F-string and D-string in 10d, two more come from the NS5 and D5-branes wrapped over $K3$, and another 22 from D3-branes wrapping the 2-cycles of $K3$. With these 26 charged objects one can construct a 26-component charge vector \vec{Q} with integer entries. For a given charge vector, a $\frac{1}{2}$ -BPS string with those charges exists if $\vec{Q}^2 \geq -2$. Since 2-forms in 6d are decomposable into their self-dual and anti-self-dual parts, the same is true of the strings. The strings arising from F1, D1, NS5 and D5 can be combined into $F1 \pm NS5$ and $D1 \pm D5$, which can be thought of as bound-state strings that are self-dual (for plus signs) and anti-self-dual (for minus signs). The remaining 22 strings are directly self-dual or anti-self-dual depending on the cycle over which they are wrapped.

We further compactify the theory on a T^2 . The resulting four-dimensional system has 28 $U(1)$ gauge fields as elaborated above and their electric-magnetic duals. Therefore we can have dyons of charge (\vec{Q}, \vec{P}) where the first entry is a 28-component vector denoting electric charge under these gauge fields and the second denotes the magnetic charge. The dyons will be $\frac{1}{2}$ -BPS if the vectors \vec{Q}, \vec{P} are parallel, and $\frac{1}{4}$ -BPS otherwise.

Note that a modular transformation of the 2-torus T^2 that changes its modular parameter as:

$$\tau \rightarrow \frac{a\tau + b}{c\tau + d} \quad (2.1)$$

with

$$\begin{pmatrix} a & b \\ c & d \end{pmatrix} \in PSL(2, Z) \quad (2.2)$$

sends the dyon charges to:

$$\begin{pmatrix} \vec{Q} \\ \vec{P} \end{pmatrix} \rightarrow \begin{pmatrix} a\vec{Q} + b\vec{P} \\ c\vec{Q} + d\vec{P} \end{pmatrix} \quad (2.3)$$

We are interested in the marginal decays of these $\frac{1}{4}$ -BPS dyons. The stability or otherwise is dictated by the charges carried by the dyons as well as the values of the moduli of $K3 \times T^2$. These are encoded as follows. Define the matrix:

$$L \equiv \text{diag}(1^6; (-1)^{22}) \quad (2.4)$$

In 4 dimensions there are, first of all, vevs of 132 moduli at infinity can be assembled into a matrix M that is symmetric and orthogonal with respect to the L metric:

$$M^T = M, \quad M^T L M = L \quad (2.5)$$

The relevant inner product for an electric charge vector, which we will call Q^2 or $\vec{Q} \cdot \vec{Q}$, is¹:

$$Q^2 \equiv \vec{Q}^T (M + L) \vec{Q} \quad (2.6)$$

Correspondingly we have:

$$\begin{aligned} P^2 &\equiv \vec{P}^T (M + L) \vec{P} \\ P \cdot Q &\equiv \vec{P}^T (M + L) \vec{Q} \end{aligned} \quad (2.7)$$

We will also make use of the quantities \vec{Q}_R, \vec{P}_R defined such that

$$Q_R^2 \equiv \vec{Q}_R^T \vec{Q}_R = \vec{Q}^T (M + L) \vec{Q} \quad (2.8)$$

and similarly for the other inner products (for details see for example [14, 15]).

In addition to the moduli appearing in M , there is the modular parameter of the 4-5 torus:

$$\tau = \tau_1 + i\tau_2 \quad (2.9)$$

¹Because our focus is on microstates, our inner products are always defined with respect to the moduli at infinity, so this notation should not cause confusion.

2.3 Decays into a pair of dyons

The BPS mass formula for general $\frac{1}{4}$ -BPS dyons is [18, 48]:

$$M_{\text{BPS}}(\vec{Q}, \vec{P})^2 = \frac{1}{\sqrt{\tau_2}}(\vec{Q} - \bar{\tau}\vec{P}) \cdot (\vec{Q} - \tau\vec{P}) + 2\sqrt{\tau_2}\sqrt{\Delta(\vec{Q}, \vec{P})} \quad (2.10)$$

where

$$\Delta(\vec{Q}, \vec{P}) \equiv Q^2 P^2 - (P \cdot Q)^2 \quad (2.11)$$

Before going on, it is useful to transform the dyon charges to bring them into a standard form. Consider the electric and magnetic charge vectors \vec{Q}, \vec{P} of the dyon and define[11]:

$$I(\vec{Q}, \vec{P}) \equiv \gcd(\vec{Q} \wedge \vec{P}) = \gcd(Q^i P^j - Q^j P^i), \text{ all } i, j \quad (2.12)$$

If for a given dyon we find that $I(\vec{Q}, \vec{P}) > 1$, we first perform an $SL(2, Z)$ transformation as in Eq. (2.3). Using some properties of finitely generated algebras (see for example Ref.[19], Chapter I, Section 8), we can always find such a transformation¹ that yields new dyon charges of the form $(m\vec{Q}', n\vec{P}')$ for some positive integers m, n and some new vectors \vec{Q}', \vec{P}' such that $I(\vec{Q}', \vec{P}') = 1$. Under this transformation $I(\vec{Q}, \vec{P})$ remains invariant, so m, n must be such that $I(\vec{Q}, \vec{P}) = mn$. If the m, n so obtained are not co-prime then the dyon with those m, n will be marginally unstable at all points of moduli space. This does not mean a bound state does not exist, but that determining its existence is more subtle and requires actually quantizing the system. Therefore we will restrict ourselves to the case where m, n are co-prime.

To summarize, in what follows we assume that our dyons have charge vectors $(m\vec{Q}, n\vec{P})$ with co-prime m, n and with $I(\vec{Q}, \vec{P}) = 1$. The special case $(m, n) = (1, 1)$ will be called a *unit torsion* dyon.

2.3 Decays into a pair of dyons

We can now examine the decay of a $\frac{1}{4}$ -BPS dyons into two other dyons. From charge conservation, the most general decay is of the form:

$$\begin{pmatrix} m\vec{Q} \\ n\vec{P} \end{pmatrix} \rightarrow \begin{pmatrix} \vec{Q}_1 \\ \vec{P}_1 \end{pmatrix} + \begin{pmatrix} m\vec{Q} - \vec{Q}_1 \\ n\vec{P} - \vec{P}_1 \end{pmatrix} \quad (2.13)$$

¹We are grateful to Nitin Nitsure for helpful discussions on this point.

where \vec{Q}_1, \vec{P}_1 are arbitrary vectors in the (6, 22)-dimensional integral charge lattice.

From the study of BPS string junctions and networks[20, 21, 22], we know that the decay products can be mutually BPS with each other and with the initial state only if the corresponding charges all lie in a plane rather than being generic 28-dimensional vectors as above. However, the properties of the networks are determined in the present context not by the charge vectors \vec{Q}, \vec{P} but by their projections \vec{Q}_R, \vec{P}_R . Indeed it is only the latter which appear in the BPS mass formula Eq. (2.10) that we will be using. Therefore the BPS condition requires that the R projections of the final-state charges are in the same plane as those of the initial-state charges. This happens automatically in some cases, while in others it requires adjusting the moduli in M to make this happen.

It follows that we must have the relation:

$$\begin{pmatrix} m\vec{Q}_R \\ n\vec{P}_R \end{pmatrix} \rightarrow \begin{pmatrix} m_1\vec{Q}_R + r_1\vec{P}_R \\ s_1\vec{Q}_R + n_1\vec{P}_R \end{pmatrix} + \begin{pmatrix} m_2\vec{Q}_R + r_2\vec{P}_R \\ s_2\vec{Q}_R + n_2\vec{P}_R \end{pmatrix} \quad (2.14)$$

where the coefficients m_i, n_i, r_i, s_i satisfy:

$$m_1 + m_2 = m, \quad n_1 + n_2 = n, \quad r_1 + r_2 = s_1 + s_2 = 0 \quad (2.15)$$

We cannot, however, assume that these coefficients are integers since the above equation refers not to the original vectors in the integral lattice but to their projections to the \vec{Q}_R, \vec{P}_R plane.

Without any additional conditions on these coefficients the decay products will both be $\frac{1}{4}$ -BPS dyons. It is possible to have one or both of them be $\frac{1}{2}$ -BPS by suitably constraining the integers, as we will see shortly.

If M, M_1, M_2 denote the BPS masses of the initial state and the two decay products (for simplicity we henceforth drop the subscript *BPS*), we can use Eqs.(2.10) and (2.14) to evaluate the condition on the moduli imposed by the marginality condition $M = M_1 + M_2$. Because of the square root in Eq. (2.10), this is most easily done by computing a combination of squared masses that vanishes when the marginality condition is satisfied.

2.3 Decays into a pair of dyons

First, define the angles θ and θ_{12} by:

$$\begin{aligned}\theta &= \tan^{-1} \frac{\tau_2}{\tau_1} \\ \theta_{QP} &= \cos^{-1} \frac{Q_R \cdot P_R}{Q_R P_R}\end{aligned}\tag{2.16}$$

where $Q_R \equiv |\vec{Q}_R|$, $P_R \equiv |\vec{P}_R|$. Geometrically, θ is the opening angle of the torus while θ_{QP} is the angle between the projected electric and magnetic charge vectors (which coincides with the angle appearing in the string junction description of the dyon). We also define a ‘‘cross-product’’ between the integers m_1, n_1, m_2, n_2 as:

$$m \wedge n = m_1 n_2 - m_2 n_1\tag{2.17}$$

Let us now find the condition that, at some point(s) in moduli space, the decay Eq. (2.14) becomes marginal: $M = M_1 + M_2$. The BPS formula Eq. (2.10) involves a square root on the RHS and another square root to extract M from M^2 . The simplest square-root-free expression that vanishes when the marginality condition is satisfied is the combination:

$$\begin{aligned}M^4 + M_1^4 + M_2^4 - 2(M^2 M_1^2 + M^2 M_2^2 + M_1^2 M_2^2) \\ = (M - M_1 - M_2)(M + M_1 + M_2)(M - M_1 + M_2)(M + M_1 - M_2)\end{aligned}\tag{2.18}$$

Now we require this expression to vanish. However, subsequently we must check that on the vanishing curve, it is really the first factor of the RHS of Eq. (2.18) that vanishes rather than any of the other factors. Notice that the second factor never vanishes (since all the M 's are positive), while vanishing of the third or fourth factor corresponds to the inverse decays $M_1 = M + M_2$ and $M_2 = M + M_1$. When we turn to a detailed analysis of marginal decay processes, it will be necessary to rule out these inverse decays before concluding that we are dealing with the correct decay mode. Only in the case where both the final products are $\frac{1}{2}$ -BPS, this check becomes unnecessary because the reverse process is forbidden: a $\frac{1}{2}$ -BPS state cannot decay into a $\frac{1}{4}$ -BPS state.

Now we use the BPS mass formula Eq. (2.10), the formula for the decay process Eq. (2.14), and the definitions of the angles in Eq. (2.16), to find

2.3 Decays into a pair of dyons

after a tedious calculation that:

$$\begin{aligned}
 M^4 + M_1^4 + M_2^4 - 2(M^2 M_1^2 + M^2 M_2^2 + M_1^2 M_2^2) = & -4\tau_2^2 \left[Q_R P_R \frac{\sin(\theta + \theta_{QP})}{\sin \theta} m \wedge n \right. \\
 & \left. + r_1 P_R \left(m Q_R \frac{\sin \theta_{QP}}{|\tau| \sin \theta} + n P_R \right) - s_1 Q_R \left(n P_R \frac{|\tau| \sin \theta_{QP}}{\sin \theta} + m Q_R \right) \right]^2 \quad (2.19)
 \end{aligned}$$

Vanishing of the RHS is a necessary condition for marginal stability.

This condition can be usefully rewritten by eliminating the angles θ, θ_{QP} and reverting to τ_1, τ_2 coordinates for the modular parameter of the torus. It is convenient to introduce the following quantity depending on charges of the initial and final states as well as the moduli:

$$\mathcal{E} \equiv \frac{1}{\sqrt{\Delta}} \left(\vec{Q}^{(1)} \circ \vec{P} - \vec{P}^{(1)} \circ \vec{Q} \right) \quad (2.20)$$

Interestingly the numerator of this quantity is the Saha angular momentum between one of the final-state dyons and the initial state, evaluated with respect to the moduli at infinity. Now we find that the equation for marginal stability is:

$$\left(\tau_1 - \frac{m \wedge n}{2ns_1} \right)^2 + \left(\tau_2 + \frac{\mathcal{E}}{2ns_1} \right)^2 = \frac{1}{4n^2 s_1^2} \left((m \wedge n)^2 + 4mnr_1 s_1 + \mathcal{E}^2 \right) \quad (2.21)$$

This is the ‘‘master equation’’ governing all two-body decays of $\frac{1}{4}$ -BPS states in this theory. However we will need careful analysis to see when the equation does actually describe such a decay and what type of decay it describes.

Note first of all that the equation is invariant under the transformation:

$$r_1 \rightarrow r_2 = -r_1, \quad s_1 \rightarrow s_2 = -s_1, \quad m_1 \rightarrow m_2 = m - m_1, \quad n_1 \rightarrow n_2 = n - n_1 \quad (2.22)$$

under which $m \wedge n$ and \mathcal{E} both change sign. This corresponds to interchange of the two decay products.

If the RHS of Eq. (2.21) can be shown to be positive definite, this will be a circle in the torus moduli space with centre at:

$$(\tau_1, \tau_2) = \left(\frac{m \wedge n}{2ns_1}, -\frac{\mathcal{E}}{2ns_1} \right) \quad (2.23)$$

2.3 Decays into a pair of dyons

and radius

$$\frac{1}{2ns_1} \sqrt{(m \wedge n)^2 + 4mnr_1s_1 + \mathcal{E}^2} \quad (2.24)$$

Because there is no restriction on the signs of r, s , it may appear that the RHS of Eq. (2.21) is not positive definite. However, after a little computation we are able to rewrite it as:

$$\begin{aligned} (m \wedge n)^2 + 4mnr_1s_1 + \mathcal{E}^2 &= \frac{1}{\Delta} \left([(m \wedge n)Q_R P_R - (ms_1 Q_R^2 - nr_1 P_R^2) \cos \theta_{QP}]^2 \right. \\ &\quad \left. + (ms_1 Q_R^2 + nr_1 P_R^2)^2 \sin^2 \theta_{QP} \right) \end{aligned} \quad (2.25)$$

which is a sum of squares. Therefore the equation does indeed describe a non-trivial circle in every case.

The next step is to check whether this circle intersects the upper half-plane. There are two cases. If $\frac{\mathcal{E}}{s_1} > 0$ then the centre of the circle is in the lower half plane. The circle will then intersect the upper half plane only if it intersects the real axis, which happens if:

$$(m \wedge n)^2 + 4mnr_1s_1 > 0 \quad (2.26)$$

It is easy to see that:

$$(m \wedge n)^2 + 4mnr_1s_1 = \text{tr} \mathbf{F}^2 - 2 \det \mathbf{F} \quad (2.27)$$

where

$$\mathbf{F} = \begin{pmatrix} nm_1 & nr_1 \\ ms_1 & mn_1 \end{pmatrix} = \begin{pmatrix} n & 0 \\ 0 & m \end{pmatrix} \begin{pmatrix} m_1 & r_1 \\ s_1 & n_1 \end{pmatrix} \quad (2.28)$$

Now if α_1, α_2 are the eigenvalues of \mathbf{F} then:

$$\text{tr} \mathbf{F}^2 - 2 \det \mathbf{F} = (\alpha_1 - \alpha_2)^2 \quad (2.29)$$

This is positive if α_1, α_2 are both real, and negative if they are complex conjugate pairs. Therefore when $\frac{\mathcal{E}}{s_1}$ is positive, only decays for which the eigenvalues of \mathbf{F} are real can produce genuine curves of marginal stability in the upper half plane of τ -space.

If $\frac{\mathcal{E}}{s_1} < 0$ then the circle has its centre in the upper half plane, and therefore always has a finite region in the upper half-plane.

2.4 Analysis of the marginal stability curves: $\frac{1}{2}$ -BPS decay products

2.4.1 Equations of the curves

To analyze the equation of marginal stability we have obtained, let us first consider the special case when both decay products are $\frac{1}{2}$ -BPS. This requires that the electric and magnetic charge vectors of the decay products be proportional. The equation for the charges of the decay products Eq. (2.13) can now be written:

$$\begin{pmatrix} m\vec{Q} \\ n\vec{P} \end{pmatrix} \rightarrow \begin{pmatrix} m_1\vec{Q} + r_1\vec{P} \\ s_1\vec{Q} + n_1\vec{P} \end{pmatrix} + \begin{pmatrix} m_2\vec{Q} + r_2\vec{P} \\ s_2\vec{Q} + n_2\vec{P} \end{pmatrix} \quad (2.30)$$

with m_i, n_i, r_i, s_i satisfying:

$$m_1 + m_2 = m, \quad n_1 + n_2 = n, \quad r_1 + r_2 = s_1 + s_2 = 0 \quad (2.31)$$

and where the electric and magnetic (upper and lower) components of each charge vector are proportional to each other. Note that this is the equation for the full, rather than projected, charge vector. The absence of any term out of the plane of \vec{Q}, \vec{P} comes from the fact that if such a term were present, it would be impossible to make the electric and magnetic charges proportional in *both* decay products. Because the above equation is for the full charge vectors, integrality of the charge lattice requires that m_i, r_i, s_i, n_i are integers. In case all four integers (for each i) have a common factor then the decay will be into three or more final states. Since we want to focus on two-body decays, we should exclude such cases.

Proportionality of electric and magnetic charges is equivalent to requiring that the determinant of the associated matrices vanish:

$$\det \begin{pmatrix} m_1 & r_1 \\ s_1 & n_1 \end{pmatrix} = 0 \quad (2.32)$$

and

$$\det \begin{pmatrix} m - m_1 & -r_1 \\ -s_1 & n - n_1 \end{pmatrix} = 0 \quad (2.33)$$

2.4 Analysis of the marginal stability curves: $\frac{1}{2}$ -BPS decay products

The first of these equations is solved by the substitution:

$$\begin{pmatrix} m_1 & r_1 \\ s_1 & n_1 \end{pmatrix} = \begin{pmatrix} ad & -ab \\ cd & -bc \end{pmatrix} \quad (2.34)$$

where a, b, c, d are defined only upto an overall reversal of sign. The second equation then tells us that

$$mn + bc m - ad n = 0 \quad (2.35)$$

Suppose now that the original dyon had unit torsion, namely $(m, n) = (1, 1)$. In this case Eq. (2.35) becomes

$$ad - bc = 1 \quad (2.36)$$

and therefore the decay products are parametrised by a matrix in $PSL(2, Z)$. In going to the coefficients a, b, c, d , we see that they are invariant under the scaling $a, b, c, d \rightarrow \lambda a, \lambda^{-1}b, \lambda c, \lambda^{-1}d$ as well as an exchange $a, b, c, d \rightarrow -b, a, -d, c$. These transformations, along with Eq. (2.36) can be used to show that a, b, c, d are unique integers[10].

Making the substitutions $(m, n) = (1, 1)$ as well as Eq. (2.34) in the curve of marginal stability Eq. (2.21), and using the $PSL(2, Z)$ property, we find that the curve reduces to:

$$\left(\tau_1 - \frac{ad + bc}{2cd}\right)^2 + \left(\tau_2 + \frac{\mathcal{E}}{2cd}\right)^2 = \frac{1}{4c^2d^2} (1 + \mathcal{E}^2) \quad (2.37)$$

where

$$\mathcal{E} \equiv \frac{1}{\sqrt{\Delta}} (cdQ^2 + abP^2 - (ad + bc)Q \cdot P) \quad (2.38)$$

This is the equation found by Sen in Ref.[10].

These curves are circles with centre at $\frac{ad+bc}{2cd}$ and radius $\frac{\sqrt{1+\mathcal{E}^2}}{2cd}$. They intersect the real axis in the pair of points

$$\frac{b}{d}, \frac{a}{c} \quad (2.39)$$

Sen showed that, for unit torsion dyons, two different curves never intersect in the upper half plane but can touch on the real axis in τ -space. This implies that

2.4 Analysis of the marginal stability curves: $\frac{1}{2}$ -BPS decay products

a given unit torsion $\frac{1}{4}$ -BPS dyon can at most be marginally unstable to decay into a single definite pair of $\frac{1}{2}$ -BPS dyons at a given point in moduli space.

While the fractions $\frac{b}{d}, \frac{a}{c}$ need not in general be positive or lie between 0 and 1, they can be brought into the form of positive fractions between 0 and 1 by a modular transformation. Suppose for example that $\frac{b}{d}$ does not lie between 0 and 1. Then for some suitable integer N , we define $b' = b - dN$ such that $0 < b' \leq d$. For the same N) we can show that $a' = a - cN$ satisfies $0 < a' \leq c$. As a result, $0 < \frac{a'}{c}, \frac{b'}{d} \leq 1$. The formula for \mathcal{E} above is unchanged under this transformation if we simultaneously re-define $\vec{Q} \rightarrow \vec{Q} - N\vec{P}$, and the curve of marginal stability is invariant if we also send $\tau_1 \rightarrow \tau_1 + N$.

To complete the discussion of decays into $\frac{1}{2}$ -BPS final states, we need to consider the case of dyons that have higher torsion, i.e. $(m, n) \neq (1, 1)$. In this case we can obtain the curve of marginal stability by starting from Eq. (2.21) and making the appropriate substitutions from Eq. (2.34) and Eq. (2.35). The coefficients ad, ab, cd, bc are still integers but they no longer describe a matrix in $PSL(2, Z)$. Instead they satisfy the condition:

$$adn - bcm = mn \tag{2.40}$$

Moreover, one can check that a, b, c, d are not unique in this case. However only the combinations ad, ab, cd, bc actually appear in the curve of marginal stability, so this curve is unique and can be written:

$$\left(\tau_1 - \frac{nad + mbc}{2ncd} \right)^2 + \left(\tau_2 + \frac{\mathcal{E}}{2ncd} \right)^2 = \frac{1}{4n^2c^2d^2} (m^2n^2 + \mathcal{E}^2) \tag{2.41}$$

where

$$\mathcal{E} \equiv \frac{1}{\sqrt{\Delta}} (mcdQ^2 + nabP^2 - (nad + mbc)Q \cdot P) \tag{2.42}$$

This is the most general curve of marginal stability for decay into $\frac{1}{2}$ -BPS dyons.

Examining the curve we find that it intersects the real axis at the points $\frac{a}{c}$ and $\frac{mb}{nd}$. Even though m, n are co-prime, we cannot be sure that mb, nd are co-prime, so the latter fraction is not necessarily reduced to lowest terms. We will discuss the geometry of these curves in a later subsection.

2.4 Analysis of the marginal stability curves: $\frac{1}{2}$ -BPS decay products

2.4.2 Farey fractions and Ford circles

In this subsection we briefly review some mathematical constructions that will facilitate the analysis of the $\frac{1}{2}$ -BPS curves of marginal stability. In the mathematical literature one encounters the notion of a Farey sequence F_n (see for example Ref.[23]). This is the set of all fractions (reduced to lowest terms) with denominators $\leq n$ and taking values in the interval between 0 and 1, arranged in order of increasing magnitude. As an example we have:

$$F_5 = \left\{ \frac{0}{1}, \frac{1}{5}, \frac{1}{4}, \frac{1}{3}, \frac{2}{5}, \frac{1}{2}, \frac{3}{5}, \frac{2}{3}, \frac{3}{4}, \frac{4}{5}, \frac{1}{1} \right\} \quad (2.43)$$

Relevant properties of Farey sequences, for us, are the following (more details can be found in Ref.[23]). For any pair of fractions $\frac{b}{d}$ and $\frac{a}{c}$ that appear consecutively in *any* Farey sequence, we have $ad - bc = \pm 1$. We can always order them so that the sign is positive, therefore $ad - bc = 1$. Given any such pair, a new fraction called the *mediant* is given by:

$$\text{mediant} \left(\frac{b}{d}, \frac{a}{c} \right) \equiv \frac{a+b}{c+d} \quad (2.44)$$

The mediant lies between the two members of the original pair and will occur between them in subsequent Farey sequences. Moreover, if we define

$$\frac{h}{k} = \frac{a+b}{c+d} \quad (2.45)$$

then $hd - kb = 1 = ak - ch$. Thus the fraction $\frac{h}{k}$ will occur after $\frac{b}{d}$ as well as before $\frac{a}{c}$ in some Farey sequence.

The above construction, which is seen to be related to the structure of the discrete group $PSL(2, Z)$, can be geometrically visualized in terms of circles called *Ford circles*. These will turn out to be helpful in understanding the properties of the Sen circles of Eq. (2.37). For a pair of co-prime integers a, c such that $0 \leq \frac{a}{c} \leq 1$, the associated Ford circle[23] $C\left(\frac{a}{c}\right)$ is a circle centred at $\left(\frac{a}{c}, \frac{1}{2c^2}\right)$ with radius $\frac{1}{2c^2}$. It is tangent to the horizontal axis at $\frac{a}{c}$, and can be thought of as “sitting above” this fraction. The size of a Ford circle is inversely proportional to the square of the denominator of the fraction. Accordingly the largest possible Ford circles, above the points $\frac{0}{1}$ and $\frac{1}{1}$, have radius $\frac{1}{2}$.

2.4 Analysis of the marginal stability curves: $\frac{1}{2}$ -BPS decay products

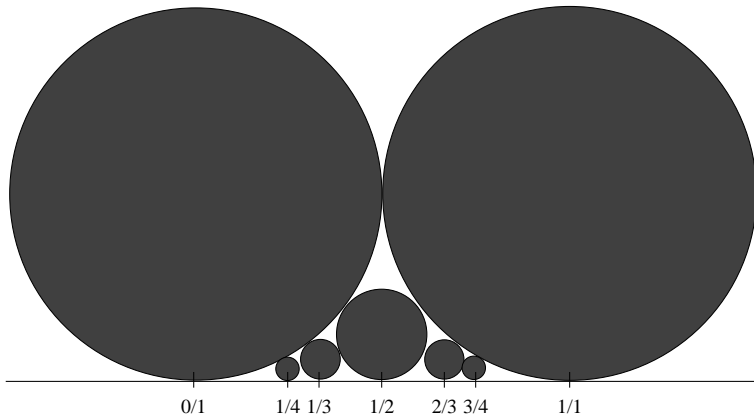


Figure 2.1: The Ford circles associated to F_4

The key property of Ford circles is that (i) two Ford circles never intersect, (ii) two Ford circles associated to the fractions $\frac{b}{a}$ and $\frac{a}{c}$ (without loss of generality we assume the second fraction to be the larger one) are tangent to each other if and only if $ad - bc = 1$. In terms of Farey sequences, if two fractions are consecutive in any Farey sequence then they are associated to a pair of touching Ford circles. Conversely if two Ford circles touch then their corresponding fractions are consecutive in some Farey sequence.

Finally we describe a construction that will be closely related to marginal decays of dyons. For any pair of touching Ford circles associated to fractions $\frac{b}{a}$ and $\frac{a}{c}$ with $ad - bc = 1$, there is another circle that (for lack of a better name) we will refer to as the “dual Ford circle” $\tilde{C}(\frac{b}{a}, \frac{a}{c})$ that is centred on the real axis and passes through the points $\frac{b}{a}$ and $\frac{a}{c}$ on the real axis. This circle has the property that it also passes through the point at which the two Ford circles touch[23].

2.4.3 Analysis of the decays: Sen circles and Ford circles

Now let us return to the decay of a unit torsion $\frac{1}{4}$ -BPS dyon into two $\frac{1}{2}$ -BPS dyons. As we have seen in the previous subsection, the decay products are defined in terms of a matrix in $PSL(2, Z)$. This matrix defines a pair of fractions $\frac{b}{a}$ and $\frac{a}{c}$ with $ad - bc = 1$. By the shift $\tau_1 \rightarrow \tau_1 + N$, as in the discussion below Eq. (2.39), we can make both the fractions lie between 0 and 1. Now the Ford circles associated to these two fractions are tangent to each other. The dual

2.4 Analysis of the marginal stability curves: $\frac{1}{2}$ -BPS decay products

Ford circle $\tilde{C}\left(\frac{b}{d}, \frac{a}{c}\right)$ has its origin on the real axis at the midpoint of these two fractions, at $\frac{ad+bc}{2cd}$. Its radius is given by half the distance between these two fractions, namely $\frac{1}{2cd}$. Thus the equation of this dual Ford circle is:

$$\left(\tau_1 - \frac{ad+bc}{2cd}\right)^2 + \tau_2^2 = \frac{1}{4c^2d^2} \quad (2.46)$$

Comparing with Eq. (2.37), we see that the dual Ford circle is the limit of the Sen circle for marginal decays of a unit torsion $\frac{1}{4}$ -BPS dyon into two $\frac{1}{2}$ -BPS dyons, as $\mathcal{E} \rightarrow 0$. (Recall that \mathcal{E} was defined in Eq. (2.38)). Conversely, the Sen circle can be thought of as a deformation of the dual Ford circle with deformation parameter \mathcal{E} . For given integers a, b, c, d , both circles are centred at the same value of τ_1 but have their centres vertically displaced from each other. The radius of the Sen circle is such that it intersects the real axis in the *same* pair of points as the dual Ford circle. Note that $\frac{\mathcal{E}}{cd}$ can be positive or negative, so the Sen circle can be displaced either downwards or upwards relative to the dual Ford circle.

This similarity is intriguing and may point to a more profound relation between Sen circles and Ford circles that we have not yet uncovered (in particular, it seems plausible that by deforming the K3 moduli one can set $\mathcal{E} \rightarrow 0$, which would make the two circles actually coincide). However, already the relation we have exhibited is sufficient to understand a key property of Sen circles, which is that they do not intersect in the upper half plane, but only on the real axis[10].

This can be seen as follows. Every Sen circle is associated to a dual Ford circle and thereby to a pair of Ford circles. Consider the two Sen circles associated to a, b, c, d and h, p, k, q with $ad - bc = pk - qh = 1$. Clearly we have $\frac{b}{d} < \frac{a}{c}$ as well as $\frac{h}{k} < \frac{p}{q}$. The two possible orderings of the fractions are $\frac{b}{d}, \frac{h}{k}, \frac{a}{c}, \frac{p}{q}$ and $\frac{b}{d}, \frac{a}{c}, \frac{h}{k}, \frac{p}{q}$. The first ordering is ruled out by the Ford circle construction, since it implies that the Ford circle of the first fraction touches that of the third one, while the Ford circle of the second fraction touches that of the fourth one. This contradicts the fact that all the Ford circles are non-overlapping. Thus only the second ordering is possible, where we have the fractions $\frac{b}{d}, \frac{a}{c}, \frac{h}{k}, \frac{p}{q}$ in increasing order. Let us consider the case where $\frac{a}{c} = \frac{h}{k}$, so that the Sen circles touch on the real axis. Clearly the dual Ford circles also touch on the real axis, which means the three fractions $\frac{b}{d}, \frac{a}{c}, \frac{p}{q}$ are consecutive terms in a Farey sequence.

2.4 Analysis of the marginal stability curves: $\frac{1}{2}$ -BPS decay products

We want to show that the Sen circles in this case do not intersect in the upper half plane. This imposes a condition on the slopes of the Sen circles at the real axis. From Eq. (2.37) we find that the slope at the real axis is given by:

$$\tan \phi = \pm \frac{1}{\mathfrak{E}} \quad (2.47)$$

where the two signs hold for the two intersection points. Now it is easy to check that the condition we are seeking is:

$$\mathcal{E}(a, b, c, d) + \mathcal{E}(a, p, c, q) > 0 \quad (2.48)$$

This is of course satisfied if both E 's are positive, though that is not in general the case. But even in the general case the condition above does hold, as we now demonstrate. From the definition of E one finds that:

$$\mathcal{E}(a, b, c, d) + \mathcal{E}(a, p, c, q) = \frac{1}{\sqrt{\Delta}} \left(c(q+d)Q^2 + a(p+b)P^2 - (a(q+d) + c(p+b))P \cdot Q \right) \quad (2.49)$$

Now we use the fact, explained in the discussion around Eq. (2.45), that if three fractions are consecutive in a Farey sequence then the middle one is the mediant of the other two. Hence we have:

$$\frac{a}{c} = \frac{p+b}{q+d} \quad (2.50)$$

from which we get:

$$Na = (p+b), \quad Nc = (q+d) \quad (2.51)$$

for some integer $N \geq 1$. It follows that:

$$\mathcal{E}(a, b, c, d) + \mathcal{E}(a, p, c, q) = \frac{N}{\sqrt{\Delta}} (c\vec{Q} - a\vec{P})^2 > 0 \quad (2.52)$$

as desired. By similar methods the non-intersecting property of Sen circles can be proved for the case where $\frac{b}{d}, \frac{a}{c}, \frac{h}{k}, \frac{p}{q}$ are all distinct fractions.

2.4.4 Analysis of the decays: higher torsion case

The above discussion was for the case of a unit torsion dyon as the initial state. Now let us look at the case where the initial state is a dyon with torsion ≥ 2 . In

2.4 Analysis of the marginal stability curves: $\frac{1}{2}$ -BPS decay products

this case the Sen circle is replaced by Eq. (2.41), which intersects the real axis at the points $\frac{a}{c}$ and $\frac{mb}{nd}$. Let us now analyze the condition Eq. (2.40) in some detail. Because m and n are co-prime, writing this condition as $adn = m(bc + n)$ tells us that m divides ad and also that n divides bc . Therefore we can rewrite Eq. (2.40) as:

$$\frac{ad}{m} - \frac{bc}{n} = 1 \quad (2.53)$$

where each of the terms on the LHS is an integer. This can only be realized if, for some (not necessarily prime or unique) factorization of m and n ;

$$m = pq, \quad n = kl \quad (2.54)$$

we have that:

$$a' = \frac{a}{p}, \quad b' = \frac{b}{k}, \quad c' = \frac{c}{l}, \quad d' = \frac{d}{q} \quad (2.55)$$

are all integers. Evidently they satisfy $a'd' - b'c' = 1$. Substituting in the curve of marginal stability for this case, Eq. (2.41), we find:

$$\left(\tau_1 - \frac{p a' d' + b' c'}{l 2c' d'} \right)^2 + \left(\tau_2 + \frac{p \mathcal{E}'}{l 2c' d'} \right)^2 = \frac{p^2}{4l^2 c'^2 d'^2} (1 + \mathcal{E}'^2) \quad (2.56)$$

where

$$\mathcal{E}' \equiv \frac{mn}{\sqrt{\Delta}} \left(\frac{q}{k} c' d' Q^2 + \frac{k}{q} a' b' P^2 - (a' d' + b' c') Q \cdot P \right) \quad (2.57)$$

This curve intersects the real axis at the points:

$$\frac{p b'}{l d'}, \quad \frac{p a'}{l c'} \quad (2.58)$$

For a fixed value of $\frac{p}{l}$, the set of intersection points is in one to one correspondence with those for the unit torsion case, where using Ford circles (or the methods of Ref.[10]) we saw that curves of marginal stability do not intersect. However the value of $\frac{p}{l}$ is not fixed. For given m, n specifying a higher torsion dyon, Eq. (2.54) permits several solutions for p and l in general. For each of them we obtain a construction in 1-1 correspondence with the set of curves of marginal stability for the unit torsion case, and it appears quite likely that curves from one of these sets can intersect with curves from another set. This would result in curves of marginal stability that intersect each other in the upper half plane.

2.4 Analysis of the marginal stability curves: $\frac{1}{2}$ -BPS decay products

To generate examples, it is convenient to revert to the notation in which the charges of the decay products are labelled by a matrix of integers $\begin{pmatrix} m_1 & r_1 \\ s_1 & n_1 \end{pmatrix}$ satisfying Eqs.(2.32) and (2.33). From these two equations we find that:

$$m_1 n + n_1 m = mn \quad (2.59)$$

from which we see that m_1 is a multiple of m . We write:

$$m_1 = m\alpha_1 \quad (2.60)$$

where α_1 is another integer. The equations now yield the following general form for the matrix:

$$\begin{pmatrix} m_1 & r_1 \\ s_1 & n_1 \end{pmatrix} = \begin{pmatrix} m\alpha_1 & \frac{mn\alpha_1(1-\alpha_1)}{s_1} \\ s_1 & n(1-\alpha_1) \end{pmatrix} \quad (2.61)$$

The strategy is now to choose a value for α_1 and then look for the set of s_1 that divide $mn\alpha_1(1-\alpha_1)$. Finally to ensure that we are dealing with a two-body decay, we must check that there is no overall common factor in either of the matrices

$$\begin{pmatrix} m_1 & r_1 \\ s_1 & n_1 \end{pmatrix}, \quad \begin{pmatrix} m - m_1 & -r_1 \\ -s_1 & n - n_1 \end{pmatrix} \quad (2.62)$$

In this way we can generate a large number of examples of curves of marginal stability for higher torsion dyons decaying into a pair of $\frac{1}{2}$ -BPS dyons.

To check the possible intersections of such curves, we recall that they intersect the real axis in the points $\frac{m_1-m}{s_1}$ and $\frac{m_1}{s_1}$. If two such intervals intersect then the curves will necessarily intersect in the upper half-plane. Let us consider a definite example. Suppose $(m, n) = (2, 3)$. Then choosing $\alpha_1 = 1$, we see that s_1 can be arbitrary. On the other hand choosing $\alpha_1 = 2$ we find that the allowed values of s_1 are 1, 2, 3, 4, 6, 12. It is easy to check that for the very simplest choices the curves do not intersect. However, picking $\alpha_1 = 1, s_1 = 7$ and $\alpha_1 = 2, s_1 = 12$ we find that all the conditions are satisfied and the decay products are given by the matrices:

$$\begin{aligned} \alpha_1 = 1, s_1 = 7 : & \quad \begin{pmatrix} 2 & 0 \\ 7 & 0 \end{pmatrix}, \quad \begin{pmatrix} 0 & 0 \\ -7 & 3 \end{pmatrix} \\ \alpha_1 = 2, s_1 = 12 : & \quad \begin{pmatrix} 4 & -1 \\ 12 & -3 \end{pmatrix}, \quad \begin{pmatrix} -2 & 1 \\ -12 & 6 \end{pmatrix} \end{aligned} \quad (2.63)$$

2.5 Analysis of the marginal stability curves: $\frac{1}{4}$ -BPS decay products

In terms of the integers a, b, c, d the two decay processes are parametrised by the matrices:

$$\begin{aligned} (i) \quad \begin{pmatrix} a & b \\ c & d \end{pmatrix} &= \begin{pmatrix} 2 & 0 \\ 7 & 1 \end{pmatrix} \\ (ii) \quad \begin{pmatrix} a & b \\ c & d \end{pmatrix} &= \begin{pmatrix} 1 & 1 \\ 3 & 4 \end{pmatrix} \end{aligned} \tag{2.64}$$

Each matrix satisfies $3ad - 2bc = 6$.

Now the curves of marginal stability for the two decay modes intersect the real axis at the following values:

$$\begin{aligned} (i) \quad \tau_1 &= 0, \frac{2}{7} \\ (ii) \quad \tau_1 &= \frac{1}{6}, \frac{1}{3} \end{aligned} \tag{2.65}$$

These two intervals are overlapping, hence the associated curves must intersect in the interior of the upper half plane. We conclude that curves of marginal stability for the decay of higher torsion dyons can in general intersect in the upper half plane, unlike what happens for unit torsion dyons. It would be important to understand the physical and mathematical reasons why the curves intersect, as well as the consequences of this fact.

2.5 Analysis of the marginal stability curves: $\frac{1}{4}$ -BPS decay products

2.5.1 Decays into a $\frac{1}{2}$ -BPS and a $\frac{1}{4}$ -BPS dyon

We now consider decays of a $\frac{1}{4}$ -BPS dyon into one $\frac{1}{2}$ -BPS and one $\frac{1}{4}$ -BPS dyon. This is parametrised as in Eq. (2.14). If the first decay product is taken to be $\frac{1}{2}$ -BPS then we must impose the condition Eq. (2.32) which is solved by Eq. (2.34). However, the coefficients m_i, r_i, s_i, n_i are no longer required to be integers and therefore nor are a, b, c, d . Moreover we want the second state to be $\frac{1}{4}$ -BPS and therefore $adn - bcm \neq mn$. Finally, as indicated earlier, we must check that

2.5 Analysis of the marginal stability curves: $\frac{1}{4}$ -BPS decay products

the curve we obtain from Eq. (2.21) actually describes the forward and not the reverse decay process.

Consider the case where the initial state is a unit torsion dyon with $(m, n) = (1, 1)$. For this case we find the curve of marginal stability to be:

$$\left(\tau_1 - \frac{m_1 - n_1}{2s_1}\right)^2 + \left(\tau_2 + \frac{\mathcal{E}}{2s_1}\right)^2 = \frac{1}{4s_1^2} \left((m_1 - n_1)^2 + 4r_1s_1 + \mathcal{E}^2 \right) \quad (2.66)$$

where

$$\mathcal{E} \equiv \frac{1}{\sqrt{\Delta}} (s_1 Q_R^2 - r_1 P_R^2 - (m_1 - n_1) Q_R \cdot P_R) \quad (2.67)$$

On replacing m_1, r_1, s_1, n_1 by their expressions in terms of a, b, c, d we can also bring it to the form:

$$\left(\tau_1 - \frac{ad + bc}{2cd}\right)^2 + \left(\tau_2 + \frac{\mathcal{E}}{2cd}\right)^2 = \frac{1}{4c^2d^2} \left((ad - bc)^2 + \mathcal{E}^2 \right) \quad (2.68)$$

with

$$\mathcal{E} \equiv \frac{1}{\sqrt{\Delta}} (cd Q_R^2 + ab P_R^2 - (ad + bc) Q_R \cdot P_R) \quad (2.69)$$

The equation is very similar to the Sen circle for decays of a unit torsion dyon into $\frac{1}{2}$ -BPS decay products. However, the constraints on a, b, c, d are quite different. Instead of analyzing this case further, we will return to it as a special case of the more general decay into two $\frac{1}{4}$ -BPS states.

2.5.2 Decays into two $\frac{1}{4}$ -BPS dyons

We now address the case in which the initial $\frac{1}{4}$ -BPS dyon decays into a pair of $\frac{1}{4}$ -BPS dyons. Again we start with the unit torsion case, $(m, n) = (1, 1)$. The relevant curve of marginal stability is the same as in the previous subsection, Eq. (2.66), except that the determinants of $\begin{pmatrix} m_i & r_i \\ s_i & n_i \end{pmatrix}$ are both nonzero. (Later we will also be able to specialize to the case where one of them is zero.)

Let us now address the constraints on the final state parameters that are required to ensure that the decay process corresponds to the correct branch of Eq. (2.18). First of all, the quantity Δ that appears in the BPS mass formula

2.5 Analysis of the marginal stability curves: $\frac{1}{4}$ -BPS decay products

Eq. (2.10) involves a square root, and we have taken all square roots to be positive. This has the following consequence. Observe that:

$$\Delta(m_i \vec{Q} + r_i \vec{P}, s_i \vec{Q} + n_i \vec{P}) = \det \begin{pmatrix} m_i & r_i \\ s_i & n_i \end{pmatrix} \Delta(\vec{Q}, \vec{P}) \quad (2.70)$$

Positivity of Δ on both sides of the equation imposes the condition:

$$\det \begin{pmatrix} m_i & r_i \\ s_i & n_i \end{pmatrix} > 0, \quad i = 1, 2 \quad (2.71)$$

Since

$$\begin{pmatrix} m_2 & r_2 \\ s_2 & n_2 \end{pmatrix} = \begin{pmatrix} 1 - m_1 & -r_1 \\ -s_1 & 1 - n_1 \end{pmatrix} \quad (2.72)$$

we find that:

$$m_1 n_1 - r_1 s_1 > \max(m_1 + n_1 - 1, 0) \quad (2.73)$$

For what follows, it will be convenient to introduce the eigenvalues β_1, γ_1 of $\begin{pmatrix} m_1 & r_1 \\ s_1 & n_1 \end{pmatrix}$ and β_2, γ_2 of $\begin{pmatrix} m_2 & r_2 \\ s_2 & n_2 \end{pmatrix}$. Because the two matrices commute (they are of the form \mathbf{F} and $1 - \mathbf{F}$) they can be simultaneously diagonalised, from which we see that:

$$\beta_1 + \beta_2 = 1 = \gamma_1 + \gamma_2 \quad (2.74)$$

From the determinant conditions above, we have:

$$\beta_1 \gamma_1 > 0, \quad (1 - \beta_1)(1 - \gamma_1) > 0 \quad (2.75)$$

We will now examine the quantities $\frac{M_1}{M}, \frac{M_2}{M}$ on the curve Eq. (2.66). For convenience, we would like to choose a particular point on the curve and evaluate these quantities there. The possible results are as follows. If we find $\frac{M_1}{M} > 1$ at a point, then the marginal stability curve cannot correspond to $M = M_1 + M_2$. It may correspond to either $M_1 = M + M_2$ or $M_2 = M + M_1$. Which of the two cases it corresponds to is then not very important, but can be distinguished by looking at $\frac{M_2}{M}$. If on the other hand we find $\frac{M_1}{M} < 1$ then we have the possibilities of being on the correct branch $M = M_1 + M_2$ or on the wrong branch $M_2 = M + M_1$. This time it is essential to distinguish the two, which can again be done by evaluating $\frac{M_2}{M}$. Being on the correct branch requires $\frac{M_i}{M} < 1$ for both $i = 1$ and 2 .

2.5 Analysis of the marginal stability curves: $\frac{1}{4}$ -BPS decay products

In any of these cases, having determined the relevant branch of Eq. (2.18) at one point on the curve, we can be sure that we will not cross over to another branch elsewhere on the same curve, since crossing from one branch to another requires passing through a point where one of the masses vanishes. But the BPS mass formula does not vanish for any value of the moduli, so this is not possible (unless the charges of that state vanish identically).

Let us assume that the matrix $\begin{pmatrix} m_1 & r_1 \\ s_1 & n_1 \end{pmatrix}$ is such that the curve Eq. (2.66) intersects the real axis. This will happen if the eigenvalues β_1, γ_1 are both real (without loss of generality we take $\gamma_1 \geq \beta_1$). Then, a convenient point at which to evaluate the mass ratios is one of the intersection points of the curve with the real axis. Setting $\tau_2 = 0$ in Eq. (2.21), we get the following equation for τ_1 :

$$n_1 - \frac{r_1}{\tau_1} = m_1 - \tau_1 s_1 \quad (2.76)$$

Now let us consider the expression $\frac{M_1^2}{M^2}$ in the limit $\tau_2 \rightarrow 0$. We have:

$$\begin{aligned} \left. \frac{M_1^2}{M^2} \right|_{\tau_2 \rightarrow 0} &= \frac{[(m_1 \vec{Q}_R + r_1 \vec{P}_R) - \tau_1 (s_1 \vec{Q}_R + n_1 \vec{P}_R)]^2}{[\vec{Q}_R - \tau_1 \vec{P}_R]^2} \\ &= \frac{[(m_1 - \tau_1 s_1) \vec{Q}_R - \tau_1 (n_1 - \frac{r_1}{\tau_1}) \vec{P}_R]^2}{[\vec{Q}_R - \tau_1 \vec{P}_R]^2} \end{aligned} \quad (2.77)$$

Using Eq. (2.76) we now get:

$$\left. \frac{M_1}{M} \right|_{\tau_2 \rightarrow 0} = |m_1 - \tau_1 s_1| \quad (2.78)$$

On the real axis, Eq. (2.66) gives:

$$\tau_1 = \frac{1}{2s_1} \left(\pm (\gamma_1 - \beta_1) + (m_1 - n_1) \right) \quad (2.79)$$

Inserting this into Eq. (2.78) we find:

$$m_1 - \tau_1 s_1 = \beta_1 \text{ or } \gamma_1 \quad (2.80)$$

Let us first consider the case $m_1 n_1 - r_1 s_1 > 1$. We will show that in this region the decay is not the desired one, but corresponds instead to a branch of Eq. (2.18)

2.5 Analysis of the marginal stability curves: $\frac{1}{4}$ -BPS decay products

describing a reverse decay. With this condition on the determinant, one of the eigenvalues (say γ_1) must be > 1 . Positivity of the second determinant, which equals $(1 - \beta_1)(1 - \gamma_1)$, tells us that if $\gamma_1 > 1$ then also $\beta_1 > 1$. Thus we have that both eigenvalues are > 1 . It follows that $\frac{M_1}{M} > 1$ and we are, as promised, on the wrong branch.

Next suppose $m_1 n_1 - r_1 s_1 = 1$. The above considerations then show that $\beta_1 = \gamma_1 = 1$. Then we $\frac{M_1}{M} = 1$. This means $M_2 = 0$ and therefore the charges associated to the second state are identically zero. In other words, $\begin{pmatrix} m_1 & r_1 \\ s_1 & n_1 \end{pmatrix} = \begin{pmatrix} 0 & 0 \\ 0 & 0 \end{pmatrix}$. This is a trivial case where the first decay product is the original state itself.

Let us note at this point that if m_1, r_1, s_1, n_1 had been taken to be integers, and the corresponding state was restricted not to be $\frac{1}{2}$ -BPS, we would necessarily have $m_1 n_1 - r_1 s_1 \geq 1$. We have shown that all such cases do not correspond to a valid decay of M into M_1 and M_2 , therefore no such decays exist for integer coefficients. This is one of the key results of Ref.[15].

That leaves the case

$$0 < m_1 n_1 - r_1 s_1 < 1, \quad 0 < m_2 n_2 - r_2 s_2 < 1 \quad (2.81)$$

which can only be satisfied for fractional coefficients.

Requiring $\beta_1 \gamma_1 < 1$ and also $\beta_2 \gamma_2 = (1 - \beta_1)(1 - \gamma_1) < 1$ we see that $0 < \beta_1, \gamma_1 < 1$ and $0 < \beta_2, \gamma_2 < 1$. From this and Eq. (2.80) we find $\frac{M_1}{M} < 1, \frac{M_2}{M} < 1$ and this indeed corresponds to the decay process that we were looking for. Thus Eq. (2.81) provides a necessary condition for the coefficients m_1, n_1, r_1, s_1 in Eq. (2.14) in order to have a decay of the original dyon into two $\frac{1}{4}$ -BPS dyons. Under this condition, our curve Eq. (2.21) describes the marginal stability locus in the τ_1, τ_2 plane. However this is a locus of co-dimension 2 or more in the full moduli space, for the following reason. Fractional m_1, r_1, s_1, n_1 means that the decay process in terms of the original integral charge vectors was into states living outside the \vec{Q}, \vec{P} plane. This is precisely the case, referred to earlier, where the moduli in M need to be adjusted to make the final state charges (after R projection) lie in the same plane as the initial state charges[15]. We will explore

the sufficient conditions on the values of m_1, r_1, s_1, n_1 as well as to understand more precisely the condition on the moduli matrix M which put the projected charge vectors in the plane of the decaying dyon.

2.6 Discussion

We have found a general equation for marginal stability of $\frac{1}{4}$ -BPS dyons to decay into two final state particles, Eq. (2.21). Analysis of the equation reveals many distinct cases with different properties. We will extend this analysis to multi-particle final states in next chapter. The construction of Ford circles and especially their dual circles proved useful in this analysis and we suspect that there may be a deeper mathematical relationship to the Sen circles of marginal instability for unit torsion dyons decaying into $\frac{1}{2}$ -BPS final states.

Chapter 3

Constraints on “rare” dyon decays

After deriving the curve of marginal stability in terms of constraint equation on the torus modular parameter, now we obtain the complete set of constraints on all the moduli of $\mathcal{N} = 4$ superstring compactifications that permit “rare” marginal decays of $\frac{1}{4}$ -BPS dyons to take place. The constraints are analyzed in some special cases. The analysis extends in a straightforward way to multi-particle decays. We will then discuss the possible relation between general multi-particle decays and multi-centred black holes.

3.1 Introduction

In the previous chapter we have analyzed in detail the lines of marginal stability corresponding to decays of $\frac{1}{4}$ BPS states into 2 $\frac{1}{2}$ BPS states. We also saw that there are many more types of marginal decays in the theory, and in one sense they are far more generic. These decays are into a pair of $\frac{1}{4}$ -BPS final states, or into three or more final states each of which can be $\frac{1}{2}$ -BPS or $\frac{1}{4}$ -BPS. In another sense these decays are “rare”, which we also discussed in details in the earlier chapter of this thesis, (at least for unit-torsion initial dyons) that they take place on curves of marginal stability that have a co-dimension > 1 in the moduli space¹.

¹Therefore they should not technically be called “curves”, but we use this terminology anyway and hope it does not cause confusion.

Therefore these have been labelled “rare decays”. In particular they cannot lead to jumps in the degeneracy formula¹. Nevertheless the existence of such decay modes is of importance in understanding the behavior of dyons as we move around in moduli space, and we will study them here for their own sake as well as for possible interesting physical consequences that they may turn out to have.

In previous chapter these curves were precisely characterized as circles in the upper half-plane labelled by the parameter τ corresponding to the $SL(2)/U(1)$ factor of the moduli space². These circles depend on the other moduli as well. However, as was demonstrated in Refs.[15, 26, 27], there are additional conditions that need to be imposed on the remaining moduli in order to make the decay possible. These latter conditions have not yet been worked out. In this chapter we will obtain these conditions and thereby completely characterize the codimension > 1 subspace on which rare decays can take place.

It is also known that there exist multi-centred dyonic black holes with two $\frac{1}{4}$ -BPS centres, or three or more centres each of which can be $\frac{1}{2}$ - or $\frac{1}{4}$ -BPS. However, because the degeneracy formula does not jump at curves of marginal stability, these multi-centred dyons have not played a role in studies of dyons in $\mathcal{N} = 4$ compactifications. In particular they have not been related to marginal decays into two $\frac{1}{4}$ -BPS final states or multiple final states, and in fact such a relation does not seem necessary for the state-counting problem. Nevertheless, in what follows we will argue that the relation between curves of marginal stability and multi-centred black holes flying apart is quite generic.

In what follows, we start by briefly reviewing the “rare” marginal decays in $\mathcal{N} = 4$ compactifications. Then we find a precise form for the constraints on moduli space in order for such rare decays to take place. We examine and solve these constraints in a variety of special cases, to give a flavour of what they look like. Then using some known results on T-duality orbits, we will obtain the constraints in the general case. Next we recursively identify the loci of marginal

¹For higher-torsion initial dyons the curves can be of codimension 1, but the degeneracy (or rather, index) is still not expected to jump, because of fermion zero modes. We will focus largely on unit-torsion dyons in this paper.

²In the type IIB on $K3 \times T^2$ description this τ is the modular parameter of the geometrical torus, hence we sometimes refer to the τ UHP as the “torus moduli space” – although technically it would be more accurate to call it the Teichmüller space of the torus.

stability for multi-particle decays. Finally we examine the special-geometry formula for generic multi-centred black holes and write it in a form that relates their separations to curves of marginal stability for $n \geq 2$ -body decays.

3.2 Marginal stability for $\mathcal{N} = 4$ dyons

The electric and magnetic charge vectors of a dyon in an $\mathcal{N} = 4$ string compactification are elements of a 28 dimensional integral charge lattice of signature (6, 22). The formulae for BPS mass involve a 28×28 matrix L , which in our basis will be taken to be:

$$\begin{pmatrix} 0 & \mathbb{I}_6 & 0 \\ \mathbb{I}_6 & 0 & 0 \\ 0 & 0 & -\mathbb{I}_{16} \end{pmatrix} \quad (3.1)$$

as well as a 28×28 matrix M of moduli satisfying $MLM^T = L$. The inner product of charge vectors appearing in the BPS mass is taken with the matrix $L+M$. In the heterotic basis where the compactification is specified by a constant metric G_{ij} , an antisymmetric tensor field B_{ij} and constant gauge potentials A_i^I (where $i = 1, 2, \dots, 6$ and $I = 1, 2, \dots, 16$), this matrix is [28, 29]:

$$L+M = \begin{pmatrix} G^{-1} & 1 + G^{-1}(B + C) & G^{-1}A \\ 1 + (-B + C)G^{-1} & (G - B + C)G^{-1}(G + B + C) & (G - B + C)G^{-1}A \\ A^T G^{-1} & A^T G^{-1}(G + B + C) & A^T G^{-1}A \end{pmatrix} \quad (3.2)$$

Here C is a symmetric 6×6 matrix constructed from A as $C = \frac{1}{2}A^T A$, more concretely $C_{ij} = \frac{1}{2}A_i^I A_j^I$.

In this basis we parametrise the charge vectors explicitly as:

$$\vec{Q} = \begin{pmatrix} \vec{Q}'_{(6)} \\ \vec{Q}''_{(6)} \\ \vec{Q}'''_{(16)} \end{pmatrix}, \quad \vec{P} = \begin{pmatrix} \vec{P}'_{(6)} \\ \vec{P}''_{(6)} \\ \vec{P}'''_{(16)} \end{pmatrix} \quad (3.3)$$

where we have broken up the original vectors into three parts with 6, 6 and 16 components respectively. In subsequent discussions we will not explicitly write out the subscripts (6), (16) that appear in the above formula.

3.2 Marginal stability for $\mathcal{N} = 4$ dyons

The BPS mass formula for $\frac{1}{4}$ -BPS dyons in $\mathcal{N} = 4$ compactifications was defined in Eq. (2.10). The inner products of charge vectors appearing in mass formula are of the form:

$$Q \circ P \equiv \vec{Q}^T (L + M) \vec{P} \quad (3.4)$$

The matrix $L + M$ has 22 zero eigenvalues and therefore the inner product only contains a projected set of 6 components from the original 28 components of the charge vector. Explicitly, the zero eigenvectors take the form:

$$\begin{pmatrix} G + B + C & A^I \\ -1 & 0 \\ 0 & -1 \end{pmatrix} \quad (3.5)$$

where each column of the above matrix describes an independent zero eigenvector.

It is convenient to replace the inner product on charge vectors in Eq. (3.4) by an ordinary product acting on some projected vectors. To do this, define $\sqrt{L + M}$ as a 28×28 matrix satisfying $\sqrt{L + M}^T \sqrt{L + M} = L + M$. This will be ambiguous upto a ‘‘gauge’’ freedom but we will select a specific solution that is particularly useful, namely:

$$\sqrt{L + M} = \begin{pmatrix} E^{-1} & E^{-1}(G + B + C) & E^{-1}A \\ 0 & 0 & 0 \\ 0 & 0 & 0 \end{pmatrix} \quad (3.6)$$

where E stands for the vielbein: $E_i^a E_i^a = G_{ij}$.

With this matrix it is evident that the projected charges only have their first 6 components nonzero, namely for any arbitrary vectors \vec{Q}, \vec{P} the projected vectors \vec{Q}_R, \vec{P}_R defined by:

$$\vec{Q}_R = \sqrt{L + M} \vec{Q}, \quad \vec{P}_R = \sqrt{L + M} \vec{P} \quad (3.7)$$

are 6-component vectors. The components of these vectors are moduli dependent and not quantized. On the projected vectors, one only needs to consider ordinary inner products, for example $\vec{Q}_R^T \vec{Q}_R$ is equal (by construction) to $\vec{Q}^T (L + M) \vec{Q}$. Hence in what follows we will denote this quantity either by $\vec{Q} \circ \vec{Q}$ or equivalently by $\vec{Q}_R \cdot \vec{Q}_R$, and analogously for other inner products.

3.2 Marginal stability for $\mathcal{N} = 4$ dyons

Within the 6-dimensional projected charge space, the electric and magnetic charge vectors of the initial dyon span a 2-dimensional plane. Decay of a $\frac{1}{4}$ -BPS dyon into a set of decay products with quantized charge vectors $(\vec{Q}^{(1)}, \vec{P}^{(1)}), \dots, (\vec{Q}^{(n)}, \vec{P}^{(n)})$ can take place only when the plane spanned by the projected charge vectors of each decay product coincides with this plane (this is the condition for all states to be mutually $\frac{1}{4}$ -BPS):

$$\begin{pmatrix} \vec{Q}_R^{(i)} \\ \vec{P}_R^{(i)} \end{pmatrix} = \begin{pmatrix} m_i & r_i \\ s_i & n_i \end{pmatrix} \begin{pmatrix} \vec{Q}_R \\ \vec{P}_R \end{pmatrix} \quad (3.8)$$

When there are just two decay products and both are $\frac{1}{2}$ -BPS, the pair of decay products defines a 2-plane. Charge conservation then implies that this plane coincides with the plane of the original charge vectors, so in this very special case the above requirement imposes no conditions on the moduli. Indeed, the numbers m_i, r_i, s_i, n_i are then integers and the above relation holds between the full (quantized) charge vectors, not only the projected ones. Marginal decay takes place on a wall of marginal stability whose equation is explicitly known (see Ref.[10] and references therein). In all other cases, the numbers m_i, r_i, s_i, n_i are non-integral and moduli-dependent. In these cases the above condition puts additional constraints on the background moduli M . Our goal here is to identify these constraints explicitly.

For a two-body decay into $\frac{1}{4}$ -BPS constituents, once the constraints are satisfied and we find the numbers m_1, r_1, s_1, n_1 (the corresponding numbers m_2, r_2, s_2, n_2 are determined by charge conservation) the condition for marginal decay is expressed in terms of the curve [26] Eq. (2.21). We rewrite the curve for the case of unit torsion in following form:

$$\left(\tau_1 - \frac{m_1 - n_1}{2s_1} \right)^2 + \left(\tau_2 + \frac{\mathcal{E}}{2s_1} \right)^2 = \frac{1}{4s_1^2} \left((m_1 - n_1)^2 + 4r_1s_1 + \mathcal{E}^2 \right) \quad (3.9)$$

Here we have restricted to the case of unit-torsion dyons, so we have put $m = n = 1$ with respect to the notation in Ref.[26]. Also, E is defined by:

$$\mathcal{E} \equiv \frac{1}{\sqrt{\Delta}} \left(\vec{Q}^{(1)} \circ \vec{P} - \vec{P}^{(1)} \circ \vec{Q} \right) \quad (3.10)$$

We notice that exchanging the role of the two final-state dyons sends $\mathcal{E} \rightarrow -\mathcal{E}$. It also sends $m_1 - n_1 \rightarrow (1 - m_1) - (1 - n_1) = -(m_1 - n_1)$ and $r_1, s_1 \rightarrow -r_1, -s_1$. The curve of marginal stability is invariant under this set of transformations, as it should be.

We now turn to the detailed study general two-body decays into $\frac{1}{4}$ -BPS constituents. We will find explicit expressions for the numbers m_1, r_1, s_1, n_1 in terms of the quantized charge vectors $\vec{Q}, \vec{P}, \vec{Q}_1, \vec{P}_1$ and the moduli M . We will also explicitly characterize the loci in moduli space where such rare decays are allowed.

3.3 Rare dyon decays

3.3.1 Analysis and implicit solution

It will be useful to define a quartic scalar invariant of four different vectors by:

$$\Delta(\vec{A}, \vec{B}; \vec{C}, \vec{D}) \equiv \det \begin{pmatrix} \vec{A} \circ \vec{C} & \vec{A} \circ \vec{D} \\ \vec{B} \circ \vec{C} & \vec{B} \circ \vec{D} \end{pmatrix} = (\vec{A} \circ \vec{C})(\vec{B} \circ \vec{D}) - (\vec{A} \circ \vec{D})(\vec{B} \circ \vec{C}) \quad (3.11)$$

As explained above, the “ \circ ” product is the moduli-dependent inner product involving the matrix $L + M$. The above quantity is antisymmetric under exchange of the first pair or last pair of vectors, and symmetric under exchange of the two pairs. The quartic invariant of two variables defined earlier is a special case of this new invariant:

$$\Delta(\vec{Q}, \vec{P}) = \Delta(\vec{Q}, \vec{P}; \vec{Q}, \vec{P}) \quad (3.12)$$

Now start with the following vector equation that is part of Eq. (3.8):

$$\vec{Q}_R^{(1)} = m_1 \vec{Q}_R + r_1 \vec{P}_R \quad (3.13)$$

Contracting this successively with \vec{Q}_R and \vec{P}_R we find:

$$\begin{aligned} \vec{Q}_R^{(1)} \cdot \vec{Q}_R &= m_1 \vec{Q}_R^2 + r_1 \vec{Q}_R \cdot \vec{P}_R \\ \vec{Q}_R^{(1)} \cdot \vec{P}_R &= m_1 \vec{Q}_R \cdot \vec{P}_R + r_1 \vec{P}_R^2 \end{aligned} \quad (3.14)$$

Multiplying the first equation by \vec{P}_R^2 and the second by $\vec{Q}_R \cdot \vec{P}_R$ and subtracting, we find:

$$m_1 \Delta(\vec{Q}_R, \vec{P}_R) = \Delta(\vec{Q}_R, \vec{P}_R; \vec{Q}_R^{(1)}, \vec{P}_R) \quad (3.15)$$

which enables us to solve for m_1 . Repeating this process we can solve for r_1, s_1, n_1 leading to the result:

$$\begin{pmatrix} m_1 & r_1 \\ s_1 & n_1 \end{pmatrix} = \frac{1}{\Delta(\vec{Q}_R, \vec{P}_R)} \begin{pmatrix} \Delta(\vec{Q}_R, \vec{P}_R; \vec{Q}_R^{(1)}, \vec{P}_R) & \Delta(\vec{Q}_R, \vec{P}_R; \vec{Q}_R, \vec{Q}_R^{(1)}) \\ \Delta(\vec{Q}_R, \vec{P}_R; \vec{P}_R^{(1)}, \vec{P}_R) & \Delta(\vec{Q}_R, \vec{P}_R; \vec{Q}_R, \vec{P}_R^{(1)}) \end{pmatrix} \quad (3.16)$$

It follows that Eq. (3.8) can be expressed as:

$$\begin{pmatrix} \vec{Q}_R^{(1)} \\ \vec{P}_R^{(1)} \end{pmatrix} = \frac{1}{\Delta(\vec{Q}_R, \vec{P}_R)} \begin{pmatrix} \Delta(\vec{Q}_R, \vec{P}_R; \vec{Q}_R^{(1)}, \vec{P}_R) & \Delta(\vec{Q}_R, \vec{P}_R; \vec{Q}_R, \vec{Q}_R^{(1)}) \\ \Delta(\vec{Q}_R, \vec{P}_R; \vec{P}_R^{(1)}, \vec{P}_R) & \Delta(\vec{Q}_R, \vec{P}_R; \vec{Q}_R, \vec{P}_R^{(1)}) \end{pmatrix} \begin{pmatrix} \vec{Q}_R \\ \vec{P}_R \end{pmatrix} \quad (3.17)$$

For fixed, quantized charge vectors \vec{Q}, \vec{P} of the initial dyon and $\vec{Q}^{(1)}, \vec{P}^{(1)}$ of the first decay product (the charge of the second product is determined by charge conservation), the above equation provides a set of constraints on the moduli that must be satisfied for the $\frac{1}{4} \rightarrow \frac{1}{4} + \frac{1}{4}$ decay to be possible. These constraints together with the curve of marginal stability Eq. (2.21) provide a necessary and sufficient set of kinematic conditions for marginal decay.

In the above form, it is rather difficult to disentangle the constraints or to physically understand their significance. Therefore we will consider a number of special cases. Along the way we will see the advantage of using T-duality to bring the charges into a convenient form and performing the analysis in that basis. Finally we write down the explicit constraint equation in the general case, again in the chosen T-duality basis.

3.3.2 Explicit solution: special cases

(i) $\frac{1}{2}$ -BPS final states

The case where the decay products are $\frac{1}{2}$ -BPS should provide no constraints on the moduli as this is a “non-rare” decay. This provides a check on our equations. Inserting the $\frac{1}{2}$ -BPS conditions:

$$\vec{P}^{(1)} = \frac{k_1}{l_1} \vec{Q}^{(1)}, \quad \vec{P}^{(2)} = \frac{k_2}{l_2} \vec{Q}^{(2)} \quad (3.18)$$

with k_i, l_i integers, we find that:

$$\begin{pmatrix} m_1 & r_1 \\ s_1 & n_1 \end{pmatrix} = \begin{pmatrix} \frac{k_2}{l_2} & -\frac{k_1}{l_1} \\ \frac{k_1 k_2}{l_1 l_2} & -\frac{k_1}{l_1} \end{pmatrix} \frac{\Delta(\vec{Q}_R^{(1)}, \vec{Q}_R^{(2)})}{\Delta(\vec{Q}_R, \vec{P}_R)} \begin{pmatrix} \frac{k_2}{l_2} & -1 \\ \frac{k_1 k_2}{l_1 l_2} & -\frac{k_1}{l_1} \end{pmatrix} \quad (3.19)$$

We also have:

$$\Delta(\vec{Q}_R, \vec{P}_R) = \left(\frac{k_2}{l_2} - \frac{k_1}{l_1} \right)^2 \Delta(\vec{Q}_R^{(1)}, \vec{Q}_R^{(2)}) \quad (3.20)$$

Substituting in the above equation, we find:

$$\begin{pmatrix} m_1 & r_1 \\ s_1 & n_1 \end{pmatrix} = \frac{1}{k_2 l_1 - k_1 l_2} \begin{pmatrix} k_2 l_1 & -l_1 l_2 \\ k_1 k_2 & -k_1 l_2 \end{pmatrix} \quad (3.21)$$

At this stage all moduli-dependence has disappeared from the matrix, and equation Eq. (3.8) indeed provides no constraints on the moduli. Rather, it reduces to an identity. It is also easy to see that $k_1 l_2 - k_2 l_1$ divides the torsion of the original dyon, so if we are also considering the unit-torsion case then $k_1 l_2 - k_2 l_1 = 1$ and m_1, r_1, s_1, n_1 are all manifestly integral [10].

(ii) Special charges and moduli

The next special case we will study has a restricted set of charges. Additionally, some of the background moduli are set to a specific value, namely zero in the chosen coordinates. We then examine the constraints on the remaining moduli. In choosing special values for the moduli, we should in principle avoid loci of enhanced gauge symmetry where the dyons we are studying would become massless.

Let us restrict ourselves to special initial-state charges given by:

$$\vec{Q}' = (Q'_1, 0, \dots, 0), \quad \vec{Q}'' = (Q''_1, 0, \dots, 0), \quad \vec{Q}''' = 0 \quad (3.22)$$

and

$$\vec{P}' = (0, P'_2, 0, \dots, 0), \quad \vec{P}'' = (0, P''_2, 0, \dots, 0), \quad \vec{P}''' = 0 \quad (3.23)$$

Next we set $B_{ij} = 0 = A_i^I$ as well as $G_{ij} = 0$, $i \neq j$. The above restrictions allow us to choose the orthonormal frames E_{ai} to be diagonal:

$$E_{ii} = R_i, \quad i = 1, 2, \dots, 6 \quad (3.24)$$

with R_i the radii of the six compactified directions in the heterotic basis.

3.3 Rare dyon decays

In the restricted subspace of moduli space that we are considering here, the matrix $\sqrt{L+M}$ reduces to:

$$\sqrt{L+M} = \begin{pmatrix} E^{-1} & E & 0 \\ 0 & 0 & 0 \\ 0 & 0 & 0 \end{pmatrix} \quad (3.25)$$

with E given as in Eq. (3.24). Therefore the projected initial-state charge vectors are:

$$\vec{Q}_R = \begin{pmatrix} \frac{Q'_1}{R_1} + Q''_1 R_1 \\ 0 \\ \dots \\ 0 \end{pmatrix}, \quad \vec{P}_R = \begin{pmatrix} 0 \\ \frac{P'_2}{R_2} + P''_2 R_2 \\ 0 \\ \dots \\ 0 \end{pmatrix} \quad (3.26)$$

For this configuration we clearly have $\vec{Q}_R \cdot \vec{P}_R = 0$ and therefore the quartic invariant Δ is:

$$\Delta(Q_R, P_R) = \left(\frac{Q'_1}{R_1} + Q''_1 R_1 \right)^2 \left(\frac{P'_2}{R_2} + P''_2 R_2 \right)^2 \quad (3.27)$$

We take the decay products to have generic charges $\vec{Q}^{(1)}, \vec{P}^{(1)}$ and $\vec{Q}^{(2)}, \vec{P}^{(2)}$ subject of course to the requirement that they add up to \vec{Q}, \vec{P} . We then have:

$$\vec{Q}_R^{(1)} = \begin{pmatrix} \frac{Q_1^{(1)'}}{R_1} + Q_1^{(1)''} R_1 \\ \frac{Q_2^{(1)'}}{R_2} + Q_2^{(1)''} R_2 \\ \dots \\ \frac{Q_6^{(1)'}}{R_6} + Q_6^{(1)''} R_6 \end{pmatrix}, \quad \vec{P}_R^{(1)} = \begin{pmatrix} \frac{P_1^{(1)'}}{R_1} + P_1^{(1)''} R_1 \\ \frac{P_2^{(1)'}}{R_2} + P_2^{(1)''} R_2 \\ \dots \\ \frac{P_6^{(1)'}}{R_6} + P_6^{(1)''} R_6 \end{pmatrix} \quad (3.28)$$

Now we can compute the quartic invariants appearing in Eq. (3.17):

$$\begin{aligned}
\Delta(\vec{Q}_R, \vec{P}_R; \vec{Q}_R^{(1)}, \vec{P}_R) &= \left(\frac{Q'_1}{R_1} + Q''_1 R_1 \right) \left(\frac{Q_1^{(1)'}}{R_1} + Q_1^{(1)''} R_1 \right) \left(\frac{P'_2}{R_2} + P''_2 R_2 \right)^2 \\
\Delta(\vec{Q}_R, \vec{P}_R; \vec{Q}_R, \vec{Q}_R^{(1)}) &= \left(\frac{Q'_1}{R_1} + Q''_1 R_1 \right)^2 \left(\frac{Q_2^{(1)'}}{R_2} + Q_2^{(1)''} R_2 \right) \left(\frac{P'_2}{R_2} + P''_2 R_2 \right) \\
\Delta(\vec{Q}_R, \vec{P}_R; \vec{P}_R^{(1)}, \vec{P}_R) &= \left(\frac{Q'_1}{R_1} + Q''_1 R_1 \right) \left(\frac{P_1^{(1)'}}{R_1} + P_1^{(1)''} R_1 \right) \left(\frac{P'_2}{R_2} + P''_2 R_2 \right)^2 \\
\Delta(\vec{Q}_R, \vec{P}_R; \vec{Q}_R, \vec{P}_R^{(1)}) &= \left(\frac{Q'_1}{R_1} + Q''_1 R_1 \right)^2 \left(\frac{P_2^{(1)'}}{R_2} + P_2^{(1)''} R_2 \right) \left(\frac{P'_2}{R_2} + P''_2 R_2 \right)
\end{aligned}$$

Had we not taken E to be diagonal, the expressions above would have quickly become very complicated to write down.

Inserting the above expressions, and cancelling some common factors, the constraint equation Eq. (3.17) becomes:

$$\begin{aligned}
\left(\frac{Q'_1}{R_1} + Q''_1 R_1 \right) \left(\frac{P'_2}{R_2} + P''_2 R_2 \right) \vec{Q}_R^{(1)} &= \left(\frac{Q_1^{(1)'}}{R_1} + Q_1^{(1)''} R_1 \right) \left(\frac{P'_2}{R_2} + P''_2 R_2 \right) \vec{Q}_R + \\
&\quad \left(\frac{Q'_1}{R_1} + Q''_1 R_1 \right) \left(\frac{Q_2^{(1)'}}{R_2} + Q_2^{(1)''} R_2 \right) \vec{P}_R \\
\left(\frac{Q'_1}{R_1} + Q''_1 R_1 \right) \left(\frac{P'_2}{R_2} + P''_2 R_2 \right) \vec{P}_R^{(1)} &= \left(\frac{P_1^{(1)'}}{R_1} + P_1^{(1)''} R_1 \right) \left(\frac{P'_2}{R_2} + P''_2 R_2 \right) \vec{Q}_R + \\
&\quad \left(\frac{Q'_1}{R_1} + Q''_1 R_1 \right) \left(\frac{P_2^{(1)'}}{R_2} + P_2^{(1)''} R_2 \right) \vec{P}_R
\end{aligned} \tag{3.29}$$

These are 6+6 equations. However, the first two components of each set are identically satisfied, as one can easily check. This is expected, and follows from the structure of Eq. (3.8) from which m_1, r_1, s_1, n_1 were determined. The remaining four components of each equation give the desired constraints on the moduli. Because of the way we have chosen \vec{Q}, \vec{P} , the RHS already vanishes on components 3 to 6, so the constraint is simply that the LHS vanishes. That in turn sets to zero

3.3 Rare dyon decays

the components 3 to 6 of the vectors $\vec{Q}^{(1)}$ and $\vec{P}^{(1)}$. Thus we find the constraints:

$$\begin{aligned}\frac{Q_i^{(1)'}}{R_i} + Q_i^{(1)''} R_i &= 0, \quad i = 3, 4, 5, 6 \\ \frac{P_i^{(1)'}}{R_i} + P_i^{(1)''} R_i &= 0, \quad i = 3, 4, 5, 6\end{aligned}\tag{3.30}$$

If the components of $\vec{Q}^{(1)}, \vec{P}^{(1)}$ are all nonvanishing, this implies that:

$$R_i = \sqrt{-\frac{Q_i^{(1)'}}{Q_i^{(1)''}}} = \sqrt{-\frac{P_i^{(1)'}}{P_i^{(1)''}}}, \quad i = 3, 4, 5, 6\tag{3.31}$$

In this special case the constraint equations have some particular features. First of all, for generic charge vectors $\vec{Q}^{(1)}$ and $\vec{P}^{(1)}$, there are no solutions. To have any solutions at all, one must choose the charges of the decay products in such a way that the second equality in the above equation can be satisfied. In other words, the sign of $Q_i^{(1)'}$ and $Q_i^{(1)''}$ must be opposite (for $i = 3, 4, 5, 6$), and the same has to be true for $P^{(1)}$. In this case we find four constraints on the moduli, which fix the compactification radii R_3, R_4, R_5, R_6 .

For this special case, the numbers m_1, r_1, s_1, n_1 in Eq. (3.8) are given by:

$$\begin{aligned}m_1 &= \frac{\frac{Q_1^{(1)'}}{R_1} + Q_1^{(1)''} R_1}{\frac{Q_1'}{R_1} + Q_1'' R_1}, & r_1 &= \frac{\frac{Q_2^{(1)'}}{R_2} + Q_2^{(1)''} R_2}{\frac{P_2'}{R_2} + P_2'' R_2} \\ s_1 &= \frac{\frac{P_1^{(1)'}}{R_1} + P_1^{(1)''} R_1}{\frac{Q_1'}{R_1} + Q_1'' R_1}, & n_1 &= \frac{\frac{P_2^{(1)'}}{R_2} + P_2^{(1)''} R_2}{\frac{P_2'}{R_2} + P_2'' R_2}\end{aligned}\tag{3.32}$$

We see that m_1, s_1 depend only on R_1 and r_1, n_1 depend only on R_2 .

So far the decay products were taken to have generic charges (consistent of course with charge conservation). The situation changes if we choose less generic decay products. Earlier we took all components of $\vec{Q}^{(1)}, \vec{P}^{(1)}$ are nonvanishing. However if $Q_i^{(1)'}$ = $Q_i^{(1)''}$ = $P_i^{(1)'}$ = $P_i^{(1)''}$ = 0 for any $i \in 3, 4, 5, 6$ then the corresponding constraint Eq. (3.30) is trivially satisfied. In this situation we will have a reduced number of constraints. As an example if the above situation holds for all directions except $i = 3$ and if $\frac{Q_3^{(1)'}}{Q_3^{(1)''}} = \frac{P_3^{(1)'}}{P_3^{(1)''}}$ then there is only a single constraint coming from the above equations. The curve of marginal stability

provides one more constraint, so the decay will take place on a codimension-2 subspace of the restricted moduli space in which we are working for this class of examples. The fact that in some situations there are no solutions (for example if we do not satisfy that $Q_i^{(1)'}$ and $Q_i^{(1)''}$ have opposite signs for $i = 3, 4, 5, 6$) simply means that our restricted moduli space fails to intersect the marginal stability locus in that case.

If the charges $Q_i^{(1)'}$, $Q_i^{(1)''}$, $P_i^{(1)'}$, $P_i^{(1)''}$ vanish for all $i \in 3, 4, 5, 6$ then there are no constraints (beyond the curve of marginal stability). This corresponds to two distinct solutions. One is that the final states are now both $\frac{1}{2}$ -BPS. The other possibility is that they are still $\frac{1}{4}$ -BPS, but apparent contradiction of having no constraints on the moduli is resolved by the fact that we are already in a restricted subspace of the moduli space.

(iii) General charges, “diagonal” moduli

In this subsection we study rare decays allowing for completely general charges \vec{Q}, \vec{P} , but we will restrict the moduli so that the formulae are tractable. The situation turns out to be rather similar to the case studied in the previous subsection.

Considerable simplification can be brought about in the formulae by using some known results on T-duality orbits from Ref.[30] (as reviewed in Appendix A of [31]). For this purpose we first change basis from the L matrix used in Ref.[31]:

$$L' = \begin{pmatrix} \sigma_1 & 0 & \cdots & 0 & 0 & \cdots & 0 \\ 0 & \sigma_1 & \cdots & 0 & 0 & \cdots & 0 \\ 0 & & \cdots & 0 & 0 & \cdots & 0 \\ 0 & \cdots & 0 & \sigma_1 & 0 & \cdots & 0 \\ 0 & & \cdots & & -L_{E_8} & & 0 \\ 0 & & \cdots & & 0 & & -L_{E_8} \end{pmatrix} \quad (3.33)$$

to the one we have defined in Eq. (3.1). Here σ_1 is a Pauli matrix, which occurs 6 times in the above, and L_{E_8} is the Cartan matrix of E_8 .

In fact using T-duality we will be able to restrict to charge vectors that have the last 16 components vanishing, therefore we can ignore these components and

3.3 Rare dyon decays

work in a space of 12-component vectors. We then use a 12×12 matrix X that satisfies

$$X L X^T = L' \quad (3.34)$$

to map the equations in Ref.[31] to our basis.

Now the relevant result of T-duality orbits states that any pair of primitive charge vectors \vec{Q}, \vec{P} can be brought via T-duality to the form:

$$\begin{aligned} \vec{Q}' &= (Q'_1, 0, \dots, 0), & \vec{Q}'' &= (Q''_1, 0, \dots, 0), & \vec{Q}''' &= 0 \\ \vec{P}' &= (P'_1, P'_2, \dots, 0), & \vec{P}'' &= (P''_1, P''_2, \dots, 0), & \vec{P}''' &= 0 \end{aligned} \quad (3.35)$$

This is close to our previous special case, but with P'_1, P''_1 turned on. It is no longer a special case but represents the general case in a special basis.

As in the previous example, we restrict the moduli by requiring $A_i^I = B_{ij} = 0$ and $G_{ij} = 0$, $i \neq j$. Then one finds the projected charges to be:

$$\vec{Q}_R = \begin{pmatrix} \frac{Q'_1}{R_1} + Q''_1 R_1 \\ 0 \\ \dots \\ 0 \end{pmatrix}, \quad \vec{P}_R = \begin{pmatrix} \frac{P'_1}{R_1} + P''_1 R_1 \\ \frac{P'_2}{R_2} + P''_2 R_2 \\ 0 \\ \dots \\ 0 \end{pmatrix} \quad (3.36)$$

The quartic invariant is then found to be:

$$\Delta(Q_R, P_R) = \left(\frac{Q'_1}{R_1} + Q''_1 R_1 \right)^2 \left(\frac{P'_2}{R_2} + P''_2 R_2 \right)^2 \quad (3.37)$$

which is actually the *same* as in the previous, simpler case where we chose a special subset of charges. Computing m_1, r_1, s_1, n_1 as in the previous subsection

and inserting them back, the constraint equation can now be written:

$$\begin{aligned}
& \left(\frac{Q'_1}{R_1} + Q''_1 R_1 \right) \left(\frac{P'_2}{R_2} + P''_2 R_2 \right) \vec{Q}_R^{(1)} = \\
& \left[\left(\frac{Q_1^{(1)'}}{R_1} + Q_1^{(1)''} R_1 \right) \left(\frac{P'_2}{R_2} + P''_2 R_2 \right) - \left(\frac{Q_2^{(1)'}}{R_2} + Q_2^{(1)''} R_2 \right) \left(\frac{P'_1}{R_1} + P''_1 R_1 \right) \right] \vec{Q}_R + \\
& \qquad \qquad \qquad \left(\frac{Q'_1}{R_1} + Q''_1 R_1 \right) \left(\frac{Q_2^{(1)'}}{R_2} + Q_2^{(1)''} R_2 \right) \vec{P}_R \\
& \left(\frac{Q'_1}{R_1} + Q''_1 R_1 \right) \left(\frac{P'_2}{R_2} + P''_2 R_2 \right) \vec{P}_R^{(1)} = \\
& \left[\left(\frac{P_1^{(1)'}}{R_1} + P_1^{(1)''} R_1 \right) \left(\frac{P'_2}{R_2} + P''_2 R_2 \right) - \left(\frac{P_2^{(1)'}}{R_2} + P_2^{(1)''} R_2 \right) \left(\frac{P'_1}{R_1} + P''_1 R_1 \right) \right] \vec{Q}_R + \\
& \qquad \qquad \qquad \left(\frac{Q'_1}{R_1} + Q''_1 R_1 \right) \left(\frac{P_2^{(1)'}}{R_2} + P_2^{(1)''} R_2 \right) \vec{P}_R
\end{aligned} \tag{3.38}$$

These equations are slightly more complicated than the previous case for which we had $\vec{Q} \circ \vec{P} = 0$, but the extra complication is only in the first two components, which are again trivially satisfied. For the remaining components we find:

$$\begin{aligned}
& \frac{Q_i^{(1)'}}{R_i} + Q_i^{(1)''} R_i = 0, \quad i = 3, 4, 5, 6 \\
& \frac{P_i^{(1)'}}{R_i} + P_i^{(1)''} R_i = 0, \quad i = 3, 4, 5, 6
\end{aligned} \tag{3.39}$$

These are exactly the *same* as the constraints we found in the previous case. The analysis is therefore also the same: the constraints cannot be satisfied for generic charges because our restricted moduli space need not intersect the marginal stability locus. When they can be satisfied there are at most four constraints, though there will be less if some of the decay product charges vanish.

3.3.3 General charges, “triangular” moduli

In this subsection we restrict the moduli in the most minimal way consistent with finding a simple form of the constraint equation. The restriction will be a kind

of “triangularity” condition:

$$(G + B + C)_{i1} = (G + B + C)_{i2} = 0, \quad i = 3, 4, 5, 6 \quad (3.40)$$

with no separate constraints on G, B, A other than the above.

As before, we use T-duality to put the initial charges into the form of Eq. (3.35). Thereafter, we are still free to make T-duality transformations involving the last four components of \vec{Q}' and \vec{Q}'' and all 16 components of \vec{Q}''' . The T-duality group is thus restricted to an $SO(4, 20; \mathbb{Z})$. These transformations will affect the charges of the decay products while leaving the initial dyon unchanged. Using them we bring the electric charges of the first decay product to the form:

$$\begin{aligned} \vec{Q}^{(1)'} &= (Q_1^{(1)'}, Q_2^{(1)'}, Q_3^{(1)'}, \dots, 0), \\ \vec{Q}^{(1)''} &= (Q_1^{(1)''}, Q_2^{(1)''}, Q_3^{(1)''}, \dots, 0), \\ \vec{Q}^{(1)'''} &= 0 \end{aligned} \quad (3.41)$$

Finally we use an $SO(3, 19; \mathbb{Z})$ subgroup of T-duality that preserves all the charge vectors that we have so far fixed, to bring the magnetic charges of the first decay product to the form:

$$\begin{aligned} \vec{P}^{(1)'} &= (P_1^{(1)'}, P_2^{(1)'}, P_3^{(1)'}, P_4^{(1)'}, \dots, 0), \\ \vec{P}^{(1)''} &= (P_1^{(1)''}, P_2^{(1)''}, P_3^{(1)''}, P_4^{(1)''}, \dots, 0), \\ \vec{P}^{(1)'''} &= 0 \end{aligned} \quad (3.42)$$

The charges of the second decay product are determined by charge conservation.

Now we use the form of the projection matrix $\sqrt{L + M}$ and write out Eq. (3.8) explicitly, after first multiplying through by E_{ij} :

$$\begin{aligned} Q_i^{(1)'} + (G + B + C)_{ij} Q_j^{(1)''} &= m_1 Q_i' + m_1 (G + B + C)_{ij} Q_j'' \\ &\quad + r_1 P_i' + r_1 (G + B + C)_{ij} P_k'' \\ P_i^{(1)'} + (G + B + C)_{ij} P_j^{(1)''} &= s_1 Q_i' + s_1 (G + B + C)_{ij} Q_j'' \\ &\quad + n_1 P_i' + n_1 (G + B + C)_{ij} P_j'' \end{aligned} \quad (3.43)$$

This is a set of $6 + 6$ equations. Recall that $C_{ij} = A_i^I A_j^I$.

3.3 Rare dyon decays

We immediately see that for our choice of T-duality frame for the initial charges, as well as using the “triangularity” condition, the RHS of the above equations vanishes for $i = 3, 4, 5, 6$. Hence we find the constraint equations still in a relatively simple form:

$$\begin{aligned} Q_i^{(1)'} + (G + B + C)_{ij} Q_j^{(1)''} &= 0, \quad i = 3, 4, 5, 6 \\ P_i^{(1)'} + (G + B + C)_{ij} P_j^{(1)''} &= 0, \quad i = 3, 4, 5, 6 \end{aligned} \quad (3.44)$$

These are then the 4+4 constraints on rare dyon decays, though still with the triangularity restriction on moduli and in a specific T-duality frame. They must be supplemented by the curve of marginal stability, for which we need to know the numbers m_1, r_1, s_1, n_1 .

The first two components of each line of equations Eq. (3.43) determine the values of m_1, r_1, s_1, n_1 . From the first line of those equations we find:

$$\begin{aligned} Q_1^{(1)'} + (G + B + C)_{1i} \vec{Q}_i^{(1)''} &= m_1 Q_1' + m_1 (G + B + C)_{1i} Q_i'' + r_1 P_1' + r_1 (G + B + C)_{1i} P_i'' \\ Q_2^{(1)'} + (G + B + C)_{2i} Q_i^{(1)''} &= r_1 P_2' + r_1 (G + B + C)_{2i} P_i'' \end{aligned} \quad (3.45)$$

Solving for r_1 from the second equation above, we get:

$$r_1 = \frac{Q_2^{(1)'} + (G + B + C)_{2i} Q_i^{(1)''}}{P_2' + (G + B + C)_{2i} P_i''} \quad (3.46)$$

Inserting this in the first equation determines m_1 :

$$\begin{aligned} m_1 &= \left(P_2' + (G + B + C)_{2i} P_i'' \right)^{-1} \left(Q_1' + (G + B + C)_{1i} Q_i'' \right)^{-1} \times \\ &\quad \left[\left(Q_1^{(1)'} + (G + B + C)_{1i} Q_i^{(1)''} \right) \left(P_2' + (G + B + C)_{2i} P_i'' \right) \right. \\ &\quad \left. - \left(Q_2^{(1)'} + (G + B + C)_{2i} Q_i^{(1)''} \right) \left(P_1' + (G + B + C)_{1i} P_i'' \right) \right] \quad (3.47) \end{aligned}$$

Similarly we solve for s_1, n_1 from the second line of Eq. (3.43) and find:

$$\begin{aligned}
n_1 &= \frac{P_2^{(1)'} + (G + B + C)_{2i} P_i^{(1)''}}{P_2' + (G + B + C)_{2i} P_i''} \\
s_1 &= \left(P_2' + (G + B + C)_{2i} P_i'' \right)^{-1} \left(Q_1' + (G + B + C)_{1i} Q_i'' \right)^{-1} \times \\
&\quad \left[\left(P_1^{(1)'} + (G + B + C)_{1i} P_i^{(1)''} \right) \left(P_2' + (G + B + C)_{2i} P_i'' \right) \right. \\
&\quad \left. - \left(P_2^{(1)'} + (G + B + C)_{2i} P_i^{(1)''} \right) \left(P_1' + r(G + B + C)_{1i} P_i \right) \right] \quad (3.48)
\end{aligned}$$

Admittedly these are somewhat complicated expressions for the numbers m_1, r_1, s_1, n_1 that one needs to plug in to determine the curve of marginal stability on the torus moduli space. It is conceivable that a more opportune choice of variables could simplify them further. Nevertheless, the constraints Eq. (3.44) on the remaining moduli are rather simple.

3.3.4 Explicit solution: the general case

We now turn to the case where the initial and final charges are completely general and the moduli are generic as well. Most of the relevant analysis has already been done in previous subsections and it only remains to write down the result. However, as we will see, the equations rapidly become messy – despite the use of T-duality transformations - once we use completely general moduli.

Let us again start by writing out Eq. (3.8) explicitly, but now without any condition on the moduli. After multiplying through by E_{ij} , we find the equations:

$$\begin{aligned}
Q_i^{(1)'} + (G + B + C)_{ij} Q_j^{(1)''} &= m_1 Q_i' + m_1 (G + B + C)_{ij} Q_j'' \\
&\quad + r_1 P_i' + r(G + B + C)_{ij} P_k'' \\
P_i^{(1)'} + (G + B + C)_{ij} P_j^{(1)''} &= s_1 Q_i' + s_1 (G + B + C)_{ij} Q_j'' \\
&\quad + n_1 P_i' + n_1 (G + B + C)_{ij} P_j'' \quad (3.49)
\end{aligned}$$

which are actually the same as Eq. (3.43) that we had before. The difference is that the RHS no longer vanishes for any of the components (earlier that was guaranteed by the triangularity condition that we had assumed on the moduli).

3.3 Rare dyon decays

Notice that even in the most general case, we have gained something by fixing the initial and final state charges using T-duality. The last 16 components of these charges have all been set to 0, and the result is that most of the terms involving the gauge field moduli A_i^I have disappeared. The only appearance of these moduli is through $C_{ij} = A_i^I A_j^I$ which in turn only appears in the combination $G + B + C$.

This time our strategy will be to choose any 4 equations from the above set of 12 to determine the variables m_1, n_1, r_1, s_1 . Then in the remaining 8 equations we insert these values for the variables and obtain the desired constraint equations. Picking the first 2 components for each charge vector, we find:

$$\begin{aligned} Q_1^{(1)'} + (G + B + C)_{1i} Q_i^{(1)''} &= m_1 Q_1' + m_1 (G + B + C)_{1i} Q_i'' + r_1 P_1' + r (G + B + C)_{1i} P_i'' \\ Q_2^{(1)'} + (G + B + C)_{2i} Q_i^{(1)''} &= r_1 P_2' + r_1 (G + B + C)_{2i} P_i'' \end{aligned} \quad (3.50)$$

Solving for r_1 from the second equation above, we get:

$$r_1 = \frac{Q_2^{(1)'} + (G + B + C)_{2i} Q_i^{(1)''}}{P_2' + (G + B + C)_{2i} P_i''} \quad (3.51)$$

and inserting this in the first equation, we find m_1 :

$$\begin{aligned} m_1 &= \left(P_2' + (G + B + C)_{2i} P_i'' \right)^{-1} \left(Q_1' + (G + B + C)_{1i} Q_i'' \right)^{-1} \times \\ &\quad \left[\left(Q_1^{(1)'} + (G + B + C)_{1i} Q_i^{(1)''} \right) \left(P_2' + (G + B + C)_{2i} P_i'' \right) \right. \\ &\quad \left. - \left(Q_2^{(1)'} + (G + B + C)_{2i} Q_i^{(1)''} \right) \left(P_1' + r (G + B + C)_{1i} P_i \right) \right] \end{aligned} \quad (3.52)$$

Similarly we solve for s_1, n_1 from the second equation and find:

$$n_1 = \frac{P_2^{(1)'} + (G + B + C)_{2i} P_i^{(1)''}}{P_2' + (G + B + C)_{2i} P_i''} \quad (3.53)$$

and

$$\begin{aligned} s_1 &= \left(P_2' + (G + B + C)_{2i} P_i'' \right)^{-1} \left(Q_1' + (G + B + C)_{1i} Q_i'' \right)^{-1} \times \\ &\quad \left[\left(P_1^{(1)'} + (G + B + C)_{1i} P_i^{(1)''} \right) \left(P_2' + (G + B + C)_{2i} P_i'' \right) \right. \\ &\quad \left. - \left(P_2^{(1)'} + (G + B + C)_{2i} P_i^{(1)''} \right) \left(P_1' + (G + B + C)_{1i} P_i \right) \right] \end{aligned} \quad (3.54)$$

We feed in these values of m_1, n_1, r_1, s_1 into the remaining 8 equations to find the most general constraint equations on the moduli:

$$\begin{aligned}
 Q_i^{(1)'} + (G + B + C)_{ij} Q_j^{(1)''} &= m_1 \left(Q_i' + (G + B + C)_{ij} Q_j'' \right) + r_1 \left(P_i' + (G + B + C)_{ij} P_j'' \right) \\
 P_i^{(1)'} + (G + B + C)_{ij} P_j^{(1)''} &= s_1 \left(Q_i' + (G + B + C)_{ij} Q_j'' \right) + n_1 \left(P_i' + (G + B + C)_{ij} P_j'' \right)
 \end{aligned}
 \tag{3.55}$$

here $i = 3, 4, 5, 6$, and m_1, n_1, r_1, s_1 are given in the above equations. We see that the values of m_1, n_1, r_1, s_1 come out the same as in the previous special case, however the constraints are much more complicated and – unlike in all the previous special cases – depend explicitly on these numbers. Nevertheless, the above equations embody the most general kinematic constraints on moduli space to allow a two-body decay of a dyon of charges \vec{Q}, \vec{P} into $\frac{1}{4}$ -BPS final state with charges $\vec{Q}^{(1)}$ and $\vec{P}^{(1)}$ (the charges of the second state being, as always, determined by charge conservation). It is quite conceivable that a more detailed study of possible T-duality bases will allow us to further simplify the most general case, and we leave such an investigation for the future.

3.4 Multi-particle decays

So far in this work, as well as in previous work[26], we have written down conditions for decay of a dyon into two $\frac{1}{4}$ -BPS final states. One could certainly imagine extending these considerations to three or more final states. Indeed, it turns out rather simple to do so and we will here discuss an iterative way to obtain the relevant formulae.

Consider the decay of a dyon of charges (\vec{Q}, \vec{P}) into n decay products of charges $(\vec{Q}^{(1)}, \vec{P}^{(1)}), (\vec{Q}^{(2)}, \vec{P}^{(2)}), \dots, (\vec{Q}^{(n)}, \vec{P}^{(n)})$. The condition for marginality of such a decay is the condition for the original dyon to go into two decay products of charges $(\vec{Q}^{(1)}, \vec{P}^{(1)})$ and $\sum_{i=2}^n (\vec{Q}^{(i)}, \vec{P}^{(i)})$, along with the condition for the second decay product to further decay into say $(\vec{Q}^{(2)}, \vec{P}^{(2)})$ and $\sum_{i=3}^n (\vec{Q}^{(i)}, \vec{P}^{(i)})$. The latter condition must in turn be iterated. Each of these is a two-body decay (with both final states being $\frac{1}{4}$ -BPS) so we already know the condition for each

one to take place. The intersection of all these loci will give the marginal stability locus for the multiparticle decay.

There is a simpler way to iterate the condition. Instead of looking at the curve where the second decay product decays into further subconstituents, as above, we can simply consider the collection of all marginal stability loci for the decays:

$$\begin{pmatrix} \vec{Q}_R \\ \vec{P}_R \end{pmatrix} \rightarrow \begin{pmatrix} \vec{Q}_R^{(i)} \\ \vec{P}_R^{(i)} \end{pmatrix} + \begin{pmatrix} \vec{Q}_R - \vec{Q}_R^{(i)} \\ \vec{P}_R - \vec{P}_R^{(i)} \end{pmatrix}, \quad i = 1, 2, \dots, n \quad (3.56)$$

For each of these, the curve is precisely Eq. (2.21) with the subscript “1” replaced by “ i ”. We write it as:

$$\mathcal{C}(m_i, r_i, s_i, n_i) \equiv \left(\tau_1 - \frac{m_i - n_i}{2s_i} \right)^2 + \left(\tau_2 + \frac{\mathcal{E}_i}{2s_i} \right)^2 - \frac{1}{4s_i^2} \left((m_i - n_i)^2 + 4r_i s_i + \mathcal{E}_i^2 \right) = 0 \quad (3.57)$$

where

$$\mathcal{E}_i \equiv \frac{1}{\sqrt{\Delta}} \left(\vec{Q}^{(i)} \circ \vec{P} - \vec{P}^{(i)} \circ \vec{Q} \right) \quad (3.58)$$

In addition to this curve we have the constraints on the remaining moduli as in Sec.3 above. Those too can be expressed in terms of the single decay product labelled “ i ”. Now to find the condition for a multi-dyon decay, we simply take the intersection of all these loci of marginal stability. As the number of final states increases, we will generically find loci of marginal stability of increasing codimension.

3.5 Multi-centred black holes

It was argued in Refs.[13, 14] that the curves of marginal stability for decays of the form:

$$\frac{1}{4}\text{-BPS} \rightarrow \frac{1}{2}\text{-BPS} + \frac{1}{2}\text{-BPS} \quad (3.59)$$

are also the curves of disintegration for two-centred $\frac{1}{4}$ -BPS black holes whose centres are individually $\frac{1}{2}$ -BPS. The method used in these works, which we will summarize and extend below, was to use a constraint equation due to Denef [25] to express the separation between the centres of such a black hole in terms of charges and moduli. Requiring that the separation be infinite places a condition

3.5 Multi-centred black holes

on charges and moduli which turns out to be precisely the curve of marginal stability, Eq. (2.21), specialized to this decay.

Now Denef's constraint equation is not confined to two-centred black holes alone, but applies to any number of centres. It has a different limitation: it is defined in the context of $\mathcal{N} = 2$, rather than $\mathcal{N} = 4$ compactifications, and relies on special geometry. Nevertheless, for the cases to which it applies, we can certainly use it in the $\mathcal{N} = 4$ context. We will do so and will find the result that the curves of marginal stability for generic decays to n final states, which we discussed in Sec.4 above, are precisely reproduced by the constraint equations for multi-centred black holes. This suggests a more generic relationship between multi-particle decays and multi-centred black holes than has been previously considered.

The constraint equation on multi-centred dyons, (see for example Ref.[13]¹) reads as follows. Let $p^{(i)I}, q_I^{(i)}$ be the charges of the i -th centre where $i = 1, 2, \dots, N$. These charges are expressed in the special-geometry basis². Let the 3-vector \vec{r}_i be the location of the i -th centre. And let the moduli be encoded in the standard holomorphic special-geometry variables X^I, F_I . Then the constraint equations are:

$$p^{(i)I} \text{Im}(F_{I\infty}) - q_I^{(i)} \text{Im}(X_{\infty}^I) + \frac{1}{2} \sum_{j \neq i} \frac{p^{(i)I} q_I^{(j)} - q_I^{(i)} p^{(j)I}}{|\vec{r}_i - \vec{r}_j|} = 0 \quad (3.60)$$

Here the subscript ∞ indicates that the corresponding moduli are measured at spatial infinity (for brevity of notation we will drop it when there is no risk of ambiguity). Note that the numerators inside the summation correspond to the Saha angular momentum between each pair of centres.

These are N equations for $\binom{N}{2}$ pairwise distances between the centres. We analyze them following the procedure in Ref.[13] for the two-centred case. First of all, one of the equations is redundant. Adding all the equations, we find:

$$p^I \text{Im}(F_{I\infty}) - q_I \text{Im}(X_{\infty}^I) = 0 \quad (3.61)$$

¹A sign in equation (3.2) of Ref.[13] should be corrected so that it reads $\frac{X^1}{X^0} = -\tau$. This leads to some sign changes in other equations there.

²As we will see, this differs by an interchange of some components from the standard basis used in $\mathcal{N} = 4$ compactifications.

where (p^I, q_I) are the charges of the entire black hole. This provides one real constraint on the extra modulus X_∞^0 . As the above equation is invariant under $X^I \rightarrow \lambda X^I$ for real X^I , as well as under $X^I \rightarrow -X^I$, we see that the magnitude of X^0 is undetermined by this condition, while the phase is determined (in terms of the $X^I, I = 1, 2, 3$) upto a two-fold ambiguity. Another real constraint is now imposed in the form of a “gauge condition”:

$$X^I \mathbf{F}_I - \bar{X}^I F_I = -i \quad (3.62)$$

This determines the magnitude of X^0 but leaves intact the two-fold ambiguity in the phase. The remaining $N - 1$ equations then provide constraints on the $\binom{N}{2}$ separations.

For the case $N = 2$ we therefore have a single equation, which completely determines the separation between the two centres. This works as follows. The relevant part of the theory is described by the holomorphic prepotential:

$$F = -\frac{X^1 X^2 X^3}{X^0} \quad (3.63)$$

where the X^I are complex scalar fields related to a subset of the $K3 \times T^2$ moduli, namely $\tau = \tau_1 + i\tau_2$ describing the 2-torus complex structure, and

$$M = \text{diag}(\hat{R}^{-2}, R^{-2}, \hat{R}^2, R^2) \quad (3.64)$$

describing a 2-parameter subset of the remaining moduli (including the $K3$ moduli). The precise relationship is:

$$\frac{X^1}{X^0} = -\tau, \quad \frac{X^2}{X^0} = iR\hat{R}, \quad \frac{X^3}{X^0} = i\frac{\hat{R}}{R} \quad (3.65)$$

The gauge condition Eq. (3.62) then tells us that:

$$|X_\infty^0|^2 = \frac{1}{8\hat{R}^2 \tau_2} \quad (3.66)$$

As in the previous sections, we will consider a dyon with charges (\vec{Q}, \vec{P}) , but now each taken to be 4-component (the first two components should be thought of as two of the six \vec{Q}' and the second two components constitute two of the six \vec{Q}''). The charges correspond to unit torsion, namely:

$$\text{g.c.d.}(Q_i P_j - P_i Q_j) = 1 \quad (3.67)$$

We begin by determining the modulus X^0 in terms of the T-duality invariants $P \circ P, Q \circ Q, P \circ Q$, where as before the inner products are defined in terms of the moduli at infinity, e.g. $P \circ P = P^T(L + M)P$.

As promised, we will use the transcription between the natural electric-magnetic basis \vec{P}, \vec{Q} for the type IIB superstring and the natural basis p^I, q_I for special geometry (see for example Ref. [13]):

$$q_I = (Q_1, P_1, Q_4, Q_2), \quad p^I = (P_3, -Q_3, P_2, P_4) \quad (3.68)$$

In addition we have:

$$\begin{aligned} \text{Im}(F_0) &= \hat{R}^2 \text{Im}(X^0 \tau), & \text{Im}(F_1) &= \hat{R}^2 \text{Im}(X^0), \\ \text{Im}(F_2) &= \frac{\hat{R}}{R} \text{Re}(X^0 \tau), & \text{Im}(F_3) &= R \hat{R} \text{Re}(X^0 \tau) \end{aligned} \quad (3.69)$$

while

$$\begin{aligned} \text{Im}(X^0) &= \text{Im}(X^0), & \text{Im}(X^1) &= -\text{Im}(X^0 \tau), \\ \text{Im}(X^2) &= R \hat{R} \text{Re}(X^0), & \text{Im}(X^3) &= \frac{\hat{R}}{R} \text{Re}(X^0) \end{aligned} \quad (3.70)$$

Inserting these into Eqs.(3.61),(3.66), one finds:

$$X^0 = \frac{1}{(2\sqrt{2}\hat{R}\tau_2)} \frac{\sqrt{\Delta}\bar{\tau} + i(Q \circ P\bar{\tau} - Q \circ Q)}{\sqrt{Q \circ Q} M_{BPS}} \quad (3.71)$$

where M_{BPS} is the BPS mass given by Eq. (2.10).

Now let us assume our dyon has n centres of charges $(\vec{Q}^{(i)}, \vec{P}^{(i)})$:

$$\begin{pmatrix} \vec{Q}^{(i)} \\ \vec{P}^{(i)} \end{pmatrix} = \begin{pmatrix} m_i & r_i \\ s_i & n_i \end{pmatrix} \begin{pmatrix} \vec{Q} \\ \vec{P} \end{pmatrix}, \quad i = 1, 2, \dots, n \quad (3.72)$$

with m_i, r_i, s_i, n_i integers satisfying:

$$\sum_{i=1}^n m_i = \sum_{i=1}^n n_i = 1, \quad \sum_{i=1}^n r_i = \sum_{i=1}^n s_i = 0 \quad (3.73)$$

From Eq. (3.68) we find that the charges of the decay products in the q_I, p^J basis are given by:

$$\begin{aligned} q_I^{(i)} &= (m_i Q_1 + r_i P_1, s_i Q_1 + n_i P_1, m_i Q_4 + r_i P_4, m_i Q_2 + r_i P_2) \\ p^{(i)I} &= (s_i Q_3 + n_i P_3, -(m_i Q_3 + r_i P_3), s_i Q_2 + n_i P_2, s_i Q_4 + n_i P_4) \end{aligned} \quad (3.74)$$

Now the first term in Eq. (3.60) can be written:

$$p^{(i)I} \text{Im}(F_I) - q_I^{(i)} \text{Im}(X^I) = \hat{R} \text{Re} \begin{pmatrix} -X^0 & X^0 \tau \end{pmatrix} \begin{pmatrix} m_i & r_i \\ s_i & n_i \end{pmatrix} \begin{pmatrix} \frac{Q_2}{R} + RQ_4 - i(\frac{Q_1}{R} + \hat{R}Q_3) \\ \frac{P_2}{R} + RP_4 - i(\frac{P_1}{R} + \hat{R}P_3) \end{pmatrix} \quad (3.75)$$

The invariants $P \circ P, Q \circ Q, Q \circ P$ are given by:

$$\begin{aligned} Q \circ Q &= \left(\frac{Q_1}{\hat{R}} + \hat{R}Q_3 \right)^2 + \left(\frac{Q_2}{R} + RQ_4 \right)^2 \\ P \circ P &= \left(\frac{P_1}{\hat{R}} + \hat{R}P_3 \right)^2 + \left(\frac{P_2}{R} + RP_4 \right)^2 \\ Q \circ P &= \left(\frac{Q_1}{\hat{R}} + \hat{R}Q_3 \right) \left(\frac{P_1}{\hat{R}} + \hat{R}P_3 \right) + \left(\frac{Q_2}{R} + RQ_4 \right) \left(\frac{P_2}{R} + RP_4 \right) \end{aligned} \quad (3.76)$$

The column vector in Eq. (3.75) depends on four combinations of Q_i, P_i and therefore cannot in general be expressed in terms of T-duality invariants. Therefore we restrict to the special case, discussed in particular in Ref.[13], for which $Q_1 = Q_3 = 0$. In this case only three independent combinations appear in the column vector and it is easy to show that:

$$\begin{aligned} p^{(i)I} \text{Im}(F_I) - q_I^{(i)} \text{Im}(X^I) &= \hat{R} \text{Re} X^0 \begin{pmatrix} -1 & \tau \end{pmatrix} \begin{pmatrix} m_i & r_i \\ s_i & n_i \end{pmatrix} \begin{pmatrix} \frac{\sqrt{Q \circ Q}}{\sqrt{Q \circ Q}} \\ \frac{Q \circ P + i\sqrt{\Delta}}{\sqrt{Q \circ Q}} \end{pmatrix} \\ &= \frac{s_1 \sqrt{\Delta}}{2\sqrt{2} \tau_2 M_{BPS}} \mathcal{C}(m_i, r_i, s_i, n_i) \end{aligned} \quad (3.77)$$

where $\mathcal{C}(m_i, r_i, s_i, n_i)$ is the curve of marginal stability for multiparticle decays, defined in Eq. (3.57).

The numerator of the second term in Eq. (3.60), denoted:

$$\mathcal{J}_{ij} \equiv p^{(i)I} q_I^{(j)} - p^{(j)I} q_I^{(i)} \quad (3.78)$$

is the angular momentum between each pair of decay products evaluated in the moduli-independent norm. We will denote the pairwise separation between the centres by:

$$L_{ij} = |\vec{r}_i - \vec{r}_j| \quad (3.79)$$

Note that $\mathcal{J}_{ij} = -\mathcal{J}_{ji}$ and $L_{ij} = L_{ji}$.

Inserting the above results into Eq. (3.60), one finds that it can be expressed as follows:

$$\tilde{\mathcal{C}}_i + \sum_{j \neq i} \frac{\mathcal{J}_{ij}}{L_{ij}} = 0 \quad (3.80)$$

where

$$\tilde{\mathcal{C}}_i \equiv \frac{s_i \sqrt{\Delta}}{\sqrt{2} \tau_2 M_{BPS}} \mathcal{C}(m_i, r_i, s_i, n_i) \quad (3.81)$$

Clearly the first term in Eq. (3.80) depends only on the charges of a single centre (as well as the initial charges) while the second term depends on the charges of a pair of centres. Note that we have $\sum_i \tilde{\mathcal{C}}_i = 0$. Thus we have shown that the curves of marginal stability for multi-centred decays appear also from considerations of multi-centred black holes and the constraints on the locations of their centres.

In the special case considered previously [13, 14] where the dyon has two $\frac{1}{2}$ -BPS centres, the corresponding curve of marginal stability is of codimension 1. In this case it is known that the degeneracy of states jumps as we cross the curve. From the supergravity point of view, it was suggested in the $\mathcal{N} = 2$ context in Ref.[25] and shown more explicitly in the present $\mathcal{N} = 4$ context in Refs.[13, 14], that this decay occurs as a result of the two centres flying apart to infinity at a curve of marginal stability. This is seen by specializing Eq. (3.80) to this case. As long as $\mathcal{J}_{12} \neq 0$, the separation $L_{12} \rightarrow \infty$ when $\tilde{\mathcal{C}}_i \rightarrow 0$. Moreover for a fixed sign of \mathcal{J}_{12} , the separation L_{12} can be positive only on one side of the curve of marginal stability. On the other side it is negative, which indicates that the corresponding two-centred black hole does not exist.

Now let us return to the more general case where there are two centres but both are $\frac{1}{4}$ -BPS. As we have seen, in this case the locus of marginal stability is not a wall in moduli space, but rather a curve of codimension ≥ 2 . Therefore the degeneracy formula cannot jump as one crosses the curve. Hence one need not have expected any relationship between marginal decays and multi-centred dyons. Nevertheless, we see that Eq. (3.80) continues to hold in the more general case (with the limitation that the charges are those that can be embedded in an $\mathcal{N} = 2$ compactification).

We interpret this as evidence that the relationship between dyon decay and the disintegration of multi-centred black holes holds more generally than required by

3.5 Multi-centred black holes

the degeneracy formula. Therefore we conjecture that even with the most general charges, n -centred black holes exist in $\mathcal{N} = 4$ string compactifications with generic $\frac{1}{4}$ -BPS centres for which Eq. (3.80) holds true. It would be worth trying to prove that this is the case, or else to show that such solutions do not exist beyond the cases that can be embedded in the charge space and moduli space of $\mathcal{N} = 2$. An intermediate possibility also exists: that in $\mathcal{N} = 4$ compactifications such multi-centred black holes do exist with arbitrary charges, but only on a subspace of the moduli space.

Examining Eq. (3.80) one sees that if the marginal stability condition $\tilde{\mathcal{C}}_i = 0$ is satisfied for a particular i , then we must have:

$$\sum_{j \neq i} \frac{\mathcal{J}_{ij}}{L_{ij}} = 0 \tag{3.82}$$

One possible solution is to have $L_{ij} \rightarrow \infty$ for all $j \neq i$. This means the i th centre has been taken infinitely far away from all the others, in agreement with the picture of marginal decay that we developed in Section 4 above. Since the pairwise Saha angular momenta $\mathcal{J}_{ij} \equiv P^{(i)} \cdot Q^{(j)} - P^{(j)} \cdot Q^{(i)}$ cannot all be positive in every equation (since $\mathcal{J}_{ij} = -\mathcal{J}_{ji}$) there could be other configurations where the $\tilde{\mathcal{C}}_i = 0$, except in the case of two centres. It is not clear to us how these other solutions should be interpreted.

Note that in the above equation the angular momentum is measured with respect to moduli-independent inner product $P \cdot Q \equiv P^T L Q$ unlike the angular momentum appearing in the curve of marginal stability Eq. (3.57) which is computed using the moduli-dependent inner product $P \circ Q \equiv P^T (L + M) Q$. One may think of the latter evolving to the former as we follow the attractor flow from infinity to the horizon of the black hole. However it would be nice to have a better physical understanding of the role of dyonic angular momenta in these discussions¹.

¹As is well-known, the dyonic angular momentum plays a physical role in the wall-crossing formulae [25, 17, 13, 14, 32] that describe how the degeneracy jumps, but in the present discussions there are no walls or jumps.

3.6 Discussion

In this work we have obtained the loci of marginal stability for decays of $\frac{1}{4}$ -BPS dyons into any number of BPS constituents in $\mathcal{N} = 4$ string compactifications. These loci appear as equations constraining the $132+2$ moduli, more precisely as a curve of marginal stability in the upper-half-plane that represents a torus moduli space (in the basis of type IIB on $K3 \times T^2$, this is the geometric torus) as well as some more complicated equations on the remaining moduli. While in this chapter we worked with unit-torsion initial dyons, it should be quite straightforward to extend our results to general torsion. We showed how to extend our analysis to multi-particle decays, and found a relation between the loci of marginal stability obtained in this way and the supergravity constraints on pairwise separations of the centres of multi-centred black holes.

The physical role of “rare” marginal dyon decays, namely all those other than of a $\frac{1}{4}$ -BPS dyon into two $\frac{1}{2}$ -BPS dyons, has yet to be explored. Because such decays take place on loci of codimension ≥ 2 in moduli space, they do not form “domain walls” across which the degeneracy can jump. Therefore, in accordance with the discussion in section 2.1, they do not affect the basic entropy or dyon counting formulae. However it is certainly possible that they have other interesting physical effects which may emerge on further investigation.

Chapter 4

String Networks

Our goal here is to develop an understanding of the marginal dyon decays using the properties of string networks. Then we will discuss the classification of arbitrary torsion string networks using dual grid diagrams.

4.1 String Networks

We will consider the system of type IIB theory compactified on $K3$. The U-duality group of this six-dimensional background is $SO(5, 21)$ [38]. On further compactification on a circle to five dimensions, the duality group does not change. Instead, each self-dual or anti-self-dual 2-form reduces to a 2-form in 5d along with a gauge field, with the two being mutually dual. Correspondingly there are dual pairs of charged particles and strings, corresponding to 6d strings that wind or do not wind on x^5 . The resulting 5d theory is T-dual to type IIA on $K3 \times S^1$ which in turn is dual to the heterotic string on T^5 [36, 37].

Compactification on a second circle leads to a 4d theory that can be thought of as IIB on $K3 \times T^2$, IIA on $K3 \times T^2$ or heterotic on T^6 . The electric states of this theory in the IIB frame are 6d strings that wind on x^4 , while the ones that wind on x^5 are magnetic. Winding a particular 6d string on more general 1-cycles of the x^4, x^5 torus produces dyons, but these are $\frac{1}{2}$ -BPS. The more general $\frac{1}{4}$ -BPS dyons arise when we take two distinct 6d strings from the set of 26 enumerated above, then wrap one on the electric and another one on the magnetic direction, and finally allow the configuration to relax into a bound state.

Now we start by describing the BPS mass formulae in the language of winding strings of the type described above. To start with, let us recall the nature of the charge vectors and their inner products. A general BPS string in 6d has a charge vector:

$$\vec{Q} = (\mathcal{Q}_1, \dots, \mathcal{Q}_5; \mathcal{Q}_6, \dots, \mathcal{Q}_{26}) \quad (4.1)$$

Upon further compactification on a 2-torus with coordinates x^4, x^5 we arrive at a 4d theory with electric and magnetic BPS states, corresponding to the BPS strings described above wrapping the x^4 or x^5 directions respectively. These states are $\frac{1}{2}$ -BPS and have either a 28 component electric charge vector \vec{Q} or a magnetic charge vector \vec{P} . More generally we have dyons with charge vectors (\vec{Q}, \vec{P}) . The inner products are defined in terms of the projected charges defined in Eq. (2.8). The modular parameter of the 4 – 5 torus is $\tau = \tau_1 + i\tau_2$ as given before. To illustrate, the charges arise out of a bound states of NS5 branes and D-branes wrapped on $K3 \times T^2$ so that in the limit of very small K3 volume, the bound brane system looks like an effective string one either cycle of the T^2 . Using the duality between the heterotic and IIB descriptions it is easy to see that strings wrapping one cycle become electric and those wrapping the other cycle constitute magnetic charges. Hence an analysis on the lines of marginal stability of these states can shed insights into the curve of marginal stability of the dyons under consideration. There is a simple relation for the BPS string tension in terms of string charge:

$$T_{BPS}^2 = Q_R^2 \quad (4.2)$$

Now for a purely electric $\frac{1}{2}$ -BPS state the mass formula defined in Eq. (2.10) reduces to:

$$M_{BPS}(\vec{Q}_R)^2 = \frac{1}{\tau_2} Q^2 \quad (4.3)$$

while a purely magnetic one has instead:

$$M_{BPS}(\vec{P}_R)^2 = \frac{|\tau|^2}{\tau_2} P^2 \quad (4.4)$$

Notice we are putting back the factor of $\sqrt{\tau_2}$ in this chapter which we removed in previous chapter as it didn't effect our calculations and also simplified them.

For the case when of a dyonic $\frac{1}{2}$ -BPS states having parallel vectors \vec{Q} and \vec{P} :

$$M_{\text{BPS}}(\vec{Q}_R, \vec{P}_R)^2 \Big|_{\vec{Q}_R \parallel \vec{P}_R} = \frac{1}{\tau_2} (\vec{Q}_R - \bar{\tau} \vec{P}_R) \cdot (\vec{Q}_R - \tau \vec{P}_R) \quad (4.5)$$

Now the above formulae can be derived from the winding string picture by noting that the minimum length of a string winding once round the electric (resp. magnetic) direction is $\sqrt{\frac{A}{\tau_2}}$ (resp. $\sqrt{\frac{A}{\tau_2}}|\tau|$) where A is the area of the 4-5 torus. More generally, the length of a string winding q times along x^4 and p times along x^5 is $\sqrt{\frac{A}{\tau_2}}|q + p\tau|$ (in what follows, we will refer to such a string as a (p, q) wound string). Now if the string in question has a charge vector \vec{Q}_R , then when it winds, the resulting BPS particle has electric and magnetic charge vectors $\vec{Q}_R = q\vec{Q}_R, \vec{P}_R = -p\vec{Q}_R$. From Eq. (4.2) we see that the BPS mass is:

$$\begin{aligned} M_{\text{BPS}}(q\vec{Q}_R, p\vec{Q}_R) &= \sqrt{\frac{A}{\tau_2}} |q + p\tau| \sqrt{\mathcal{Q}^2} \\ &= \sqrt{\frac{A}{\tau_2}} \sqrt{(\vec{Q} - \bar{\tau} \vec{P}) \cdot (\vec{Q} - \tau \vec{P})} \end{aligned} \quad (4.6)$$

which agrees with Eq. (4.5) upto an overall factor of \sqrt{A} which is accounted for by the relation between the metric in 6d and 4d. Henceforth we drop this factor of \sqrt{A} .

Let us now turn to the $\frac{1}{4}$ -BPS dyons. These have non-parallel charge vectors \vec{Q}, \vec{P} . The BPS mass formula for these is given by Eq. (2.10) The key point[3] is that these correspond to BPS *string junctions*[21, 22] wrapped over the 4-5 torus. To see this, consider a junction where a string of charge vector \vec{Q}_1 and another string of charge vector \vec{Q}_2 (not parallel to \vec{Q}_1) merge into a string of charge $\vec{Q}_1 + \vec{Q}_2$ and then split back into the original constituents. (This is not by any means the most general configuration, a point to which we will return in the following section.) This can be extended to a periodic string network, in other words one that can be wrapped on a 2-torus. The corresponding dyon has electric and magnetic charge vectors:

$$\vec{Q}_R = \vec{Q}_{1R}, \quad \vec{P}_R = -\vec{Q}_{2R} \quad (4.7)$$

Thus the BPS mass formula Eq. (2.10) becomes:

$$M_{\text{BPS}}^2 = \frac{1}{\tau_2} (\vec{Q}_{1R} + \bar{\tau} \vec{Q}_{2R}) \cdot (\vec{Q}_{1R} + \tau \vec{Q}_{2R}) + 2\sqrt{\Delta(\vec{Q}_{1R}, \vec{Q}_{2R})} \quad (4.8)$$

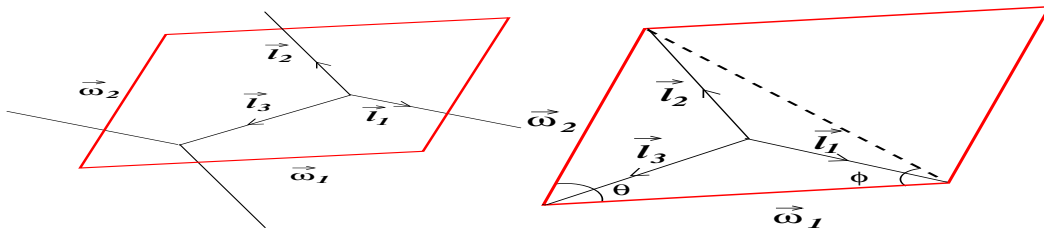


Figure 4.1: A simple periodic network. Same network with a different basic cell.

which is more or less the same formula as before, but expressed in terms of the charge vectors of two different BPS strings of the 6d theory.

Following [22, 40], this can be rewritten as the contribution of different segments of the junction. First of all, suppose that $\text{Re } \tau = \tau_1 = 0$ and also the charge vectors are orthogonal: $\vec{Q}_{1R} \cdot \vec{Q}_{2R} = 0$. In this case the torus is rectangular and the junction degenerates to a pair of intersecting strings (the intervening string shrinks away), so we have:

$$\begin{aligned} m_{\text{network}} &= \sqrt{\frac{1}{\tau_2} (Q_{1R}^2 + S^2 Q_{2R}^2) + 2|Q_{1R}||Q_{2R}|} \\ &= \frac{|\vec{Q}_{1R}|}{\sqrt{\tau_2}} + \sqrt{\tau_2} |\vec{Q}_{2R}| \end{aligned} \quad (4.9)$$

A more general situation, where the torus is slanted but the junction is still degenerate, arises for arbitrary τ_1 if $\vec{Q}_1 \cdot \vec{Q}_2 = -\frac{\tau_1}{|\tau|} |\vec{Q}_1| |\vec{Q}_2|$. In this case we find that:

$$m_{\text{network}} = \frac{|\vec{Q}_1|}{\sqrt{\tau_2}} + \sqrt{\frac{\tau_1^2 + S^2}{\tau_2}} |\vec{Q}_2| \quad (4.10)$$

Therefore the BPS mass is the sum of the BPS masses of two strings of charge vectors \vec{Q}_1, \vec{Q}_2 that are separately wrapped on the electric and magnetic directions to make $\frac{1}{2}$ -BPS particles. This is, in fact, a point of marginal stability.

Finally we consider the basic network of Fig.4.1. We want to show that M_{BPS} in Eq. (2.10) is equal to:

$$m_{\text{network}} = l_1 |\vec{Q}_1| + l_2 |\vec{Q}_2| + l_3 |\vec{Q}_1 + \vec{Q}_2| \quad (4.11)$$

To see this, note that the generators of the torus ω_1, ω_2 , are given by:

$$\begin{aligned}\vec{\omega}_1 &= \vec{l}_1 - \vec{l}_3 \\ \vec{\omega}_2 &= \vec{l}_2 - \vec{l}_3\end{aligned}\tag{4.12}$$

where the \vec{l}_i are all outward-pointing vectors at the junction. Define the angles $\theta, \theta_{12}, \theta_{23}, \theta_{31}$ as follows:

$$\begin{aligned}\vec{\omega}_1 \cdot \vec{\omega}_2 &= |\vec{\omega}_1| |\vec{\omega}_2| \cos \theta \\ \vec{l}_1 \cdot \vec{l}_2 &= l_1 l_2 \cos \theta_{12} \\ \vec{l}_2 \cdot \vec{l}_3 &= l_2 l_3 \cos \theta_{23} \\ \vec{l}_3 \cdot \vec{l}_1 &= l_1 l_3 \cos \theta_{31}\end{aligned}\tag{4.13}$$

satisfying $\theta_{12} + \theta_{23} + \theta_{31} = 2\pi$.

Then the modular parameter τ and area A of the torus are:

$$\begin{aligned}\tau &= \frac{|\vec{\omega}_2|}{|\vec{\omega}_1|} e^{i\theta} \\ A &= |\vec{\omega}_1| |\vec{\omega}_2| \sin \theta\end{aligned}\tag{4.14}$$

From the force balance condition for BPS string junctions, it follows that:

$$\begin{aligned}\vec{Q}_1 \cdot \vec{Q}_2 &= |\vec{Q}_1| |\vec{Q}_2| \cos \theta_{12} \\ \sin \theta_{13} |\vec{Q}_1| &= \sin \theta_{23} |\vec{Q}_2| \\ |\vec{Q}_1 + \vec{Q}_2| &= -\cos \theta_{31} |\vec{Q}_1| - \cos \theta_{32} |\vec{Q}_2|\end{aligned}\tag{4.15}$$

Inserting the above relations in Eq. (4.8) and dropping a factor of the area A as before, we find:

$$\begin{aligned}M_{\text{BPS}}^2 &= (l_1^2 + l_3^2 - 2 l_1 l_3 \cos \theta_{13}) Q_1^2 + (l_2^2 + l_3^2 - 2 l_2 l_3 \cos \theta_{23}) Q_2^2 \\ &\quad + 2 |\vec{\omega}_1| |\vec{\omega}_2| (\cos \theta_{12} \cos \theta + \sin \theta_{12} \sin \theta) |\vec{Q}_1| |\vec{Q}_2|\end{aligned}\tag{4.16}$$

It is easily shown that

$$|\vec{\omega}_1| |\vec{\omega}_2| (\cos \theta_{12} \cos \theta + \sin \theta_{12} \sin \theta) = l_1 l_2 - l_1 l_3 \cos \theta_{23} - l_2 l_3 \cos \theta_{31} + l_3^2 \cos \theta_{12}\tag{4.17}$$

4.2 Classification of periodic string networks

and therefore

$$\begin{aligned}
M_{\text{BPS}}^2 &= (l_1^2 + l_3^2 - 2 l_1 l_3 \cos \theta_{13}) \mathcal{Q}_1^2 + (l_2^2 + l_3^2 - 2 l_2 l_3 \cos \theta_{23}) \mathcal{Q}_2^2 \\
&\quad + 2 (l_1 l_2 - l_1 l_3 \cos \theta_{23} - l_2 l_3 \cos \theta_{31} + l_3^2 \cos \theta_{12}) |\vec{\mathcal{Q}}_1| |\vec{\mathcal{Q}}_2| \quad (4.18)
\end{aligned}$$

Finally, using Eq. (4.15), we end up with:

$$M_{\text{BPS}} = l_1 |\vec{\mathcal{Q}}_1| + l_2 |\vec{\mathcal{Q}}_2| + l_3 |\vec{\mathcal{Q}}_1 + \vec{\mathcal{Q}}_2| = m_{\text{network}} \quad (4.19)$$

as desired.

From the above considerations we see that the $\frac{1}{4}$ -BPS state we have considered, with charge vectors \vec{Q}, \vec{P} , is equivalent to a string junction made of three types of strings with charge vectors $\vec{\mathcal{Q}}_1 = \vec{Q}, \vec{\mathcal{Q}}_2 = \vec{P}$ and $\vec{\mathcal{Q}}_1 + \vec{\mathcal{Q}}_2$. In the following sections we first examine the simplest junctions and study their possible modes of marginal decay. Thereafter we generalize these considerations to include the most general $\frac{1}{4}$ -BPS states and study a number of their properties.

4.2 Classification of periodic string networks

From the discussions of the previous section, classifying $\frac{1}{4}$ -BPS dyons amounts to classifying all periodic string networks on the torus. Previous discussions of this classification problem were mostly in the context of non-periodic networks with infinitely extended external strings, see Refs.[39, 40]. Recently some aspects of periodic networks were discussed in Ref.[11]. Below we will provide a complete classification procedure for periodic string networks, in the process re-deriving and extending some of the considerations in Ref.[11].

4.2.1 Some general properties

Start with a state with dyonic charge vector (\vec{Q}, \vec{P}) . Because of the force-balance condition, all the strings in the network must lie in the linear span of \vec{Q}, \vec{P} . The corresponding string network, when inscribed on a torus, will have a net number of strings of total charge \vec{Q} winding around the x^4 direction and another number of strings of total charge \vec{P} winding on the x^5 direction. In the standard representation of the torus as a parallelogram, the most convenient way to identify

4.2 Classification of periodic string networks

these charges is to add up the charge vectors of all the strings going “out” of the parallelogram towards the right and the top respectively.

Suppose V, E, F are the total number of vertices, edges and faces in the network. The fact that the network is on a torus means that $V - E + F = 0$. Suppose also that the network is completely non-degenerate, meaning that all vertices are three-string junctions (as opposed to the situation when a string degenerates to zero length, in which case two three-point vertices merge to form a four-point vertex, which should really be thought of as two strings crossing each other). It follows that $2E = 3V$. Therefore the number of vertices is always even and the number of edges is a multiple of 3.

Next, write:

$$\vec{Q} = m\vec{Q}_1, \quad \vec{P} = n\vec{Q}_2 \tag{4.20}$$

where m, n are the largest integer factors in \vec{Q}, \vec{P} respectively. As defined before when $m = n = 1$ we call the dyon has *unit torsion*. The corresponding network necessarily has a single string of charge \vec{Q}_1 going out towards the right of the torus and a single string of charge \vec{Q}_2 going out towards the top. The unique way to join these into a non-degenerate network is the one depicted in Fig.4.1. This is a hexagonal network with $V = 2, E = 3$. It follows that all unit torsion string networks on the torus are hexagonal. To make contact with the observations in Ref.[11] we note that I in that reference is just mn in our discussion, therefore the networks that we say have unit torsion are those having $I = 1$ ¹.

Arbitrary torsion networks have a more complicated structure. Suppose first that $(m, n) \neq (1, 1)$ and are relatively prime. We will refer to this case as an irreducible $\frac{1}{4}$ -BPS dyon. At a generic point in moduli space, it is represented by a non-degenerate string web with m strings of charge \vec{Q}_1 wrapping x^4 and n strings of charge \vec{Q}_2 wrapping x^5 . The total number of vertices in this network is $2mn$. One way to see this is that if the strings just cross each other forming a completely degenerate network then we have mn four-point intersections, but in the fully non-degenerate case each four-point intersection is blown up into a pair of three-point vertices which are therefore $2mn$ in number. It also follows that

¹In an M-theory lift they correspond to genus-2 surfaces. Here we focus primarily on the string network representation.

4.2 Classification of periodic string networks

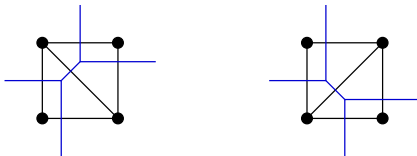


Figure 4.3: Dual grid diagrams and networks for $(m, n) = (1, 1)$

This is a well-defined question. We have already seen that when $(m, n) = (1, 1)$ the topology is that of a hexagonal lattice and therefore unique. For the other cases, a method to obtain all possible topologies can be found by adapting the idea of dual grid diagrams[40] to the present case, which differs from the cases considered in the older literature in two ways: (i) instead of two possible types of strings (F and D) and their bound states, we have 26 types of strings and their bound states, and (ii) the resulting networks are to be drawn on a torus.

We have seen that fixing the charges of a dyon amounts to choosing two unit torsion charge vectors \vec{Q}_1, \vec{Q}_2 in terms of which the charges are represented as $m\vec{Q}_1, n\vec{Q}_2$. Since BPS networks are planar, and the directions of the strings are determined by the charge vectors, it follows that all charges appearing in a planar BPS network are in the linear span (with integer coefficients) of \vec{Q}_1, \vec{Q}_2 . Therefore after fixing \vec{Q}_1, \vec{Q}_2 , all possible networks and their degeneration can be understood in terms of the two integers m, n . This essentially makes this problem similar to the one of F- and D-string junctions for which dual grid diagrams were originally proposed.

Now we address the more nontrivial issue of periodicity. Let us represent an m, n dyon by a rectangular grid of m points by n points. The outer walls of the rectangle are drawn as solid lines. Additional solid lines are drawn joining any pair of points in the grid, but intersecting lines are not allowed. When no more lines can be added, the diagram is called non-degenerate. In this case the interior of the rectangle has been divided up into triangles. Degenerate diagrams can be drawn by removing any subset of internal lines of a non-degenerate diagram. The allowed non-degenerate dual grid diagrams for $(1, 1)$ and $(1, 2)$ dyons are shown in Figs. 4.3, 4.4. Some of them are related to others by obvious symmetries. In

4.2 Classification of periodic string networks

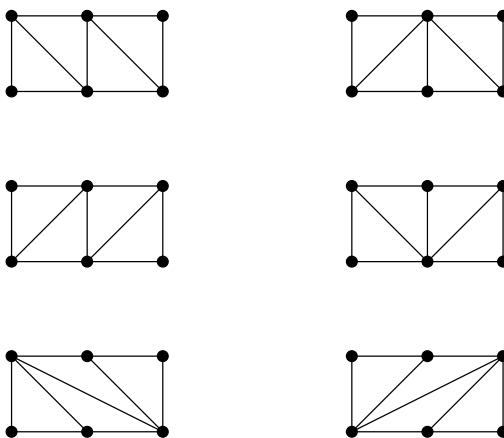


Figure 4.4: Dual grid diagrams for $(m, n) = (1, 2)$

what follows, the grid diagrams of interest to us will always be the non-degenerate ones.

Given such a diagram, a periodic network is constructed as follows. Draw strings passing transversely through every line of the grid diagram. The charge vector of each string coming in from the left is \vec{Q}_1 and of each one coming in from the bottom is \vec{Q}_2 . The remaining charge vectors can be assigned by charge conservation at a vertex, or equivalently by noting that a line in the grid diagram described by the 2-vector $(n, -m)$ is crossed by an (m, n) string. Once a string network has been drawn in this way we can forget about the original grid diagram. We are left with an open string network (“open” in the sense that some strings are emerging from it) with m strings of charge vector \vec{Q}_1 coming in from the left and going out to the right, and n strings of charge vector \vec{Q}_2 coming in from below and emerging at the top. This non-periodic network will constitute the unit cell of a periodic network of strings.

Next we adjust the angles between the strings at every vertex to ensure force balance. For much of the following discussion we will find it convenient to choose $\vec{Q}_1 \cdot \vec{Q}_2 = 0$ in which case the incoming and outgoing strings are either horizontal or vertical, but the general case is not much more complicated. Some dual grid diagrams and their corresponding open networks after performing this operation are shown in Fig.4.5.

4.2 Classification of periodic string networks

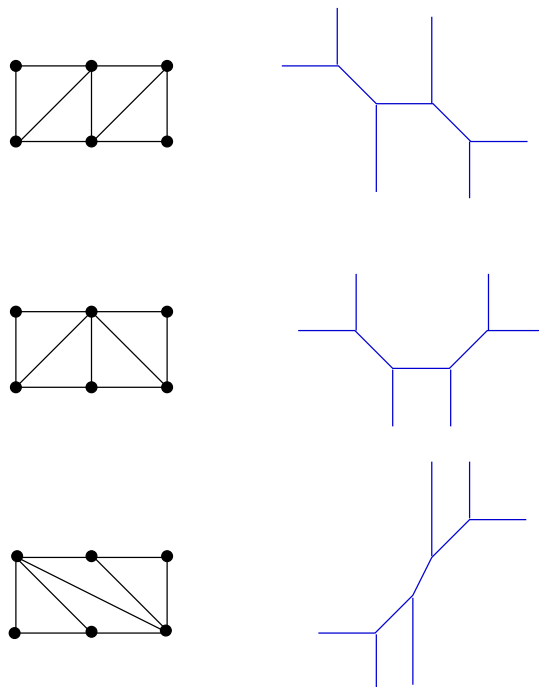


Figure 4.5: Some grid diagrams and their corresponding networks, for $(m, n) = (1, 2)$

Now we can allow the internal and external lengths in the open network to vary. However, this variation must be consistent with the possibility of making a periodic network out of the given open network. This restricts the number of independent parameters, for which we now derive a formula.

Consider a dual grid diagram with m rows and n columns. We will show that the total number of freely adjustable parameters consistent with making the corresponding string network periodic is $mn + 2$.

Before doing this, we single out a class of special cases where all diagonals in the network are "simple", namely they are created by joining a single horizontal and a single vertical string. In the dual grid diagram this corresponds to all diagonals lying at 45 degrees, or equivalently being diagonals of a unit square. There are 2^{mn} such grid diagrams, corresponding to an independent choice of orientation of the diagonal in each unit square. An example of a "simple" grid diagram is shown in Fig 4.6.

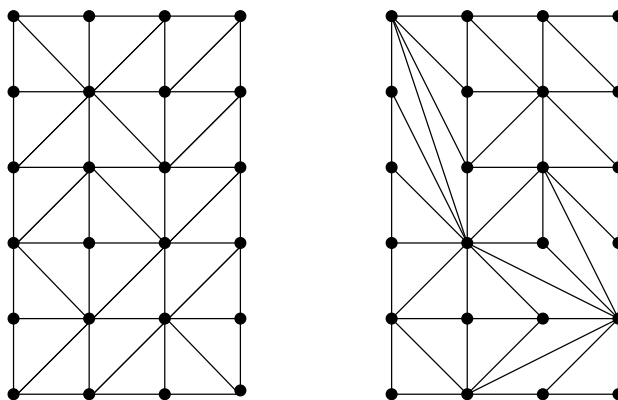


Figure 4.6: A simple and a non-simple 5×3 grid diagram.

More complicated diagonals in the network occur when a vertical or horizontal string joins a diagonal one such that the outgoing string is slanted at more than 45 degrees. In the dual diagram this corresponds to diagonals that extend across more than one unit square, as on the right hand side of Fig.4.6.

For the counting, let us start with the simplest of all (m, n) grid diagrams, in which all diagonals are parallel. This, along with its accompanying open network which is a hexagonal lattice, is illustrated in Fig.4.7. It is easy to count the number of free parameters in the corresponding network. There are mn lines of each type: horizontal, vertical and diagonal, making $3mn$ altogether. Incorporating them into a network with fixed angles puts constraints on the lengths of these $3mn$ lines. We can think of these constraints as follows. In a given row there is a set of $n - 1$ spacings between consecutive vertical lines. These must be matched with those of the following row, leading to $n - 1$ constraints per row, or $m(n - 1)$ “row-type” constraints. Similarly there are $n(m - 1)$ “column-type” constraints. Finally when we make the open network periodic, we find constraints on the external lines. The horizontal ones are all determined by the periodicity requirement in terms of one horizontal line, making $(m - 1)$ constraints, and similarly there are $(n - 1)$ constraints on the vertical ones. This exhausts all the

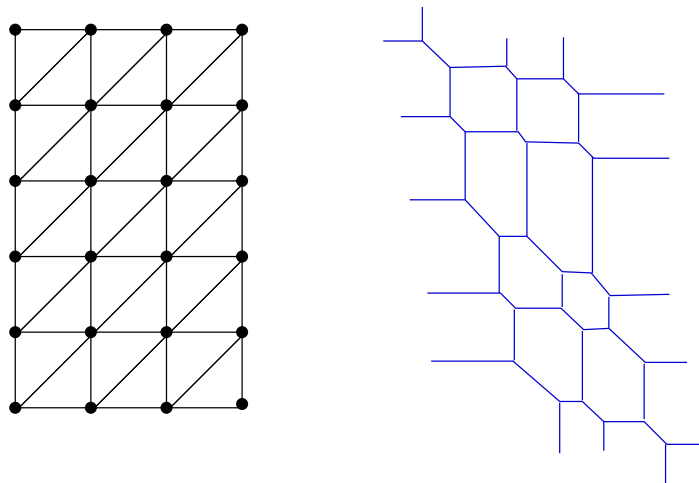


Figure 4.7: The simplest (m, n) grid diagram.

constraints¹. Thus we have:

$$3mn - m(n - 1) - n(m - 1) - (m - 1) - (n - 1) = mn + 2 \quad (4.21)$$

as the final number of free parameters in a network of the type shown in Fig.4.7.

Turning now to more general, but still “simple”, grid diagrams as on the left side of Fig.4.6, we notice that any such diagram can be obtained from the one of Fig.4.7 by a series of “flops” which consist of individual diagonals within unit squares being replaced by the opposite diagonals of these squares. These “flops” can be thought of as a four-string junction inside the network having its intermediate line shrink to zero and grow back with the opposite orientation. After a flop, the number of adjustable parameters is the same as before since we have merely replaced a diagonal by another one. In fact for all simple grid diagrams, the counting can be done as before by identifying lengths and constraints, and leads to the same result as for the simplest case.

Now let us turn to the most general case, like the one shown on the right hand side of Fig.4.6. Although it seems less obvious, here too one can obtain the grid diagram by a series of “flops” starting from the simplest one of Fig.4.7. This time

¹In addition there is a discrete choice involving a cyclic permutation of the outgoing lines, which will play an important role in what follows but is not relevant for parameter counting.

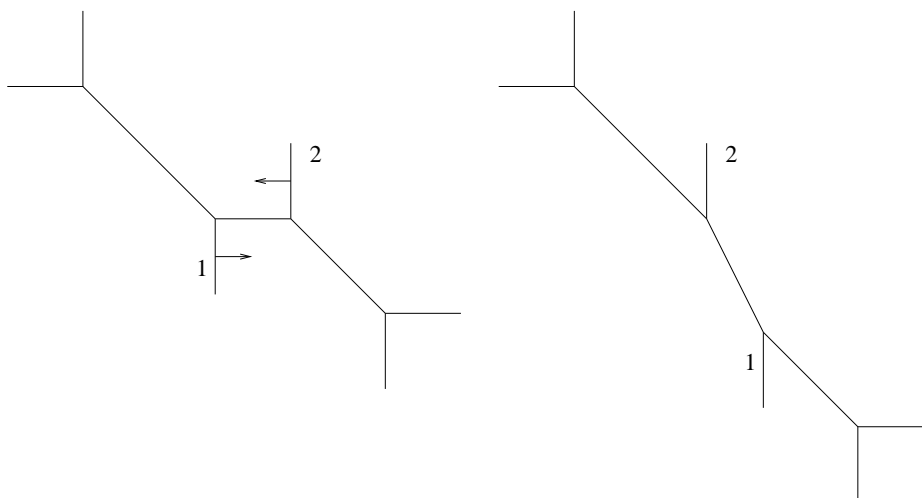


Figure 4.8: A flop where a horizontal line is replaced by a diagonal.

the flops are not solely of the diagonals, but also of the horizontal and vertical internal lines. An example of such a flop is depicted in Fig 4.8. We conclude that all periodic $m \times n$ string networks have the same number of independent parameters, namely $mn + 2$.

There is a useful check to this formula. If we try to inscribe a periodic network with $mn + 2$ length parameters on a 2-torus, this fixes three parameters of the network in terms of the three torus parameters: the complex modular parameter and the area. That leaves $mn - 1$ free parameters for the toroidal network, precisely equal to the number of zero modes that we have already determined.

It is worth mentioning here that the parameter space is bounded by the requirement that all the lengths be positive or zero. The boundary is reached when one or more strings shrink to zero length, causing a degeneration of some segment of the whole network into crossed strings. A “flop”, where a new string then grows back with a different orientation, corresponds in some ways to a negative length parameter, much like what happens at Calabi-Yau singularities.

4.2.3 Periodic identifications

To complete our classification, we now need to address the issue of periodic identifications. For definiteness, consider the open network depicted in Fig.4.7. We see that it has three strings emerging from top and bottom. To make a periodic network out of this, we need to pairwise identify these strings. Clearly there are three distinct ways to do this, which are just cyclic permutations of each other. Similarly, when we identify the five horizontal strings at left with their counterparts on the right, we encounter a five-fold choice corresponding to cyclic permutations. In more generality, given a specific (m, n) grid diagram and its associated open network, we want to ask how many ways this network can be closed into a periodic one on a torus. The possible ways can be labelled by a pair of integers (r, s) , $0 \leq r \leq m, 0 \leq s \leq n$. What we will see is that for a given dual grid diagram, not all (r, s) lead to valid networks. The reason is that in some cases the length constraints can only be solved by assigning a negative length to one or more of the lines. In this case the given (non-degenerate) grid diagram does not lead to a periodic network, though some “flopped” version of it may be allowed, since as mentioned above, a negative length can typically be thought of as a positive length after a flop.

Let us work this out in detail for the case of a $(1, 3)$ network. This, with all its length parameters labelled, is shown in Fig.4.9. Note that v_{ij} are to be understood as the total lengths of the vertical lines after suitable identifications of the upper and lower verticals. We have introduced $\sqrt{2}$ factors in the definition of the diagonal lengths to simplify the resulting formulae.

Let us make this periodic by identifying the first vertical line on the top with the first one below. In terms of our previous notation this can be labelled as an $(r, s) = (0, 0)$ identification. The resulting constraint equations can be read off from the figure, and are:

$$\begin{aligned}
 h_{12} + d_{11} &= h_{12} + d_{12} \\
 h_{13} + d_{12} &= h_{13} + d_{13} \\
 v_{11} + d_{11} &= v_{12} + d_{12} = v_{13} + d_{13}
 \end{aligned}
 \tag{4.22}$$

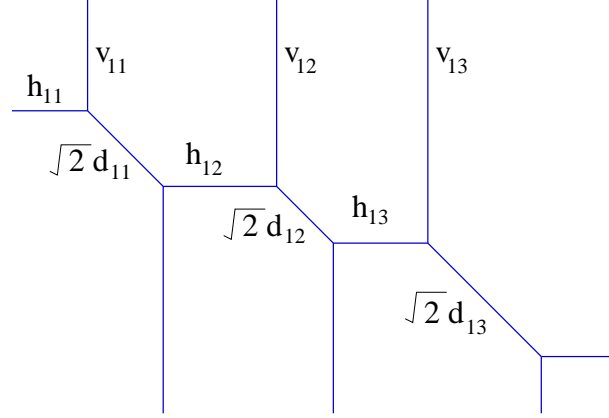


Figure 4.9: A (1, 3) open network with labelled lengths.

As expected, these are 4 equations on 9 variables and they leave 5 independent variables. These variables must be taken to be one diagonal (since all diagonals are set equal), one vertical (for the same reason) and three horizontals, all of which remain independent and arbitrary.

Now let us consider the next identification, in which the first line on the top is identified with the second line below. In this case, which corresponds to $(r, s) = (0, 1)$, the equations are:

$$\begin{aligned}
 h_{12} + d_{11} &= h_{13} + d_{13} \\
 h_{13} + d_{12} &= h_{11} + d_{11} \\
 v_{11} + d_{11} + d_{12} &= v_{12} + d_{12} + d_{13} = v_{13} + d_{13} + d_{11}
 \end{aligned} \tag{4.23}$$

This time we can arbitrarily choose, for example, three diagonals, one horizontal and one vertical, or else three horizontals, one diagonal and one vertical.

Finally the identification obtained by matching the first line on top to the third line below, namely $(r, s) = (0, 2)$, leads to the equations:

$$\begin{aligned}
 h_{12} + d_{11} &= h_{11} + d_{11} \\
 h_{13} + d_{12} &= h_{12} + d_{12} \\
 v_{11} &= v_{12} = v_{13}
 \end{aligned} \tag{4.24}$$

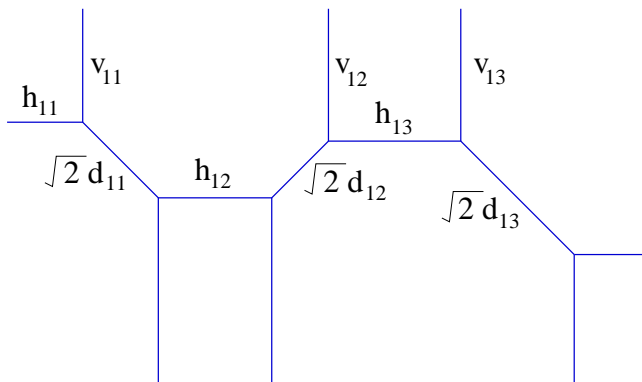


Figure 4.10: A different (1, 3) open network with labelled lengths.

This time all the verticals are equal and the remaining independent variables are three diagonals and a horizontal or the other way around.

We see that all the periodic identifications are allowed for the particular open network in Fig.4.9. However, if we choose a different network with the same charges, as in Fig.4.10, then things will be rather different.

In this case, if we match the first vertical lines on top and bottom, the resulting equations are:

$$\begin{aligned}
 h_{12} + d_{11} + d_{12} &= h_{12} \\
 h_{13} &= h_{13} + d_{12} + d_{13} \\
 v_{11} + d_{11} &= v_{12} + d_{12} = v_{13} + d_{13}
 \end{aligned} \tag{4.25}$$

which has no solutions if we require all lengths to be positive. If we allow one diagonal, say d_{12} , to be negative then we can have solutions, but those will correspond to the network of Fig.4.9 which we have already taken into account.

This only shows that the $(r, s) = (0, 0)$ identification does not work for the network of Fig.4.10. With $(r, s) = (0, 1)$ we instead have:

$$\begin{aligned}
 h_{12} + d_{11} + d_{12} &= h_{13} + d_{12} + d_{13} \\
 h_{13} &= h_{11} + d_{11} \\
 v_{11} + d_{11} &= v_{12} + d_{13} = v_{13} + d_{13} + d_{11}
 \end{aligned} \tag{4.26}$$

which does admit sensible solutions, for example we can choose all the diagonals independently along with one horizontal and one vertical length. Similarly one can check that $(r, s) = (0, 2)$ is also allowed.

We can generalize from this example to reach the following conclusions. First, for every dual grid diagram and its corresponding open string network there are several possible periodic networks, depending on the (r, s) shift in the identification of vertical and horizontal external lines. Second, some of these may be disallowed by the positivity condition on lengths.

4.3 Discussion

In this chapter we discussed the process of marginal decay of a $\frac{1}{4}$ -BPS in terms of BPS string junctions. We showed how we arrive at the mass formula of a general dyon by calculating the effective length of strings wrapping the T^2 for the basic network. The marginal dyon decay is essentially the process when the length of one of the strings in the string junction vanishes. Implementing this condition on the torus modular parameter we arrive at the curve of marginal stability. Classifying $\frac{1}{4}$ -BPS dyons amounts to classifying all periodic string networks on the torus. We provided a complete classification procedure for periodic string networks. For an arbitrary torsion network, this required us to study the dual grid diagrams. For a given dual grid diagram, the force balance condition and periodicity restricts the number of allowed topologically distinct non-degenerate networks. We illustrated this fact using few higher torsion string networks.

Chapter 5

Kinematical Analogy for Marginal Dyon Decay

Now we explore a kinematical analogy for the previously discussed marginal decay of $\frac{1}{4}$ -BPS dyons in 4-dimensional $\mathcal{N} = 4$ string compactifications. In this analogy, the electric and magnetic charges play the role of spatial momenta, the BPS mass plays the role of energy, and $\frac{1}{2}$ -BPS dyons correspond to massless particles. Using $SO(12, 1)$ “Lorentz” invariance and standard kinematical formulae in particle physics, we provide simple derivations of the curves of marginal stability. We also show how these curves map into the momentum ellipsoid, and propose some applications of this analogy.

5.1 Introduction and review

The system and notations we will be working with are the same as that in the previous chapters. we work in the duality frame corresponding to IIB compactification on $K3 \times T^2$ or the heterotic string on T^6 , the two being related by duality. In what follows we will use the duality frame appropriate for type IIB. For purposes of the BPS mass formula, the relevant inner products for the charge vectors are:

$$Q^2 \equiv \vec{Q}^T (M + L) \vec{Q}, \quad P^2 \equiv \vec{P}^T (M + L) \vec{P}, \quad P \cdot Q \equiv \vec{P}^T (M + L) \vec{Q} \quad (5.1)$$

We define these right-moving projections of the charge vectors, \vec{Q}_R, \vec{P}_R , by:

$$Q_R^2 \equiv \vec{Q}_R^T \vec{Q}_R = \vec{Q}^T (M + L) \vec{Q} = Q^2 \quad (5.2)$$

and similarly for the other inner products. In this way the moduli-dependent inner product Eq. (5.1) for the charge vectors is replaced by a standard moduli-independent product while the moduli-dependence is moved to the vectors themselves¹. In what follows, we will not always write the suffix R , since the inner products are by definition the same whether we are dealing with the projected or unprojected vector. The BPS mass formula for general $\frac{1}{4}$ -BPS dyons is [18, 48, 10] defined before Eq. (2.10), where τ is the modular parameter of the torus².

5.1.1 Kinematic Analogy

The formula Eq. (2.10) has a striking analogy to the energy-momentum dispersion relation for a relativistic point particle, $E^2 = \vec{p}^2 + m^2$. In this analogy, the BPS mass plays the role of the energy of the particle, while the dyonic charges play the role of momenta:

$$\vec{p} = \frac{1}{\sqrt{\tau_2}} (\vec{Q} - \tau \vec{P}) \quad (5.3)$$

Conservation of dyonic charge corresponds to momentum conservation in the kinematical system. For this, it is crucial that τ be complex (in fact it has a strictly positive imaginary part). Then conservation of the imaginary part of the momentum is equivalent to conservation of the dyon's magnetic charge, while the real part ensures conservation of electric charge.

To complete the analogy, note that the condition of marginal stability in a decay: $M^{\text{BPS}} = M_1^{\text{BPS}} + M_2^{\text{BPS}} + \dots$ corresponds to energy conservation. Finally, the mass of the analogue particle is $\sqrt{2} \left(\Delta(\vec{Q}, \vec{P}) \right)^{\frac{1}{4}}$. A $\frac{1}{2}$ -BPS dyon has its electric and magnetic charge vectors proportional, so $\Delta(\vec{Q}, \vec{P}) = 0$. It therefore corresponds to a massless particle.

¹This refers to all moduli other than those of the 2-torus, which are always displayed explicitly and do not appear in the inner product.

²Our conventions are those in Ref.[10] and differ by a factor of $\frac{1}{\sqrt{\tau_2}}$ from those in Ref[26].

Because the momentum vector defined in Eq. (5.3) is complex, some care must be taken in defining the inner product. As each of \vec{Q}, \vec{P} is effectively 6-dimensional (recall that they are all projected using a moduli-dependent matrix, as in Eq. (5.2)), one can convert the momenta to real vectors in a 12-dimensional space with Lorentz group $SO(12, 1)$. As we have noted, these Lorentz symmetries are symmetries of the dispersion relation and the kinematics of the decay process, but not of the underlying string theory.

This point can be clarified by considering a general dyonic particle having a momentum \vec{k} in the noncompact three-dimensional space. For such a particle the full dispersion relation is:

$$\begin{aligned} E^2 &= \vec{k}^2 + (M^{\text{BPS}})^2 \\ &= \vec{k}^2 + \frac{1}{\tau_2}(\vec{Q} - \bar{\tau}\vec{P}) \cdot (\vec{Q} - \tau\vec{P}) + 2\sqrt{\Delta(\vec{Q}, \vec{P})} \end{aligned} \quad (5.4)$$

If we restrict our attention to electrically charged particles, $\vec{P} = 0$, the above equation simplifies to:

$$E^2 = \vec{k}^2 + \frac{1}{\tau_2}\vec{Q}^2 \quad (5.5)$$

which can be thought of as the dispersion relation for either a massive particle in 4d or a massless particle in 10d. This is the expected situation for a Kaluza-Klein particle whose electric charges are momenta along the toroidal directions. The dependence on the modulus τ , though present, is trivial in this case and can be removed by rescaling the metric appropriately. However, once we introduce magnetic charges as well then the dispersion relation is nontrivially τ -dependent and also contains the Δ factor. Now if we put $\vec{k} = 0$ then we have the kinematic analogy of interest in the present work.

To recover the curves of marginal stability, consider a general two-body decay of a particle with energy-momentum (E, \vec{p}) into a pair of particles of energy-momentum (E_1, \vec{p}_1) and (E_2, \vec{p}_2) . There are two Lorentz frames that are useful: the rest frame of the initial particle and the lab frame where the initial particle has a given spatial momentum. By working in the rest frame, the Lorentz invariant $p \cdot p_1$ is easily shown to be:

$$p \cdot p_1 = \frac{1}{2}(m^2 + m_1^2 - m_2^2) \quad (5.6)$$

The same Lorentz invariant in the lab frame can be written:

$$p \cdot p_1 = m_1^2 + \sqrt{\vec{p}_1^2 + m_1^2} \sqrt{\vec{p}_2^2 + m_2^2} - \vec{p}_1 \cdot \vec{p}_2 \quad (5.7)$$

Equating the two, we have:

$$\sqrt{\vec{p}_1^2 + m_1^2} \sqrt{\vec{p}_2^2 + m_2^2} - \vec{p}_1 \cdot \vec{p}_2 = \frac{m^2 - m_1^2 - m_2^2}{2} \quad (5.8)$$

To apply this to the decay of a $\frac{1}{4}$ -BPS dyon, we make the substitution in Eq. (5.3) as well as:

$$\vec{p}_1 = \frac{1}{\sqrt{\tau_2}}(\vec{Q}_1 - \tau \vec{P}_1), \quad \vec{p}_2 = \frac{1}{\sqrt{\tau_2}}(\vec{Q}_2 - \tau \vec{P}_2) \quad (5.9)$$

to find:

$$\begin{aligned} \sqrt{|\vec{Q}_1 - \tau \vec{P}_1|^2 + 2\tau_2 \sqrt{\Delta_1}} \sqrt{|\vec{Q}_2 - \tau \vec{P}_2|^2 + 2\tau_2 \sqrt{\Delta_2}} &- \operatorname{Re}(\vec{Q}_1 - \tau \vec{P}_1) \cdot (\vec{Q}_2 - \tau \vec{P}_2) \\ &= \tau_2(\sqrt{\Delta} - \sqrt{\Delta_1} - \sqrt{\Delta_2}) \end{aligned} \quad (5.10)$$

where $\Delta_i = \Delta(\vec{Q}_i, \vec{P}_i)$. For fixed charge vectors \vec{Q}_i, \vec{P}_i and moduli matrix M this is an equation for the torus modular parameter τ . In other words, this is the general curve of marginal stability!

We can relate this to previously derived forms of the curve, as in [10, 15, 26]. First let us consider the case of decay of a primitive ($\gcd(\vec{Q} \wedge \vec{P}) = 1$) $\frac{1}{4}$ -BPS dyon into two $\frac{1}{2}$ -BPS dyons. In this case the product particles are massless. Moreover, the charge vectors of the decay products are given by[10]:

$$\begin{aligned} \vec{Q}_1 &= a\vec{N}_1, & \vec{P}_1 &= c\vec{N}_1 \\ \vec{Q}_2 &= b\vec{N}_2, & \vec{P}_2 &= d\vec{N}_2 \end{aligned} \quad (5.11)$$

where

$$\vec{N}_1 = d\vec{Q} - b\vec{P}, \quad \vec{N}_2 = -c\vec{Q} + a\vec{P} \quad (5.12)$$

and $ad - bc = 1$. Thus the equation reduces to:

$$|a - c\tau| |b - d\tau| \frac{|\vec{N}_1| |\vec{N}_2|}{\sqrt{\Delta}} - \operatorname{Re} \{ (a - c\tau)(b - d\tau) \} \frac{\vec{N}_1 \cdot \vec{N}_2}{\sqrt{\Delta}} = \tau_2 \quad (5.13)$$

Let

$$\mathcal{E} = -\frac{\vec{N}_1 \cdot \vec{N}_2}{\sqrt{\Delta(\vec{N}_1, \vec{N}_2)}} \quad (5.14)$$

It is easily checked that

$$\sqrt{1 + \mathcal{E}^2} = \frac{|\vec{N}_1||\vec{N}_2|}{\sqrt{\Delta(\vec{N}_1, \vec{N}_2)}} \quad (5.15)$$

Using the above equations and the fact that $\Delta(\vec{N}_1, \vec{N}_2) = \Delta(\vec{Q}, \vec{P})$, the curve becomes:

$$|a - c\tau||b - d\bar{\tau}| \sqrt{1 + \mathcal{E}^2} + \text{Re}\{(a - c\tau)(b - d\bar{\tau})\} \mathcal{E} = \tau_2 \quad (5.16)$$

Now one can take the second term to the right side and square both sides, whereupon the resulting quartic (in τ) re-factorises into a perfect square of the familiar Sen circle equation. However there is a neater way to proceed. The above equation is the same as:

$$|(a - c\tau)(b - d\bar{\tau})(\mathcal{E} + i)| + \text{Re}(a - c\tau)(b - d\bar{\tau})(\mathcal{E} + i) = 0 \quad (5.17)$$

which is equivalent to the two conditions:

$$\begin{aligned} \text{Im}(a - c\tau)(b - d\bar{\tau})(\mathcal{E} + i) &= 0 \\ \text{Re}(a - c\tau)(b - d\bar{\tau})(\mathcal{E} + i) &< 0 \end{aligned} \quad (5.18)$$

The first of these is directly the equation of the Sen circle:

$$\left(\tau_1 - \frac{ad + bc}{2cd}\right)^2 + \left(\tau_2 + \frac{\mathcal{E}}{2cd}\right)^2 = \frac{1}{4c^2d^2}(1 + \mathcal{E}^2) \quad (5.19)$$

while the second one restricts us to the $\tau_2 > 0$ region of that circle.

Next consider decays into two $\frac{1}{4}$ -BPS dyons, or one $\frac{1}{4}$ -BPS and one $\frac{1}{2}$ -BPS dyon. In this case the charges of the final states are parametrised as:

$$\begin{aligned} \vec{Q}_1 &= m_1\vec{Q} + r_1\vec{P}, & \vec{P}_1 &= s_1\vec{Q} + n_1\vec{P} \\ \vec{Q}_2 &= (m - m_1)\vec{Q} - r_1\vec{P}, & \vec{P}_2 &= -s_1\vec{Q} + (n - n_1)\vec{P} \end{aligned} \quad (5.20)$$

where the charges of the initial dyon are now $(m\vec{Q}, n\vec{P})$ with $\text{gcd}(\vec{Q} \wedge \vec{P}) = 1$.

Substituting the above into Eq. (5.10), transposing the second term to the right hand side and squaring, one find the earlier derived curve Eq. (2.21):

$$\left(\tau_1 - \frac{m \wedge n}{2ns_1}\right)^2 + \left(\tau_2 + \frac{\mathcal{E}}{2ns_1}\right)^2 = \frac{1}{4n^2s_1^2} \left((m \wedge n)^2 + 4mnr_1s_1 + \mathcal{E}^2 \right) \quad (5.21)$$

where

$$\mathcal{E} \equiv -\frac{\vec{Q}_1 \cdot \vec{P}_2 - \vec{Q}_2 \cdot \vec{P}_1}{\sqrt{\Delta}} = \frac{1}{\sqrt{\Delta}} (ms_1 Q^2 - nr_1 P^2 - (m \wedge n)Q \cdot P) \quad (5.22)$$

and $m \wedge n = m_1n_2 - m_2n_1$. This is the general curve of marginal stability found in [26].

5.1.2 Momentum ellipsoid

For two-body decay of an unstable particle in the lab frame, the final-state particle momenta are constrained to lie on an ellipsoid of revolution, obtained by rotating an ellipse in the forward and transverse momenta $p_{1,\parallel}$ and $p_{1,\perp}$ along the azimuthal angles around the beam axis. It is tempting to guess that the curve of marginal stability coincides with this ellipse, We will see below that this is roughly true but the relationship is more complicated than one might have expected.

Indeed this approach, in which p and p_1 are treated as the independent variables, is not the easiest way to *derive* the curves of marginal stability, which in fact we have already done in the previous section by treating the final-state momenta p_1, p_2 as the independent variables. Nevertheless it is of some conceptual interest to understand how the curves of marginal stability are related to the momentum ellipsoid. One reason why the embedding we will obtain is rather complicated is that the momentum of the initial particle (which determines one axis of the ellipse) itself depends on the modular parameter τ .

To find the momentum ellipsoid, we first eliminate \vec{p}_2 in Eq. (5.8) in favour of \vec{p}, \vec{p}_1 . Then, taking the second term to the right hand side and squaring, we end up with the equation:

$$m^2 \left(p_{1,\parallel} - \frac{|\vec{p}|(m^2 - m_1^2 - m_2^2)}{2m^2} \right)^2 + (\vec{p}^2 + m^2) p_{1,\perp}^2 = \frac{1}{4} \lambda(m^2, m_1^2, m_2^2) \left(1 + \frac{\vec{p}^2}{m^2} \right) \quad (5.23)$$

where

$$\lambda(a, b, c) \equiv a^2 + b^2 + c^2 - 2ab - 2bc - 2ca \quad (5.24)$$

Here $p_{1,\parallel}$ and $p_{1,\perp}$ are the components of \vec{p}_1 along and transverse to the beam. The momentum ellipsoid is the ellipse in Eq. (5.23) rotated about the beam axis.

For decays into two $\frac{1}{2}$ -BPS states, we put $m_1 = m_2 = 0$ and the momentum ellipsoid simplifies considerably into:

$$\frac{\left(p_{1,\parallel} - \frac{|\vec{p}|}{2}\right)^2}{\frac{1}{4}(\vec{p}^2 + m^2)} + \frac{p_{1,\perp}^2}{\frac{1}{4}m^2} = 1 \quad (5.25)$$

Evidently the major axis of the ellipse is proportional to $\sqrt{\vec{p}^2 + m^2}$, which from Eq. (5.3) is τ -dependent. Therefore the momentum ellipsoid itself varies with τ , and the curve of marginal stability is technically not a subspace of a particular ellipsoid. This can be remedied by defining a new variable \tilde{p}_1 via:

$$\tilde{p}_1 \equiv \frac{p_{1,\parallel} - \frac{|\vec{p}|}{2}}{\sqrt{1 + \frac{\vec{p}^2}{m^2}}} \quad (5.26)$$

in terms of which the ellipse becomes a circle with a τ -independent radius:

$$\tilde{p}_1^2 + p_{1,\perp}^2 = \frac{1}{4}m^2 \quad (5.27)$$

From Eqs.(5.3),(5.9) we find:

$$p_{1,\parallel} = \frac{1}{\sqrt{\tau_2}} \frac{\operatorname{Re}\left((\vec{Q} - \tau\vec{P}) \cdot (\vec{Q}_1 - \tau\vec{P}_1)\right)}{|\vec{Q} - \tau\vec{P}|} \quad (5.28)$$

$$p_{1,\perp} = \frac{1}{\sqrt{\tau_2}} \frac{1}{|\vec{Q} - \tau\vec{P}|} \sqrt{|\vec{Q} - \tau\vec{P}|^2 |\vec{Q}_1 - \tau\vec{P}_1|^2 - \left(\operatorname{Re}(\vec{Q} - \tau\vec{P}) \cdot (\vec{Q}_1 - \tau\vec{P}_1)\right)^2}$$

from which one obtains:

$$\begin{aligned} \tilde{p}_1 &= \frac{1}{\sqrt{\tau_2}} \frac{1}{|\vec{Q} - \tau\vec{P}|} \frac{(ad + bc - 2cd\tau_1)Q^2 + (2ab\tau_1 - (ad + bc)|\tau|^2)P^2 + (-2ab + 2cd|\tau|^2)Q \cdot P}{\sqrt{\frac{1}{\tau_2}|\vec{Q} - \tau\vec{P}|^2 + 2\sqrt{\Delta(\vec{Q}, \vec{P})}}} \\ p_{1,\perp} &= \frac{1}{\sqrt{\tau_2}} \frac{1}{|\vec{Q} - \tau\vec{P}|} \sqrt{\Delta(\vec{Q}, \vec{P})} \sqrt{\left(\operatorname{Re}(a - c\tau)(b - d\tau)\right)^2 + (\mathcal{E}^2 + 1)\tau_2^2} \end{aligned} \quad (5.29)$$

where \mathcal{E} has been defined in Eq. (5.14). As promised, this is rather complicated. One might hope to find a better parametrisation that leads to a simpler embedding.

5.1.3 Multiparticle decays and the issue of codimension

As is well known, kinematics alone does not determine whether a decay actually takes place. In the present situation, an additional constraint is furnished by the fact that a BPS particle cannot decay into a non-BPS final state. If we violate this condition, the matrix element for the decay will vanish by supersymmetry.

In order for the particles in the final state to be BPS relative to each other, it is known that $\vec{Q}_{i,R}, \vec{P}_{i,R}$ must lie in the same plane as \vec{Q}_R, \vec{P}_R . Along with the kinematics, this condition implies that all decays other than two-body decays into $\frac{1}{2}$ -BPS particles occur on codimension ≥ 2 subspaces of moduli space, as noted in Refs.[15, 26].

We can incorporate this property into the kinematical analogy. Let us impose on our 12-dimensional space the structure of a linear symplectic manifold. Thus there is a polarization - a closed, non-degenerate 2-form that divides the space into 6 electric and 6 magnetic directions, each one a Lagrangian subspace analogous to coordinates and momenta in a phase space.

Consider a particle of arbitrary 12-momentum. We use the polarization to divide this momentum into its electric and magnetic parts, each being a 6-vector. Now consider the “diagonal” 6-manifold obtained by identifying the electric and magnetic subspaces. In this 6-manifold, the linear span of the electric and magnetic parts of the 12-momentum defines a plane (if these 6-vectors are non-parallel) or a line (if they are parallel). The former case is $\frac{1}{4}$ -BPS while the latter is $\frac{1}{2}$ -BPS.

In a two-body decay, if the original particle defines a plane in the “diagonal” space while the final particles define lines, then by momentum conservation the BPS condition is automatically satisfied. If the final state particles are $\frac{1}{2}$ -BPS but three or more in number, or if at least one of them is $\frac{1}{4}$ -BPS, then the dimensionality of the subspace of the diagonal space spanned is at least three. In this case, additional conditions on the moduli besides the marginal stability condition are required to make the decay possible[15, 26]. The embedding of codimension ≥ 2 curves in the full moduli space has, however, not yet been given a precise description.

5.1.4 Decay widths on marginal stability curves

The kinematical analogy suggests that one consider decay and scattering processes involving dyons on curves of marginal stability. As a simple example, consider an ensemble of $\frac{1}{4}$ -BPS dyons of a given charge, at a curve of marginal stability for decay into two $\frac{1}{2}$ -BPS dyons. The ensemble will decay with a width given by a formula analogous to the classic formula for decay of a particle of mass m into two identical massless particles, which in three noncompact space dimensions and in the rest frame of the decaying particle is (see for example Ref.[34]):

$$\Gamma = \frac{1}{32\pi\hbar m} |\mathcal{M}|^2 \quad (5.30)$$

where \mathcal{M} is the matrix element for the process.

To apply this formula to the present case the kinematics needs to be re-done in the lab frame of the decaying particle, and in 12 dimensions. We also need to take into account the quantization rule for the analogue momenta, inherited from the quantization of the original electric and magnetic charges. Finally, the matrix element \mathcal{M} needs to be computed. It seems quite plausible that everything here is computable in string theory. One can similarly consider scattering cross-sections for dyons.

Discussion

We have presented an analogy that maps the marginal stability conditions for $\frac{1}{4}$ -BPS dyons into energy-momentum conservation in an analogue particle problem in 12+1 dimensions. $\frac{1}{4}$ -BPS states behave like massive particles and $\frac{1}{2}$ -BPS states like massless particles. The analogy provides a simple way to understand curves of marginal stability and useful both in deriving these curves in other situations and in suggesting ways to think about physical processes involving $\frac{1}{4}$ -BPS dyons.

Chapter 6

Conclusions

In the thesis we extensively discussed the process of marginal decay of a $\frac{1}{4}$ BPS dyonic states. We derived the curve of marginal stability in the torus moduli space for the most general $\frac{1}{4}$ BPS dyon decay in $N = 4$ supersymmetric string theory. Earlier works had shown that when the product dyons are $\frac{1}{2}$ BPS, the decay happens across a curve of codimension 1 and hence it leads to a jump in the entropy of the system. This was done for the case of original dyon having unit torsion. Furthermore in the gravity description this jump can be accounted for by appearance and disappearance of two centered small black holes . We extended this to the most general case when either one or both the products can be $\frac{1}{4}$ BPS dyon with the original dyon having arbitrary torsion and derived the equation of curve of marginal stability for this process. Some solutions of our equation turned out to be "spurious", in the sense that they described a possible reverse decay instead of forward decay. We provided an algorithm to rule out these reverse decay channels. For the case when both products are $\frac{1}{2}$ BPS, we discovered a similarity of the marginal curves with well known mathematical construction of Farey sequence and Ford circles. This helped us in establishing the non-intersecting behaviour of the curves in the upper half plane. We analyzed the marginal curves for the case of higher torsion. It was easy to produce example for this case where we showed that the curves do intersect in the upper half plane. The intersection point of these curves

In the next chapter we have obtained the complete set of constraint equations on all the moduli of the theory for the $\frac{1}{4}$ BPS dyon decay to happen. These

constraints come from the condition that the initial and final dyons are mutually supersymmetric. The initial and final dyons are made mutually supersymmetric by bringing the planes of the final charge vectors to the plane formed by the initial electric and magnetic charges. For the case when both the product dyons are $\frac{1}{2}$ BPS, the charge vectors already lie in the same plane. Therefore because of enough supersymmetry, there is only one constraint equation coming from the mass conservation in this case and hence the curve of marginal stability is of codimension 1. However when either one or both of the products are $\frac{1}{4}$ BPS, the moduli are adjusted to bring their charge vectors in a plane. We derived the most general set of these constraint equations on the moduli which are to be satisfied for the marginal decay to happen. The number of constraints can be any arbitrary number depending on the components on initial and final charges. We showed that the maximum number of these constraint equation will be 9. We also extended our analysis to the multi-centered decays, and found a relation between the loci of marginal stability obtained in this way and the supergravity constraints on pairwise separations of the centres of multi-centered black holes.

Studying the string networks provided us a deep insight about the dynamics of marginal decay of a dyon. We showed how we arrive at the mass formula for a unit torsion dyon. It was effectively the product of the string tension and the string length in a basic cell. A string network wrapped on a torus is necessarily a periodic network. We provided a classification procedure for such periodic networks. An arbitrary torsion dyon is represented by a rather complicated string network, but we can easily calculate the number of zero bosonic modes using the networks. A counting problem would involve quantizing these zero bosonic modes which we have not addressed in our work. Dual grid diagrams are useful tools while studying the string network. For a given grid diagram number of topologically distinct non-degenerate diagrams can be drawn. We explained the procedure of constructing the periodic string networks for a given dual grid diagram.

Further we discussed an intriguing analogy between the decay of a $\frac{1}{4}$ BPS dyon and that of an unstable particle in particle physics. This gave an alternative approach to the problem of marginal dyon decay and we could derive the equation of curve of marginal stability in much simpler way using this analogy.

References

- [1] D. Shih, A. Strominger, and X. Yin, *Recounting dyons in $N = 4$ string theory*, *JHEP* **10** (2006) 087, [[hep-th/0505094](#)].
- [2] A. Strominger, C. Vafa, *Microscopic origin of the Bekenstein-Hawking entropy*, *Phys. Lett.***D379**(1996) 99–104, [[hep-th/9601029](#)].
- [3] D. Gaiotto, *Re-recounting dyons in $N = 4$ string theory*, [hep-th/0506249](#).
- [4] D. P. Jatkar and A. Sen, *Dyon spectrum in CHL models*, *JHEP* **04** (2006) 018, [[hep-th/0510147](#)].
- [5] J. R. David, D. P. Jatkar, and A. Sen, *Product representation of dyon partition function in CHL models*, *JHEP* **06** (2006) 064, [[hep-th/0602254](#)].
- [6] J. R. David and A. Sen, *CHL dyons and statistical entropy function from $D1$ - $D5$ system*, *JHEP* **11** (2006) 072, [[hep-th/0605210](#)].
- [7] J. R. David, D. P. Jatkar, and A. Sen, *Dyon spectrum in $N = 4$ supersymmetric type II string theories*, *JHEP* **11** (2006) 073, [[hep-th/0607155](#)].
- [8] J. R. David, D. P. Jatkar, and A. Sen, *Dyon spectrum in generic $N = 4$ supersymmetric $Z(N)$ orbifolds*, *JHEP* **01** (2007) 016, [[hep-th/0609109](#)].
- [9] A. Dabholkar and D. Gaiotto, *Spectrum of CHL dyons from genus-two partition function*, [hep-th/0612011](#).
- [10] A. Sen, *Walls of marginal stability and dyon spectrum in $N=4$ supersymmetric string theories*, [hep-th/0702141](#).

REFERENCES

- [11] A. Dabholkar, D. Gaiotto, and S. Nampuri, *Comments on the spectrum of CHL dyons*, [hep-th/0702150](#).
- [12] N. Banerjee, D. P. Jatkar, and A. Sen, *Adding charges to $N = 4$ dyons*, [0705.1433](#).
- [13] A. Sen, *Two centered black holes and $N=4$ dyon spectrum*, [0705.3874](#).
- [14] M. C. N. Cheng and E. Verlinde, *Dying dyons don't count*, [0706.2363](#).
- [15] A. Sen, *Rare decay modes of quarter BPS dyons*, [0707.1563](#).
- [16] R. Dijkgraaf, E. P. Verlinde, and H. L. Verlinde, *Counting dyons in $N = 4$ string theory*, *Nucl. Phys.* **B484** (1997) 543–561, [[hep-th/9607026](#)].
- [17] F. Denef and G. W. Moore, *Split states, entropy enigmas, holes and halos*, [hep-th/0702146](#).
- [18] M. Cvetič and D. Youm, *Dyonic bps saturated black holes of heterotic string on a six torus*, *Phys. Rev.* **D53** (1996) 584–588, [[hep-th/9507090](#)].
- [19] S. Lang, *Algebra*. Addison-Wesley, 1993.
- [20] O. Aharony, A. Hanany, and B. Kol, *Webs of (p,q) 5-branes, five dimensional field theories and grid diagrams*, *JHEP* **01** (1998) 002, [[hep-th/9710116](#)].
- [21] K. Dasgupta and S. Mukhi, *BPS nature of 3-string junctions*, *Phys. Lett.* **B423** (1998) 261–264, [[hep-th/9711094](#)].
- [22] A. Sen, *String network*, *JHEP* **03** (1998) 005, [[hep-th/9711130](#)].
- [23] T. Apostol, *Modular Functions and Dirichlet Series in Number Theory*. Springer-Verlag, 1976.
- [24] A. Sen, *Black Hole Entropy Function, Attractors and Precision Counting of Microstates*, [arXiv:0708.1270](#).
- [25] F. Denef, *Supergravity Flows and D-brane Stability*, *JHEP* **08** (2000) 050, [[hep-th/0005049](#)].

REFERENCES

- [26] A. Mukherjee, S. Mukhi, and R. Nigam, *Dyon Death Eaters*, *JHEP* **10** (2007) 037, [[arXiv:0707.3035](#)].
- [27] A. Mukherjee, S. Mukhi, and R. Nigam, *Kinematical Analogy for Marginal Dyon Decay*, [arXiv:0710.4533](#).
- [28] J. Maharana and J. H. Schwarz, *Noncompact Symmetries in String Theory*, *Nucl. Phys.* **B390** (1993) 3–32, [[hep-th/9207016](#)].
- [29] A. Sen, *Electric Magnetic Duality in String Theory*, *Nucl. Phys.* **B404** (1993) 109–126, [[hep-th/9207053](#)].
- [30] C. Wall, *On the Orthogonal Groups of Unimodular Quadratic Forms*, *Math. Annalen* **147** (1962) 328.
- [31] S. Banerjee and A. Sen, *Duality Orbits, Dyon Spectrum and Gauge Theory Limit of Heterotic String Theory on T^6* , *JHEP* **03** (2008) 022, [[arXiv:0712.0043](#)].
- [32] E. Diaconescu and G. W. Moore, *Crossing the Wall: Branes vs. Bundles*, [arXiv:0706.3193](#).
- [33] M. C. N. Cheng and E. P. Verlinde, *Wall Crossing, Discrete Attractor Flow, and Borchers Algebra*, [arXiv:0806.2337](#).
- [34] D. J. Griffiths, *Introduction to elementary particles*. Wiley, New York, 1987.
- [35] J. Distler, A. Hanany *(0,2) noncritical strings in six dimensions*, *Nucl. Phys.* **B490** (1997) 75–90, [[hep-th/9611104](#)].
- [36] A. Sen, *String string duality conjecture in six-dimensions and charged solitonic strings*, *Nucl. Phys.* **B450** (1995) 103–114, [[hep-th/9504027](#)].
- [37] J. Harvey, A. Strominger, *The heterotic string is a soliton*, *Nucl. Phys.* **B449** (1995) 535–552, [[hep-th/9504047](#)].
- [38] E. Witten, *String theory dynamics in various dimensions*, *Nucl. Phys.* **B443** (1995) 85–126, [[hep-th/9503124](#)].

REFERENCES

- [39] O. Bergman, *Three-pronged strings and 1/4 BPS states in $N = 4$ super-Yang-Mills theory*, *Nucl. Phys.* **B525** (1998) 104–116, [[hep-th/9712211](#)].
- [40] O. Bergman, B. Kol, *String webs and 1/4 BPS monopoles*, *Nucl. Phys.* **B536** (1998) 149–174, [[hep-th/9804160](#)].
- [41] A. Dabholkar, D. Gaiotto, S. Nampuri, *Comments on the spectrum of CHL dyons*, [[hep-th/0702150](#)].
- [42] A. Dabholkar, D. Gaiotto, S. Nampuri *Comments on the spectrum of CHL dyons*, [[hep-th/0612011](#)].
- [43] K. Dasgupta, S. Mukhi, *Orbifolds of M-theory*, *Nucl. Phys.* **B465** (1996) 399–412, [[hep-th/9512196](#)].
- [44] E. Witten, *Five-branes and M-theory on an orbifold*, *Nucl. Phys.* **B463** (1996) 383–397, [[hep-th/9512219](#)].
- [45] H. Ooguri, A. Strominger, C. Vafa, *Black hole attractors and the topological string*, *Phys. Rev.* **D70** (2004) 106007, [[hep-th/0405146](#)].
- [46] H. Ooguri, C. Vafa, E. P. Verlinde, *Hartle-Hawking wave-function for flux compactifications*, *Lett. Math. Phys.* **74** (2005) 311–342, [[hep-th/0502211](#)].
- [47] T. J. Hollowood, A. Iqbal, C. Vafa, *Matrix Models, Geometric Engineering and Elliptic Genera*, [[hep-th/0310272](#)].
- [48] M. J. Duff, J. T. Liu, J. Rahmfeld, *Four-dimensional string-string-string triality*, *Nucl. Phys.* **B459** (1996) 125–159, [[hep-th/9508094](#)].